



Schweizerische Eidgenossenschaft
Confédération suisse
Confederazione Svizzera
Confederaziun svizra

Federal Department of the Environment, Transport, Energy and
Communications (DETEC)

Federal Office of Transport FOT
Public Transport Energy Strategy 2050 Programme
(SETP 2050)

Potential analysis for vacuum transport technologies in public transport in Switzerland

Life-cycle analysis with focus on energy consumption and environmental impact of a vacuum transport infrastructure

Final report

Giacomo Pareschi, EuroTube Foundation

Neugutstrasse 66, 8600 Dübendorf, giacomo.pareschi@eurotube.org, eurotube.org

Julian Ehwald, EuroTube Foundation

Neugutstrasse 66, 8600 Dübendorf, julian.ehwald@eurotube.org, eurotube.org

Nuannuan Leng, EuroTube Foundation

Neugutstrasse 66, 8600 Dübendorf, nuannuan.leng@eurotube.org, eurotube.org

Paul Beckert, Paul Scherrer Institut

Forschungsstrasse 111, 5232 Villigen PSI, paul.beckert@t-online.de, www.psi.ch/de

Baoling Guo, HES-SO Valais-Wallis

Rue de l'Industrie 23, 1950 Sion, baoling.guo@hevs.ch, www.hevs.ch/en

Advisory Board

Mr Jean-Loup Robineau, PLANAIR SA
Mr Nicolas Macabrey, PLANAIR SA

Legal information

Publisher:
Federal Office of Transport FOT
Programme: Energy Strategy 2050 in Public Transport (SETP 2050)
CH-3003 Bern

Programme Director
Tristan Chevroulet, FOT

Project number: 237
Source
Accessible free of charge via the Internet
www.bav.admin.ch/energie2050

The author(s) alone are responsible for the content and conclusions of this report.

Dübendorf, 14.09.2023

Contents

| | |
|---------------------------------------------------------------|-----------|
| List of tables | 1 |
| List of figures | 4 |
| List of abbreviations | 5 |
| Executive summary in English | 6 |
| Executive summary in German | 7 |
| Executive summary in French | 8 |
| Summary in English | 9 |
| Summary in German | 13 |
| Summary in French | 17 |
| 1 Initial situation | 21 |
| 1.1 Why hyperloop now? | 21 |
| 1.1.1 The predicted future of transport | 21 |
| 1.1.2 Future options for transport | 21 |
| 1.1.3 The potential of hyperloop | 21 |
| 1.1.4 Financial situation | 22 |
| 1.1.5 Switzerland's role in pioneering transport technologies | 23 |
| 2 Objectives of the work | 24 |
| 3 Approach and current state of knowledge | 25 |
| 3.1 Overview of the hyperloop system | 25 |
| 3.2 Overview of methodology | 27 |
| 3.3 Passenger demand model | 28 |
| 3.3.1 Data declaration | 28 |
| 3.3.2 Passenger simulation model | 29 |
| 3.3.3 Traffic extrapolation to 2050 | 30 |
| 3.4 Operational requirements and fleet sizing | 30 |
| 3.4.1 Rush hour and fleet sizing | 30 |
| 3.5 System design | 32 |
| 3.5.1 Vehicle systems and energy consumption | 32 |
| 3.5.2 Overground infrastructure | 38 |
| 3.5.3 Underground infrastructure | 39 |
| 3.5.4 Additional infrastructure | 39 |
| 3.6 Numerical simulation and interfaces with other modules | 41 |
| 3.7 Life-cycle assessment (LCA) | 43 |
| 3.7.1 Goal and scope definition | 43 |
| 3.7.2 Life-cycle inventory (LCI) analysis | 44 |
| 3.7.3 Life-cycle impact assessment (LCIA) | 45 |
| 3.7.4 Interpretation | 46 |
| 3.8 Economic assessment | 47 |
| 4 General hyperloop energy assessment | 50 |
| 4.1 Overview of simulated scenarios | 50 |
| 4.2 Reference case parameters | 50 |
| 4.3 Energy consumption | 50 |
| 4.3.1 Track-side vs pod-side acceleration | 50 |
| 4.3.2 Sensitivity Analysis | 53 |
| 4.3.3 Role of aerodynamics | 55 |
| 4.4 LCA for linear infrastructure | 57 |
| 4.5 Cost of linear infrastructure | 57 |
| 5 Results for a small network (Swiss case) | 59 |
| 5.1 Passenger demand | 60 |
| 5.1.1 Scenarios description for passenger simulation | 60 |
| 5.1.2 Average daily hyperloop passengers on each segment | 61 |
| 5.1.3 Mode split of passenger-kilometres | 61 |
| 5.1.4 Shift from each mode of transport to hyperloop | 62 |
| 5.2 System operation and fleet sizing | 63 |
| 5.2.1 Fleet sizing | 63 |

| | | |
|----------|-----------------------------------------------------------------------|------------|
| 5.3 | Network life-cycle assessments | 66 |
| 5.3.1 | Travel time sensitivity | 67 |
| 5.3.2 | Energy consumption | 67 |
| 5.3.3 | Life-cycle assessment | 68 |
| 5.4 | Network economic assessments | 71 |
| 6 | Overall assessment of hyperloop in Switzerland | 74 |
| 6.1 | Cost and emissions trade-off | 74 |
| 6.2 | Environmental benchmark with alternative modes of transport | 77 |
| 6.3 | Economic benchmark with alternative modes of transport | 79 |
| 6.3.1 | Comparison with other sources | 79 |
| 6.4 | Further economic considerations | 80 |
| 7 | Conclusion | 81 |
| 7.1 | Key Findings | 81 |
| 7.2 | Identified bottlenecks in technology | 82 |
| 7.3 | Limitations of the model and outlook | 83 |
| A | Calibration of passenger simulation | 91 |
| B | Intermodality | 91 |
| C | Freight use case | 92 |
| D | The impact of the electricity mix | 92 |
| E | Technical descriptions | 93 |
| E.1 | Alternative levitation technologies | 93 |
| E.2 | Levitation System Details | 93 |
| F | Detailed study on launcher power management | 94 |
| F.1 | Modelling of the train traction system | 94 |
| F.2 | Modelling of electrical network with moving loads | 96 |
| F.3 | Substation configuration | 97 |
| F.3.1 | MVAC vs MVDC | 97 |
| F.3.2 | Energy management system | 99 |
| G | Sankey diagram of the life-cycle assessment | 102 |

List of Tables

| | | |
|----|--------------------------------------------------------------------------------------------------------------------------------------------------------------------------------------------------------------------------|----|
| 1 | Functionalities of a hyperloop system and technological concepts assumed in this study. Bold represents the chosen concept, where sometimes several were investigated and some omitted in the modelling process. | 33 |
| 2 | Modelling of drag coefficient dependencies on key system design parameters. | 37 |
| 3 | Alignment of climate and techno-economic scenarios between global and Swiss perspectives. | 45 |
| 4 | List of impact assessment methods, categories, indicators and units that are used in this study to evaluate the hyperloop system. | 46 |
| 5 | Examples for characterising the results of the LCI (impact category climate change from the IPCC 2013). | 47 |
| 6 | Main technical and scenario parameters assumed for the hyperloop system. | 51 |
| 7 | Parameters changed compared to Table 6 for the investigation of the Swiss network. | 59 |
| 8 | Comparison of travel times with car and rail today and the Hyperloop variants fast, slow, and slow with the need to slow down for switching as well. Passenger transit times are excluded. | 63 |
| 9 | Main input parameters and output results of the average best-performing configurations for a Swiss hyperloop network; 1 Rp. = 0.01 CHF. | 75 |
| 10 | General inputs of passenger and freight pods | 95 |
| 11 | Launching frequencies of passenger and freight pods | 95 |

List of Figures

| | | |
|----|--------------------------------------------------------------------------------------------------------------------------------------------------------------------------------------------------------------------------------------------------------------------------------------------------------------------------------------------------------------------|----|
| 1 | Comparison of the specific life-cycle emissions per passenger-kilometre between different modes of transport, split into the main sources of emissions for a hyperloop configuration with 600 kph and direct connections between cities. Given in gram of CO ₂ -equivalent warming potential. | 10 |
| 2 | Relative contribution to infrastructure cost per component for an underground solution with exits at full speeds (implying long exit ramps). | 10 |
| 3 | Vergleich der spezifischen Lebenszyklus-Emissionen pro Personenkilometer zwischen verschiedenen Verkehrsmitteln, aufgeteilt in die Hauptemissionsquellen für eine Hyperloop-Konfiguration mit 600 km/h und Direktverbindungen zwischen Städten. Angegeben in Gramm CO ₂ -äquivalent Erwärmungspotenzial. | 14 |
| 4 | Relativer Beitrag zu den Infrastrukturkosten pro Komponente für eine unterirdische Lösung. | 14 |
| 5 | Comparaison des émissions spécifiques du cycle de vie par passager-kilomètre entre différents moyens de transport, réparties selon les principales sources d'émission. Exprimé en grammes d'équivalent CO ₂ de potentiel de réchauffement. | 18 |
| 6 | Contribution relative aux coûts d'infrastructure par composant pour une solution souterraine | 18 |
| 7 | Breakdown of resistive forces acting on a train at constant speed. Based on TGV measurements [21]. | 22 |
| 8 | Total forecasted infrastructure investment needs by mode, from 2022 to 2050. Note: Estimates are based on a linear extrapolation of G20 investment requirement projections from 2017 to 2040 [31]. | 23 |
| 9 | Essential subsystems with the corresponding components included in a hyperloop system. | 25 |
| 10 | Envisaged pressure regimes of key players in the hyperloop field. | 25 |
| 11 | Schematic relations between the different modules of the study. Each module is explained in the given section and the quantities in the parallelograms are the main KPIs of this study. | 28 |
| 12 | Zones of Switzerland in NPVM 2017. | 29 |
| 13 | Hourly distribution of passenger traffic by car and by train. The distributions refer to an <i>average working day</i> but are normalised with respect to the total traffic of an <i>average day</i> of the year. The sum of the columns thus slightly exceeds 100%. | 31 |
| 14 | Passenger capacity of a hyperloop line (left y-axis) achievable for a given headway between travelling vehicles (x-axis) and seat capacity of the pods (different colours). The right x-axis shows the minimum emergency braking rate required to safely operate at a given headway. | 32 |
| 15 | Energy and mass flows modelled within the simulation. | 35 |
| 16 | Left to right: Blockage ratios of 0.36, 0.6 and 0.83: Ratio of the inner area of the tube that pod and sleeper occupy together. | 36 |
| 17 | EuroTube's concept of the <i>GammaShellPipe</i> , for which the design is completed and first pipes will be produced in 2024. For this study, an upscaled version was used (doubling of diameter and span). Pillars are placed at the interface of two tubes. | 38 |
| 18 | Overview of layers included in tunnelling solution. | 39 |
| 19 | Underground system for a hyperloop with bypass system, valves, on-/off-ramps and safety tunnel above the main line | 41 |
| 20 | Internal structure of the design module. | 42 |
| 21 | Phases of an LCA [53] | 43 |
| 22 | Scheme of the cut-off allocation used for the LCI of the hyperloop system. The diagram serves as a simplified illustration and does not represent all connections between the system components. | 45 |
| 23 | Breakdown of specific energy consumption (left, a) and pod weight (right, b) for the track-side and pod-side acceleration systems. In a) also the recuperation energy is shown as negative and the resulting net energy consumption is depicted by the yellow dots. The payload is for 100% load factor, which is the scenario the system is designed for. | 52 |
| 24 | Specific energy consumption of the hyperloop system (in MJ/pkm) for various input designs settings. Each row explores a different dimension: first and third values correspond to the left and right margins of the bars; the second value is captured by the dashed line and indicates the reference case. | 54 |

| | | |
|----|--------------------------------------------------------------------------------------------------------------------------------------------------------------------------------------------------------------------------------------------------------------------------------------------------------------------------------------------------------------------------------------------------------------------------------------------------------------------------------------------------------------------------------------------------------------------------------------------------------------------------------------------------------------------------------------------------------------------------------------------------------------------------------------------------------------------------------------------------------------------------------------------------------------------------|----|
| 25 | Aerodynamic sensitivities | 56 |
| 26 | GWP per meter of infrastructure for a lifetime of 100 years. This does not include stations, launching devices or vehicles but is used to illustrate the breakdown into subsystem contributions as well as comparison between ways of construction. | 57 |
| 27 | Cost per unidirectional kilometre for construction of linear infrastructure. Additional cost such as vehicles, stations and track-side launching are network dependent. | 58 |
| 28 | Average daily hyperloop passengers on each segment in 2050. | 61 |
| 29 | Mode split pkm (≥ 50 km). | 62 |
| 30 | Mode split pkm (≥ 100 km). | 62 |
| 31 | Shift from each mode of transport to hyperloop in 2050. | 62 |
| 32 | Rush hour passenger traffic (y-axis) and journey distance (x-axis) for each Swiss connection. These are the two main features used to group the routes into two categories, so that each that can be served by a unique vehicle type. The bubble size is proportional to the average daily traffic. | 64 |
| 33 | Pod traffic at rush hour on each segment of the network for the “fast hyperloop” scenario; the colours identify the origin – destination routes travelled by the pods. | 64 |
| 34 | Daily passenger and pod traffic in both directions for each route of the network for the “fast hyperloop” scenario. Also the travel time and the minimum number of vehicles dedicated to each route is indicated. The colour refers to the assigned vehicle type. | 65 |
| 35 | Six examples of pod acceleration profiles that have been tested in the study. The colour indicates whether the pod is being accelerated by the launcher, by its own propulsion, or it is simply cruising. a) is the reference case from section 4, with a slow 1 m/s^2 acceleration to the top speed of 900 km/h fully propelled by the launcher; case b) depicts a launcher-propelled 2 m/s^2 acceleration to 600 km/h; in case c) the acceleration is provided by the launcher up to 450 km/h, then by the pod; case d) shows a fully self-accelerated pod, but with a gradually lower acceleration rate at higher speeds; case e) displays a fully concave acceleration profile propelled by the launcher; case f) combines all of the above, with a concave acceleration profile propelled by both launcher and pod. All these combinations and more have been tested in the simulation. | 66 |
| 36 | Bi-directional daily passenger flow by hyperloop (y-axis) for a given total travel time (x-axis) on each route. The travel time includes the time needed to change mode (if required) at both origin and destination. Passenger numbers include modal shift from road, rail, and plane and are set in 2050. | 67 |
| 37 | Annual electricity consumption (left and right y-axes) and passenger traffic (x-axis) for different system configurations. The colour indicates the share of the acceleration phase propelled by the track-side launcher. The points to the left correspond to system configurations with a cruising speed of 600 km/h, the points to the right to 900 km/h. | 68 |
| 38 | Breakdown of the specific energy consumption per pkm for various system configurations, grouped by cruising speed (600 or 900 km/h) and share of acceleration propelled by the track-side launcher. | 69 |
| 39 | Breakdown of the specific LCA emissions per pkm for various system configurations, grouped by cruising speed (600 or 900 km/h) and share of acceleration propelled by the track-side launcher. | 70 |
| 40 | Annualised life-cycle emissions (y-axis) and passenger traffic (x-axis) for different system configurations. The colour indicates which through stations employ high- or slow-speed transit bypasses. The points to the left correspond to system configurations with a cruising speed of 600 km/h, the points to the right to 900 km/h. | 70 |
| 41 | Breakdown of the full CAPEX of the network for various system configurations, grouped by cruising speed (600 or 900 km/h) and share of acceleration propelled by the track-side launcher. | 71 |
| 42 | Breakdown of the annual OPEX of the network for various system configurations, grouped by cruising speed (600 or 900 km/h) and share of acceleration propelled by the track-side launcher. | 72 |
| 43 | Annualised system costs (y-axis) and passenger traffic (x-axis) for different system configurations. The colour indicates which through stations employ high- or slow-speed transit bypasses. The points to the left correspond to system configurations with a cruising speed of 600 km/h, the points to the right to 900 km/h. | 73 |

| | | |
|----|-----------------------------------------------------------------------------------------------------------------------------------------------------------------------------------------------------------------------------------------|-----|
| 44 | Breakdown of the total costs of the system (CAPEX depreciation and OPEX) per pkm for various system configurations, grouped by cruising speed (600 or 900 km/h) and share of acceleration propelled by the track-side launcher. | 73 |
| 45 | Summary of total costs (y-axis) and life-cycle GHG emissions (x-axis) for all tested network configurations. The colours indicates the presence of slow- or high-speed bypasses at through stations. | 74 |
| 46 | Pod acceleration profile for the average best-performing hyperloop configurations, using the notation of Fig. 35. | 76 |
| 47 | Comparison of the specific life-cycle emissions per passenger-kilometre between different modes of transport, split into the main sources of emissions. | 77 |
| 48 | Cost per passenger-kilometre for different modes of transport. The railway and aviation data are taken from annual reports of the corresponding entities for the year 2022. | 79 |
| 49 | Life-cycle GHG emissions of different transport systems for a given GHG intensity of the electricity consumed during operation (or e-kerosene production). | 92 |
| 50 | hyperloop rail line with launcher in green and recuperator in orange | 94 |
| 51 | Capsule train traction model with Matlab/Simulink | 96 |
| 52 | Speed and position profiles of each capsule train | 96 |
| 53 | Equivalent circuits of the electrical railway network | 97 |
| 54 | Modelling solution of the moving train loads | 97 |
| 55 | Complete simulation model of hyperloop electrical microgrid with Matlab/Simulink | 98 |
| 56 | MVAC (Medium Voltage Alternating Current) Topology | 98 |
| 57 | Fig. MVDC (Medium Voltage Direct Current) Topology | 99 |
| 58 | Voltage profile of each capsule train for 15kV DC electrification system | 99 |
| 59 | Voltage profile of each capsule train for 25kV AC electrification system | 100 |
| 60 | Line power loss under different voltage configurations | 100 |
| 61 | Substation total power curves for DC electrification system | 101 |
| 62 | HPS module integration in hyperloop microgrid | 101 |
| 63 | Partial zoom results of substation power curves and HPS behaviour curves | 104 |

List of abbreviations

| Abbreviation | Meaning |
|-----------------|-------------------------------------------------------------------|
| AC | Alternating Current |
| BC | Boundary Condition |
| BR | Blockage Ratio |
| CAPEX | Capital Expenditures |
| CHF | Swiss Franc |
| CFL | Courant–Friedrichs–Lewy (condition) |
| CST | Cargo sous terrain |
| DAC | Direct Air Capture |
| DC | Direct Current |
| DSO | Distribution System Operator |
| EDS | Electrodynamic suspension |
| EDLC | Electric Double Layer Capacitor |
| EM | Electromagnetic |
| EMS | Electromagnetic suspension |
| ENTSO-E | European Network of Transmission System Operators for Electricity |
| ETF | EuroTube Foundation |
| ETH | Eidgenössische Technische Hochschule (Zürich) |
| FOT | Federal Office of Transport |
| GHG | Greenhouse Gases |
| GUI | Graphical User Interface |
| GWP | Global Warming Potential |
| HES-SO | Haute Ecole Spécialisée de Suisse occidentale |
| HPS | High-Power Storage |
| HSR | High Speed Rail |
| HTS | High Temperature Superconductor |
| HVAC | Heating, Ventilation and Air Conditioning |
| IAM | Integrated Assessment Models |
| IEA | International Energy Agency |
| ISO | International Organisation for Standardisation |
| KPI | Key Performance Indicator |
| IPCC | Intergovernmental Panel on Climate Change |
| LCA | Life-Cycle Assessment |
| LCI | Life-Cycle Inventory |
| LCIA | Life-Cycle Impact Assessment |
| LIM | Linear Induction Motor |
| LSW | Leading Shock Wave |
| MNA | Modified Nodal Analysis |
| MV (MVAC, MVDC) | Medium Voltage (-AC, -DC) |
| OPEX | Operational Expenditures |
| PFC | Passive Flow Control |
| pkm | passenger-kilometre |
| PSI | Paul Scherrer Institute |
| PtL | Power to Liquid |
| ReBCO | Rare-earth Barium Copper Oxide |
| SAF | Sustainable Aviation Fuel |
| SBB | Schweizerische Bundesbahnen (Swiss Federal Railway) |
| SOC | State Of Charge |
| SST | Substation |
| TDIP | Technology Development Impact Projections |
| TES | Thermal Energy Storage |
| TRL | Technology Readiness Level |
| TSO | Transmission System Operator |
| VAC | Vacuum |
| vkm | vehicle-kilometre |

Executive summary in English

Switzerland's public transport system is integral to its living standards. With the nation's growth and evolution, there is an escalating demand for mobility. The transport sector in Switzerland is responsible for nearly 40% of all CO₂ emissions, underscoring the need for sustainable solutions. Vacuum transport (VT) is proposed as one such solution, offering high speeds with a reduced ecological impact by magnetically levitating in a partially vacuumed tube.

Our study evaluates the integration of VT into Switzerland's transport framework, examining energy use, environmental effects, capacity, and costs. The environmental impact of VT is found to be similar to that of conventional trains, with infrastructure construction being a major contributor to emissions. This means that a system applied to a small Swiss network could achieve as little as 0.075 kWh/pkm or 8.5g CO₂/pkm.

The construction cost for a Swiss VT-network is estimated between 15-25 bill. CHF (excluding any type of development cost), mainly due to the much lower tunnel diameter that VT envisions compared to railway. For context, budgets for upcoming rail system improvements are in a similar range. By 2050, the Geneva-Lausanne-Bern-Zurich route is projected to have robust passenger demand, with VT capable of potentially capturing a significant portion.

Technological components for VT largely exist, but challenges remain, especially in the development of levitation systems and thermal batteries. The study also highlights the importance of design choices, such as speed and acceleration profiles, in determining the system's performance. Safety considerations and regulatory decisions are yet to be detailed, and as are recommendations on how to best implement sensible permitting and financing procedures.

In conclusion, while VT has the potential to bring significant environmental and socio-economic benefits, its practical implementation in Switzerland requires substantial research work and validation analyses. VT could potentially bridge an important gap in existing transport networks. It is however yet to be proven in real-world applications that the system can meet the expectations set in this study.

Executive summary in German

Das öffentliche Verkehrssystem trägt wesentlich zum hohen Lebensstandard der Schweiz bei. Mit dem Wachstum und steigendem Wohlstand des Landes steigt die Nachfrage nach Mobilität. Der Verkehrssektor in der Schweiz ist für fast 40% aller CO₂-Emissionen verantwortlich, womit nachhaltige Lösungen von hoher Notwendigkeit sind. Vakuumtransport (VT) stellt eine Alternative dar, bei der Fahrzeuge durch magnetisches Schweben in einer teilwevakuierten Röhre mit hoher Geschwindigkeit befördert werden. Unsere Studie bewertet das Potential einer Integration von VT in das Schweizer Verkehrssystem und untersucht Energieverbrauch, Umweltauswirkungen, Kapazität und Kosten.

Die Umweltauswirkungen von VT sind im Bereich von herkömmlichen Zügen, wobei der Infrastrukturbau den Hauptbeitrag zu den Emissionen leistet. Unsere Modellierung ergibt für ein Schweizer Ost-West Netzwerk Werte von bis zu 0.075 kWh/pkm oder 8.5g CO₂/pkm inklusive Bauemissionen. Die Baukosten für ein Schweizer VT-Netzwerk werden auf 15 – 25 Mrd. CHF geschätzt, wobei der vorgesehene, wesentlich kleinere Tunneldurchmesser die Hauptkostensenkung im Vergleich mit z.B. Eisenbahntunnels darstellt. Zur Einschätzung: Die Budgets für bevorstehenden Ausbauschritte 2025 und 2035 der Bahn liegen in einem ähnlichen Bereich.

Technologische Komponenten für VT existieren bereits zu weiten Teilen, jedoch bleiben Herausforderungen bestehen, insbesondere bei der Entwicklung von Schwebesystemen und thermischen Batterien. Die Ergebnisse unterstreichen die Bedeutung von grundlegenden Konzeptfragen wie Geschwindigkeits- und Beschleunigungsprofilen. Sicherheitsüberlegungen und regulatorische Entscheidungen müssen im Detail ausgearbeitet werden, ebenso wie Empfehlungen zur sinnvollen Umsetzung von Genehmigungs- und Finanzierungsverfahren.

Abschliessend kann festgestellt werden, dass VT das Potenzial für erhebliche ökologische und sozioökonomische Vorteile mit sich bringt. Seine praktische Umsetzung in der Schweiz erfordert jedoch umfangreiche Forschungsarbeiten und Validierungsanalysen. VT könnte eine wichtige Lücke in den zukünftigen Verkehrsnetzen schliessen. Es bleibt jedoch zu beweisen, ob das System in der Praxis den in dieser Studie gesetzten Erwartungen gerecht werden kann.

Executive summary in French

Le système de transport public de la Suisse est essentiel à ses normes de vie. Avec la croissance et l'évolution de la nation, il y a une demande croissante pour la mobilité. Le secteur des transports en Suisse est responsable de près de 40% de toutes les émissions de CO₂, soulignant le besoin de solutions durables. Le transport sous vide (VT) est proposé comme une telle solution, offrant des vitesses élevées avec un impact écologique réduit en lévitant magnétiquement dans un tube partiellement vidé.

Notre étude évalue l'intégration du VT dans le cadre de transport de la Suisse, examinant l'utilisation de l'énergie, les effets environnementaux, la capacité et les coûts. L'impact environnemental du VT est trouvé similaire à celui des trains conventionnels, avec la construction d'infrastructures étant un contributeur majeur aux émissions. Cela signifie qu'un système appliqué à un petit réseau suisse pourrait atteindre aussi peu que 0.075 kWh/pkm ou 8.5g CO₂/pkm.

Le coût de construction pour un réseau VT suisse est estimé entre 15-25 milliards de CHF, principalement en raison du diamètre de tunnel beaucoup plus bas que le VT envisagé par rapport au chemin de fer. Pour contexte, les budgets pour les améliorations prochaines du système ferroviaire sont dans une gamme similaire. D'ici 2050, la route Genève-Lausanne-Berne-Zurich devrait avoir une forte demande de passagers, avec VT capable de capturer potentiellement une portion significative.

Les composants technologiques pour VT existent en grande partie, mais des défis demeurent, en particulier dans le développement des systèmes de lévitation et des batteries thermiques. L'étude souligne également l'importance des choix de conception, tels que les profils de vitesse et d'accélération, dans la détermination de la performance du système. Les considérations de sécurité et les décisions réglementaires restent à détailler, tout comme les recommandations sur la manière de mettre en œuvre au mieux des procédures d'autorisation et de financement sensées.

En conclusion, bien que le VT ait le potentiel d'apporter des avantages environnementaux et socio-économiques significatifs, sa mise en œuvre pratique en Suisse nécessite un travail de recherche substantiel et des analyses de validation. Le VT pourrait potentiellement combler un écart important dans les réseaux de transport existants. Il reste cependant à prouver dans les applications réelles que le système peut répondre aux attentes énoncées dans cette étude.

Summary in English

The availability of a high-quality public transport system has become a key to Switzerland’s high living standards. At the same time, the increase in population and economic growth inevitably leads to a higher demand for transport. As the impact of the changing climate is becoming increasingly more pressing, the need for emission reduction is inevitable also in the transport sector. In Switzerland in particular, the transport sector contributes to almost 40% of all CO₂ emissions [1]. It is therefore apparent that tomorrow’s transport infrastructure needs to adapt to live up to both societal and environmental requirements at the same time. New modes of transport, in combination with extensions and improvements of the existing ones, are required.

Vacuum transport (VT) is a concept that generally addresses transport at a range between a hundred and a thousand kilometres, by travelling at speeds comparable to aeroplanes, but with a considerably lower ecological footprint. VT is a guided transport system that strongly mitigates the limitations of current railway – aerodynamic and rolling resistances – by magnetically levitating above the track in a tube with a partial vacuum. Therefore, not only could it be possible to add a new mode of ultra-high-speed rail to the current network, but also to shift large parts of emission-intensive short-haul flights to sustainable, fully electric ground-based transport. However, the promising vision of VT will only have a chance at becoming reality if it can guarantee benefits to society that outweigh its costs: from improved accessibility, capacity, and comfort to reduced travel time and most importantly low ecological impact.

This study evaluates the potential of integrating a VT system into Switzerland’s transport infrastructure. We present estimates on energy use, environmental effects, transport capacity, and cost. Our methodology allows for flexible assessments based on different design choices. The estimation of the environmental impacts is based on the ecoinvent database, a transparent and widely recognised resource of life-cycle data in academia and industry. The feasibility and implication of connecting the system to the power grid have also been investigated.

This work aims at presenting and assessing the environmental and energy-related impacts of a feasible concept of VT system, focusing on an aggregation and coherent synthesis of all its parts rather than the detailed development of any component in particular. Every technological principle included and modelled is either already in use or has been investigated in industry or academia. Therefore, it is shown that already today’s technology is not too far from providing all technology for a functional VT system. Furthermore, with the expected technological advancements through cumulative investments and the developments in the construction sector, VT systems are expected to be built at substantially lower energy and environmental footprint in the years to come. It has yet to be shown whether or not the systems can perform at the level modelled in this study at a full-scale, real-world application.

Findings

Our in-depth life-cycle assessment reveals that VT’s environmental impact, in terms of greenhouse gas emissions and operational energy consumption, is on par with conventional trains, as depicted in Fig. 1. For optimal configurations, the operational energy could reach as little as 0.075 kWh/pkm or 8.5 gCO₂ per pkm when including infrastructure. However, the emissions are significantly influenced by the electricity mix. Notably, the construction of the tunnel (or tube) alone accounts for half of the emissions, with the guide way – comprising aluminium and steel profiles for guidance and propulsion – being the second-largest contributor. In terms of environmental impact, VT behaves inversely to aviation: the lion share of emissions comes from the construction of the infrastructure, with then very little emissions during operation. Aviation, on the other hand, needs only the construction of airports, but causes immense subsequent emissions during operation.

Regarding the financial performance of the system, our initial estimates suggest a total cost in the range of 0.15–0.17 CHF per passenger-kilometre for the proposed network, translating to roughly 775–850 mill. CHF per year. Around 60% of this cost comes from purely operational expenditures, i.e. personnel, electricity, etc. With this, VT is in a range between aviation and railway. Aviation is economically more efficient due to lack of infrastructure apart from airports. The potential cost advantages of VT come into play particularly on high-capacity lines, where the heavy infrastructure over low-speed trains can be justified. Additionally, VT operates in smaller

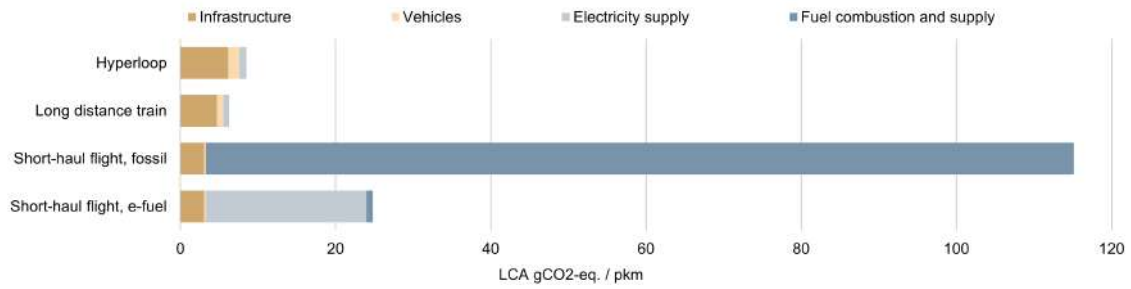


Figure 1: Comparison of the specific life-cycle emissions per passenger-kilometre between different modes of transport, split into the main sources of emissions for a hyperloop configuration with 600 kph and direct connections between cities. Given in gram of CO₂-equivalent warming potential.

vehicles (70-200 passengers) and therefore can adapt closely to the demand, resulting in a high load factor on vehicles. When considering socio-economic benefits, factors such as reduced travel time and noise reduction could potentially lead to societal savings exceeding 500 mill. CHF annually.

The projected construction cost for a Swiss VT network is estimated between 15–25 bill. CHF. It is worth noting that unforeseen costs, especially in underground solutions, could potentially increase this estimate, similarly to the Gotthard project where the budget increased by 50%. In comparison, the gradual improvements planned for the railway system in the combined extension steps for 2025 and 2035 have a reserved budget of roughly 20 bill. CHF [2, 3]. While considerable, this means that the cost for such a VT network is a realisable investment and would be a fundamental decision similar to the construction of the Gotthard tunnel.

Fig. 2 shows the distribution of cost factors in construction for a purely underground solution, which costs just short of 40 mill. CHF per two-lane kilometre of infrastructure.

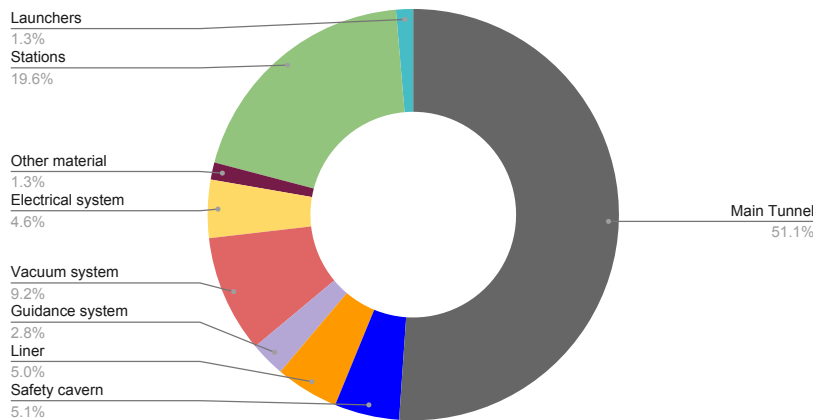


Figure 2: Relative contribution to infrastructure cost per component for an underground solution with exits at full speeds (implying long exit ramps).

By 2050, projections for the Geneva-Lausanne-Bern-Zurich line indicate robust passenger demand, where the VT is poised to capture a significant market share. Factors such as travel time, station locations, and streamlined processes play a crucial role in influencing passenger choices. The strategic placement of VT stations is essential for accessibility.

In terms of capacity, the system would be able to cover the full rush hour demand between Zurich and Bern. Doubts regarding the VT’s capacity seem largely unfounded, given that no major player still follows the 28-person vehicle concept suggested in Tesla and SpaceX’ Hyperloop Alpha Paper [4]. The vision has moved to larger vehicles, especially since aerodynamic drag has little dependence on vehicle length, making longer vehicles more energy-efficient.

When adapting a VT system for Switzerland, it is evident that the ideal system configuration and performance are closely intertwined. While the general consensus is to develop high-speed

switches, for a Swiss network of the projected size, this might not be as beneficial due to the extensive construction required for off- and on-ramps. Interestingly, the top speed is recommended to be reduced compared to a continental network, with a hybrid of track- and pod-side acceleration appearing optimal for environmental impact. The application of the general results for VT also show the extremely strong dependency of the performance on the network topology, demand per segment and distances. It shall therefore be understood that results presented in this study are not straightforwardly generalisable to other contexts or applications. For the specifically modelled Swiss system, it seems that emissions and cost are minimised for approximately the same conditions.

On the technological front, many of the essential technologies for constructing a VT are already in existence and have undergone proof of concept. The most influential parameters about the system's performance are less about technology predictions and more about design choices, such as speed, acceleration profiles, and operating pressures.

Limitations and Outlook

Opportunities for improvements have been identified both in terms of the modelling techniques and in actual technological development.

On a purely technical side, levitation systems are pivotal for VT's operation and must be built and validated at a larger scale. The idea of a vacuum-sealed, easy-to-maintain tunnel, while promising, has not been tested in real-world conditions. Its success is crucial not only for Switzerland but for the broader adoption of VT technology globally and could be one of the key products to be developed. Thermal batteries, conceptualised using phase-changing materials like water, are still in the theoretical stage and require practical development. The efficiencies projected for motors in this study, are yet to be achieved and crucial for the system to reach the performance suggested.

Many limitations exist also on the modelling side. Questions remain about the applicability of air leakage rates from overground systems to tunnels. The levitation system, even though based on current research, could encounter unexpected challenges when implemented on a full scale. Cooling of the tunnels, a frequent point of discussion, might be more influential than initially anticipated, potentially overshadowing the energy demand for maintaining the partial vacuum conditions. Furthermore, predicting passenger demand is intricate, with factors like ticket pricing, governance, and broader economic trends playing as much of a role as the modelled travel time dependency.

Despite extensive work, many challenges persist also in the aerodynamic modelling of the system. The pressure drag experienced by the vehicle, even in vacuum, remains a major energy consumption contributor. Reliable Key Performance Indicators (KPIs) can only be established with in-depth simulations of drag forces. Furthermore, the materials needed to build track-side accelerations are based on small prototypes and their accuracy when scaled up can be questioned. More economical designs of the tube as well as in-depth modelling of required rail thickness would substantially reduce construction and operational emissions.

There are unresolved queries beyond this study's scope. In governance, a crucial choice looms: should VT's safety regulations align more with aviation's inherent safety, where systems are designed to prevent failure at all cost, or with railways' fail-safe approach, which allows for immediate evacuations in emergencies? It can be observed that the on-going standardisation by the EU (JTC-20) and first safety certifications by renowned TÜV can largely be built on existing aerospace and railway metrics [5, 6].

Conclusion

A framework has been established to evaluate different design configurations and address fundamental VT design questions. This method can be further utilised and expanded upon in future research. The introduction of a VT system in Switzerland could serve as a pioneering flagship in transport, reminiscent of the AlpTransit introduction in recent decades. Even if VT is not introduced in Switzerland, the research and development of related technologies could benefit the Swiss industry through the export of technological know-how and innovative products.

While the performance of the system described in this study has not been demonstrated in actual conditions, the current efforts such as the establishment of the European Hyperloop Centre [7] and investments made at a European level [8, 9] underscore the strong scientific and political interest. It is clear that more research, developments, and careful considerations are required before it can be fully realised. Overall, the study suggests that a VT system could effectively offer the speed of an aeroplane with the ecological footprint and capacity of a train; this at a cost that, although considerable, is well within the realm of possibility for infrastructure projects of this size. Introducing such a system would bridge a significant growing gap in transport networks and could be a complementary measure that can bring capacity relief, redundancy, and consumer- and environment-friendly competitiveness to future long-distance public transport.

Summary in German

Die Verfügbarkeit von zuverlässigem und schnellem öffentlichen Verkehr spielt eine wichtige Rolle für den hohen Lebensstandard in der Schweiz. Gleichzeitig führen das Bevölkerungs- und Wohlstandswachstum zu einer erhöhten Verkehrsnachfrage. Mit den sich immer stärker zeigenden Auswirkungen des Klimawandels wird die Reduktion von Emissionen auch im Verkehrssektor notwendig, welcher in der Schweiz fast 40% aller CO₂-Emissionen verursacht [1]. Es ist somit offensichtlich, dass die zukünftige Verkehrsinfrastruktur sich sowohl der Nachfrage wie auch den entsprechenden Umwelanforderungen anpassen muss. Neue Transportmittel, in Kombination mit Ausbau und Verbesserung der bestehenden Infrastruktur, sind notwendig.

Vakuumtransport (VT) ist ein Konzept, das in seiner ursprünglichsten Form auf den Verkehr zwischen hundert und tausend Kilometern Distanz zugeschnitten ist, sich mit der Geschwindigkeit eines Flugzeuges fortbewegt, jedoch wesentlich weniger Energie verbraucht. Die Limitierungen für konventionelle Eisenbahnen – Luft- und Rollwiderstand – werden beim VT durch magnetische Levitation in teilevakuieren Röhren grossteils eliminiert. Somit könnte nicht nur die bestehende Bahn durch eine neue Hochgeschwindigkeitsinfrastruktur ergänzt werden, sondern auch Grossteile von emissionsreichen Kurzstreckenflügen auf ein nachhaltiges, vollelektrisches Transportmittel verlagert werden. Die vielversprechende Vision von VT kann nur Realität werden, wenn sie Vorteile für die Gesellschaft mit sich bringt, die die Kosten übersteigen: Kapazität, Komfort, Fahrzeitverkürzung und vor allem reduzierte Emissionen.

Diese Studie bewertet das Potential einer Integration von einem VT-System in die zukünftige Verkehrsinfrastruktur. Wir präsentieren Schätzungen für Energiebedarf, Umweltauswirkungen, Kapazität und Kosten. Die Berechnungen der Umwelteinflüsse basieren auf der Ecoinvent-Datenbank, einer transparenten und in Wissenschaft und Industrie weit anerkannten Ressource für Lebenszyklusdaten. Die Machbarkeit eines Anschlusses des Systems an das Schweizer Stromnetz wurden ebenfalls untersucht.

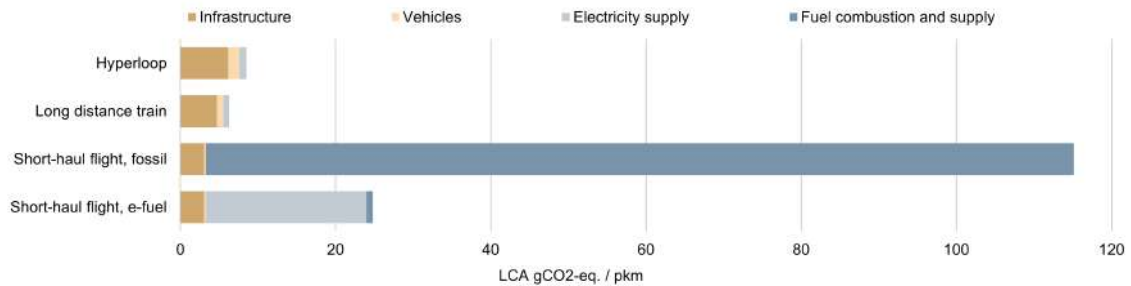
Diese Arbeit hat zum Ziel, die Umwelt- und Energieauswirkungen eines spezifischen (von vielen möglichen) VT-Konzepts zu präsentieren und zu bewerten. Dabei liegt der Fokus auf einer gesamthaften Betrachtung aller seiner Teile, anstatt auf der detaillierten Entwicklung von bestimmten Komponenten. Jedes technologische Prinzip, das einbezogen und modelliert wurde, wird entweder bereits verwendet oder wurde in der Industrie oder Wissenschaft untersucht. Damit wird nahegelegt, dass die heutige Technologie nicht allzu weit davon entfernt ist, alle Funktionen für ein VT-System bereitzustellen. Es ist ausserdem davon auszugehen, dass die Realisierung von VT-Systemen aufgrund der erwarteten technologischen Fortschritte durch Investitionen und Entwicklungen im Bausektor vereinfacht wird. Es bleibt jedoch zu zeigen, dass das modellierte System in einer realen Anwendung die geschätzten Kennzahlen tatsächlich erreicht.

Ergebnisse

Unsere Lebenszyklusanalyse zeigt, dass sich die Umweltauswirkungen, sowohl die Treibhausgasemissionen als auch der Energiebedarf, sich in einem ähnlichen Bereich wie jene der Eisenbahn befinden. Grafik 3 zeigt, dass für optimale Konfigurationen der Energiebedarf lediglich 0.075 kWh/pkm (Passagierkilometer) beträgt, und die Emissionen inklusive Bau bei ungefähr 8.5 gCO₂ /pkm liegen. Es soll jedoch festgehalten werden, dass die Treibhausgasemissionen stark vom Strommix abhängen. Die Hauptquelle für Treibhausgase ist der Bau des Tunnels/der Röhre, welche ungefähr die Hälfte beisteuert. Das Schienenkonzept – bestehend aus Aluminium- und Stahlprofilen für Führung und Antrieb – stellt den zweitgrössten Anteil dar. In Bezug auf die Umweltauswirkungen verhält sich VT genau entgegengesetzt zur Luftfahrt: Der Grossteil der Emissionen stammt aus dem Bau der Infrastruktur, während im Betrieb nur sehr geringe Emissionen anfallen. Die Luftfahrt hingegen benötigt lediglich den Bau von Flughäfen, verursacht aber im Betrieb immense, kontinuierliche Emissionen.

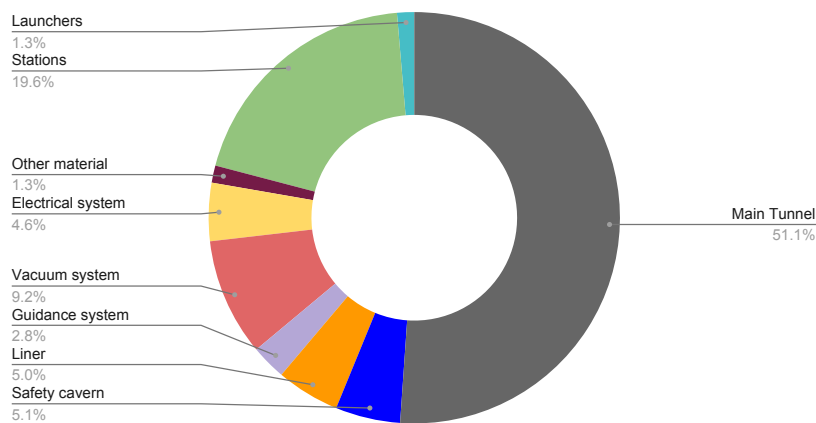
Die ersten Schätzungen ergeben Gesamtkosten im Bereich von 0.15 – 0.17 CHF pro Passagierkilometer für das vorgeschlagene Netzwerk, was jährlich in etwa 775 – 850 Mio. CHF entspricht. Rund 60% dieser Kosten entstehen durch rein betriebliche Ausgaben, also Personal, Strom usw. Damit liegt VT preislich zwischen Luftfahrt und Eisenbahn. Die Luftfahrt ist wirtschaftlich effizienter, da abgesehen von Flughäfen praktisch keine Infrastruktur benötigt wird. Der potenzielle

Kostenvorteil von VT gegenüber der Eisenbahn im Rahmen dieser Studie könnte auf sein simples, stark frequentiertes Netzwerk zurückzuführen sein. Im Vergleich dazu bedient die Bahn ein viel grösseres, weitverzweigtes Netz. Zudem sind bei VT kleinere Fahrzeuge vorgesehen (70-200 Passagiere) womit sich der Betrieb besser der Nachfrage anpassen kann, was wiederum zu einem hohen Auslastungsfaktor der Fahrzeuge führt. Unter Berücksichtigung sozioökonomischer Aspekte könnten Faktoren wie reduzierte Reisezeit und Lärminderung potenziell zu gesellschaftlichen Einsparungen von über 500 Mio. CHF jährlich führen.



Grafik 3: Vergleich der spezifischen Lebenszyklus-Emissionen pro Personenkilometer zwischen verschiedenen Verkehrsmitteln, aufgeteilt in die Hauptemissionsquellen für eine Hyperloop-Konfiguration mit 600 km/h und Direktverbindungen zwischen Städten. Angegeben in Gramm CO₂-äquivalent Erwärmungspotenzial.

Eine erste Schätzung der Baukosten für ein Schweizer VT-Netz im Mittelland beträgt 15 – 25 Mrd. CHF. Es soll darauf hingewiesen werden, dass unvorhergesehene Kosten – speziell im Tunnelbau – potentiell die Ausgaben bedeutend erhöhen könnten (ähnlich dem Gotthard-Basistunnel, wo das Budget um 50% erhöht werden musste). Zum Vergleich: Die Kosten für die geplanten Ausbauschritte 2025 und 2035 betragen zusammen ebenfalls ca. 20 Mrd. CHF [2, 3]. Diese Kosten sind zwar in der Tat immens, aber im Bereich des für Infrastrukturprojekte Realistischen und würden eine grundlegende Entscheidung wie damals für den Bau der AlpTransit darstellen. Grafik 4 zeigt eine Kostenaufschlüsselung für eine unterirdische Linie, welche ca. 40 Mill. CHF pro Kilometer für beide Richtungen beträgt.



Grafik 4: Relativer Beitrag zu den Infrastrukturkosten pro Komponente für eine unterirdische Lösung.

Die im Rahmen dieser Arbeit erstellten Prognosen sehen hohe Passagierzahlen auf einem potentiellen Netz Genf-Lausanne-Bern-Zürich vor. Faktoren wie Reisezeit, Einbindung der Stationen in bestehende Bahnhöfe und gute Zugänglichkeit spielen eine entscheidende Rolle.

In Bezug auf die Kapazität könnte das System die gesamte Stosszeiten-Nachfrage zwischen Zürich und Bern abdecken. Zweifel an der Kapazität von VT scheinen weitgehend unbegründet, da kein bedeutender Akteur mehr dem Konzept eines 28-Personen-Fahrzeugs folgt, wie es im Hyperloop Alpha Paper von Tesla und SpaceX [4] vorgeschlagen wurde. Die Vision hat sich zu

grösseren Fahrzeugen verschoben, insbesondere da die Fahrzeuglänge nur wenig Einfluss auf den aerodynamische Widerstand hat, was längere Fahrzeuge energieeffizienter macht.

Bei der konkreten Modellierung eines VT-Systems für die Schweiz wird deutlich, dass die ideale Systemkonfiguration und Kennzahlen eng miteinander verknüpft sind. Während der allgemeine europäische Konsens darin besteht, Hochgeschwindigkeitsweichen zu entwickeln, könnte dies für ein schweizerisches Netzwerk der projizierten Grösse aufgrund des umfangreichen Baus von Ab- und Auffahrten nicht notwendig sein. Es wird empfohlen, die Höchstgeschwindigkeit im Vergleich zu einem kontinentalen Netzwerk zu reduzieren, wobei eine Kombination aus Beschleunigung durch eine aktive Fahrbahn und Motor auf dem Fahrzeug für die Umweltauswirkungen optimal erscheint. Es zeigt sich auch eine extrem starke Abhängigkeit der Kennzahlen von der Netzwerktopologie, der Nachfrage pro Segment und den einzelnen Entfernungen. Es sollte daher festgehalten werden, dass die in dieser Studie präsentierten Ergebnisse nicht auf andere Netzwerke oder Betrachtungen übertragbar sind. Für das modellierte System scheinen Emissionen und Kosten unter ungefähr denselben Bedingungen minimiert zu werden.

Viele der wesentlichen Technologien für den Bau von VT bestehen bereits und haben einen Machbarkeitsnachweis durchlaufen. Die einflussreichsten Parameter bezüglich der Systemleistung hängen weniger stark von Technologieprognosen und mehr von Designentscheidungen, wie Geschwindigkeit, Beschleunigungsprofil und Betriebsdruck ab.

Limitierungen und Ausblick

In der technologischen Entwicklung sind diverse Fortschritte notwendig: Unter anderem sind v.a. Schwebesysteme entscheidend für die Effizienz von VT und müssen in grösserem Massstab gebaut und validiert werden. Die Idee eines vakuumversiegelten, leicht zu wartenden Tunnels, obwohl vielversprechend, wurde noch nicht unter realen Bedingungen getestet. Das Konzept eines solchen Tunnels ist nicht nur für die Schweiz, sondern auch für die breitere Einführung der VT-Technologie weltweit entscheidend und stellt eines der Schlüsselprodukte dar, welche entwickelt werden müssen. Thermische Batterien, die mit phasenwechselnden Materialien wie Wasser konzipiert wurden, befinden sich noch im theoretischen Stadium und erfordern praktische Entwicklung. Die in dieser Studie projizierten Effizienzen für Motoren müssen noch erreicht werden und sind entscheidend, damit das System die hier berechneten Kennzahlen erreicht.

Auch auf der Modellierungsseite gibt es Raum für Verbesserung: Die Übertragbarkeit von Leckageraten von Röhren auf Tunnel muss validiert werden. Das modellierte Schwebesystem, obwohl es auf aktueller Forschung basiert, basiert auf Simulationen und muss in der Realität validiert werden. Die Kühlung der Tunnel könnte einflussreicher sein als ursprünglich angenommen und möglicherweise den Energiebedarf für die Aufrechterhaltung des Vakuums überschreiten. Darüber hinaus ist die Vorhersage der Passagiernachfrage ein äusserst komplexer Bereich, wo Faktoren wie Ticketpreise, Governance und allgemeine wirtschaftliche Trends genauso eine Rolle spielen wie die modellierte Reisezeitabhängigkeit.

Bei der aerodynamischen Modellierung des Systems bleiben viele Herausforderungen bestehen. Der Druckwiderstand, den das Fahrzeug selbst im Vakuum erfährt, stellt einen wesentlichen Bestandteil des Energieverbrauchs dar. Zuverlässige Kennzahlen können nur mit detaillierten Simulationen der Luftwiderstandskräfte bestimmt. Die Rohmaterialvolumen, welche für den Bau der Beschleunigungsmotoren auf der Fahrbahn benötigt werden, basieren auf der Skalierung von kleinen Prototypen, welche in ihrer Genauigkeit in Frage gestellt werden kann. Sparsamere Designs der Röhre sowie eine vertiefte Berechnung der Schienenstärken könnten die geschätzten Bauemissionen erheblich reduzieren.

Es bestehen ungeklärte Punkte ausserhalb dieser Studie: In der Regulierung stellt sich eine entscheidende Frage: Sollen die Sicherheitsrichtlinien sich mehr an der intrinsischen Sicherheit von Flugzeugen orientieren, wo ein Ausfall um jeden Preis verhindert werden muss, oder eher an der von Eisenbahnen, welche eine regelmässige Evakuierung zulässt? In der laufenden Standardisierung durch die EU (JTC-20) und die ersten Sicherheitszertifizierungen durch den renommierten TÜV scheint es als ob weitgehend auf bestehenden Luftfahrt- und Eisenbahnmetriken aufgebaut werden könnte.

Zusammenfassung

Ein Framework wurde etabliert, um verschiedene Konfigurationen zu bewerten und grundlegende Konzeptfragen zu klären. Diese Methode kann in zukünftigen Forschungen weiter genutzt und erweitert werden. Die Einführung eines VT-Systems in der Schweiz könnte als wegweisendes Leuchtturmprojekt im Verkehr dienen, das an die Einführung von AlpTransit in den letzten Jahrzehnten erinnert. Selbst wenn VT nicht eingeführt wird in der Schweiz, könnte die Forschung und Entwicklung verwandter Technologien der Schweizer Industrie durch den Export von technologischem Know-how und innovativen Produkten zugutekommen. Obwohl die Kennzahlen des in dieser Studie beschriebenen Systems unter tatsächlichen Bedingungen noch nicht nachgewiesen wurden, unterstreichen die aktuellen Bemühungen wie die Gründung des European Hyperloop Centre [7] und Investitionen auf europäischer Ebene [8, 9] das starke wissenschaftliche und politische Interesse an der Technologie.

Es ist klar, dass weitere Forschung, Entwicklung und sorgfältige Abwägungen erforderlich sind, bevor ein solches System vollständig realisiert werden kann. Insgesamt legt die Studie nahe, dass ein VT-System effektiv die Geschwindigkeit eines Flugzeugs mit dem ökologischen Fussabdruck und der Kapazität eines Zuges bieten könnte; dies zu Kosten, die, obwohl beträchtlich, für Infrastrukturprojekte dieser Grösse durchaus im Bereich des Möglichen liegen. Die Einführung eines solchen Systems würde eine bedeutende, wachsende Lücke in den Verkehrsnetzen von morgen schliessen und könnte eine ergänzende Massnahme sein, die Kapazitätsentlastung, Redundanz und wettbewerbsfähige, verbraucher- und umweltfreundliche Lösungen für den zukünftigen Fernverkehr bietet.

Summary in French

La mise à disposition d'un réseau de transport public de grande qualité est un élément clé des standards de vie élevés en Suisse. Parallèlement, l'augmentation démographique et la croissance économique accroissent la demande en matière de transport. Face à l'urgence climatique grandissante, la réduction des émissions dans le secteur du transport devient impérative. En Suisse, ce secteur est responsable de près de 40% des émissions totales de CO₂ [1]. Il est donc clair que l'infrastructure de transport de demain devra répondre simultanément aux enjeux sociétaux et écologiques. De nouveaux moyens de transport, conjugués à des améliorations des infrastructures actuelles, sont indispensables.

Un train sous vide, voyageant à des vitesses similaires à celles des avions mais pour une empreinte écologique bien moindre, s'inscrit sur des distances allant de cent à mille kilomètres. C'est un système guidé qui, en lévitant magnétiquement dans un tube sous vide partiel, contourne les contraintes aérodynamiques et de friction propres au rail conventionnel. Il pourrait ainsi non seulement enrichir le réseau actuel par une nouvelle ligne à très grande vitesse, mais aussi rediriger une part importante des vols courts-courriers, gros émetteurs de CO₂, vers un mode de transport terrestre entièrement électrique. Toutefois, la vision prometteuse d'un transport sous vide ne pourra se concrétiser que si ses bénéfices pour la société surpassent ses coûts, qu'il s'agisse d'accessibilité, de capacité, de confort, de gain de temps ou d'impact écologique réduit.

Cette étude vise à évaluer la pertinence de l'intégration d'un train sous vide dans les infrastructures de transport suisses. Elle offre des estimations sur la consommation énergétique, l'impact environnemental, la capacité de transport, et le coût global. Notre approche permet une évaluation flexible en fonction des différents choix de conception. Les impacts environnementaux sont estimés à partir de la base de données ecoinvent, reconnue pour sa transparence et son utilisation tant dans le monde académique qu'industriel. La faisabilité et les implications d'une connexion au réseau électrique ont également été examinées.

L'objectif de ce travail est de dresser un bilan des impacts environnementaux et énergétiques d'un système Hyperloop viable, en privilégiant une vision globale plutôt qu'un examen détaillé de chaque composant. Chaque principe technologique évoqué est soit déjà en opération, soit à l'étude dans le secteur industriel ou académique. Ainsi, nous démontrons que la technologie actuelle se rapproche déjà des besoins d'un système de transport sous vide fonctionnel. De plus, au vu des avancées technologiques attendues et des évolutions dans le secteur de la construction, il est prévu que les systèmes de train sous vide soient construits avec une empreinte énergétique et écologique réduite dans un futur proche. Reste à voir si ces systèmes pourront fonctionner à l'échelle réelle selon les modalités présentées dans cette étude.

Résultats

Notre évaluation approfondie du cycle de vie révèle que l'impact environnemental du transport sous vide, en termes d'émissions de gaz à effet de serre et de consommation énergétique opérationnelle, est comparable à celui des trains conventionnels, comme illustré à la Fig. 5. Pour des configurations optimales, l'énergie opérationnelle pourrait atteindre seulement 0.075 kWh/pkm ou 8.5 gCO₂ par pkm en incluant l'infrastructure. Cependant, les émissions sont fortement influencées par le mix électrique. Notamment, la construction du tunnel (ou tube) représente à elle seule la moitié des émissions, la voie de guidage – comprenant des profils en aluminium et en acier pour la direction et la propulsion – étant le deuxième contributeur majeur. En termes d'impact environnemental, le système se comporte à l'inverse de l'aviation : la majeure partie des émissions provient de la construction de l'infrastructure, avec ensuite très peu d'émissions pendant son exploitation. L'aviation, en revanche, nécessite uniquement la construction des aéroports, mais provoque d'énormes émissions ultérieures pendant son exploitation.

Sur le plan financier, nos premières estimations indiquent un coût total situé entre 0,15 et 0,17 CHF par passager-kilomètre pour le réseau envisagé, soit approximativement 775-850 millions de CHF annuels. Environ 60% de ce coût provient des dépenses opérationnelles, telles que les salaires, l'électricité, etc. Ainsi, le transport sous vide se positionne entre l'aviation et le chemin de fer en termes de coûts. L'aviation est économiquement plus avantageuse grâce à l'absence d'infrastructure autre que les aéroports. Les atouts financiers du transport sous vide se manifestent notamment sur

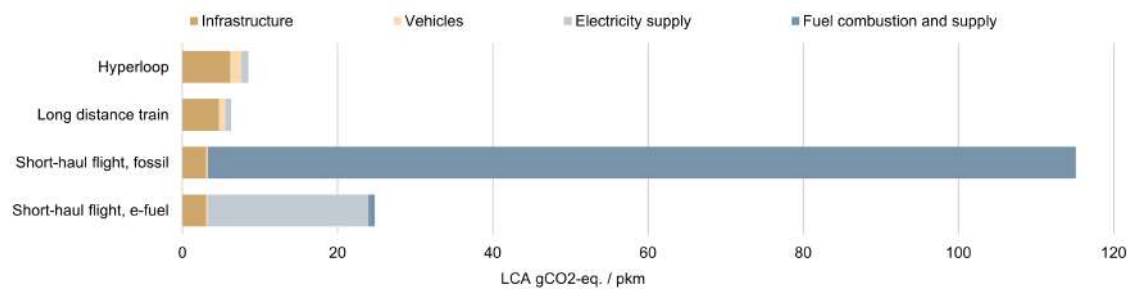


Figure 5: Comparaison des émissions spécifiques du cycle de vie par passager-kilomètre entre différents moyens de transport, réparties selon les principales sources d'émission. Exprimé en grammes d'équivalent CO₂ de potentiel de réchauffement.

les lignes à forte capacité, où l'importante infrastructure est justifiée face aux trains plus lents. De plus, le transport sous vide opère avec des véhicules plus petits (70-200 passagers) lui permettant une adaptation fine à la demande, assurant ainsi un taux de remplissage élevé. Si l'on prend en compte les avantages socio-économiques, tels que la diminution du temps de trajet et la réduction du bruit, on pourrait potentiellement réaliser des économies sociétales dépassant 500 millions de CHF par an.

Le coût de construction estimé pour un réseau Hyperloop en Suisse se situe entre 15 et 25 milliards de CHF. Il est important de souligner que des coûts imprévus, surtout pour des solutions souterraines, pourraient augmenter cette estimation, à l'instar du projet du Gothard dont le budget a augmenté de 50%. En comparaison, les améliorations planifiées pour le système ferroviaire, prévues pour 2025 et 2035, disposent d'un budget d'environ 20 milliards de CHF [2, 3]. Bien que conséquent, cela signifie que le coût d'un tel réseau de transport sous vide est envisageable et représenterait un investissement majeur, comparable à la construction du tunnel du Gothard.

La Fig. 6 montre la répartition des facteurs de coût dans la construction pour une solution entièrement souterraine, qui coûte un peu moins de 40 millions de CHF par kilomètre d'infrastructure à deux voies.

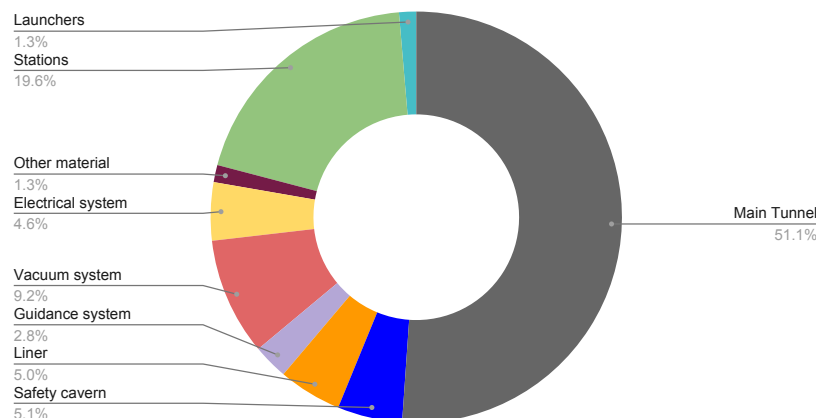


Figure 6: Contribution relative aux coûts d'infrastructure par composant pour une solution souterraine

D'ici 2050, les projections pour la ligne Genève-Lausanne-Berne-Zurich indiquent une forte demande de passagers, où le transport sous vide est bien placé pour capter une part de marché importante. Des éléments tels que le temps de trajet, l'emplacement des stations et l'optimisation des processus jouent un rôle crucial dans les choix des passagers. Le positionnement stratégique des stations est essentiel pour assurer l'accessibilité.

En termes de capacité, le système serait en mesure de répondre à la demande de pointe entre Zurich et Berne. Les doutes sur la capacité de transport sous vide semblent largement infondés, étant donné qu'aucun acteur majeur ne suit plus le concept de véhicule de 28 personnes suggéré dans

le document Hyperloop Alpha de Tesla et SpaceX [4]. La vision s'est orientée vers des véhicules plus grands, surtout depuis que la traînée aérodynamique dépend peu de la longueur du véhicule, rendant les véhicules plus longs plus écoénergétiques.

Lors de l'adaptation d'un système Hyperloop pour la Suisse, il est évident que la configuration idéale du système et ses performances sont étroitement liées. Bien que le consensus général soit de développer des commutateurs à grande vitesse, pour un réseau suisse de la taille projetée, cela pourrait ne pas être aussi avantageux en raison des importantes constructions nécessaires pour les voies d'accès et de sortie. De manière intéressante, il est recommandé de réduire la vitesse maximale par rapport à un réseau continental, avec une combinaison d'accélération côté voie et côté capsule qui semble optimale pour l'impact environnemental. L'application des résultats généraux pour le transport sous vide montre également la très forte dépendance des performances au réseau, à la demande par segment et aux distances. Il est donc important de comprendre que les résultats présentés dans cette étude ne sont pas directement généralisables à d'autres contextes ou applications. Pour le système suisse spécifiquement modélisé, il semble que les émissions et les coûts soient minimisés pour des conditions approximativement identiques.

Sur le plan technologique, de nombreuses technologies essentielles à la construction d'un système de transport sous vide existent déjà et ont été testées. Les paramètres les plus influents concernant la performance du système sont moins liés aux prédictions technologiques qu'aux choix de conception, tels que la vitesse, les profils d'accélération et les pressions de fonctionnement.

Limitations et Perspectives

Des opportunités d'amélioration ont été identifiées, tant en termes de techniques de modélisation qu'en termes de développement technologique.

D'un point de vue purement technique, les systèmes de lévitation sont essentiels pour le fonctionnement d'un transport sous vide et doivent être construits et validés à une plus grande échelle. L'idée d'un tunnel étanche au vide et facile à entretenir, bien que prometteuse, n'a pas été testée dans des conditions réelles. Son succès est crucial non seulement pour la Suisse, mais aussi pour l'adoption plus large de la technologie à l'échelle mondiale, et pourrait être l'un des produits clés à développer. Les batteries thermiques, conceptualisées en utilisant des matériaux à changement de phase comme l'eau, sont encore au stade théorique et nécessitent un développement pratique. Les rendements projetés pour les moteurs dans cette étude doivent encore être atteints et sont essentiels pour que le système atteigne les performances suggérées.

Du côté de la modélisation, des zones d'ombre persistent. Par exemple, il reste à déterminer si les taux de fuite d'air observés pour les systèmes en surface peuvent être transposés aux tunnels souterrains. De plus, même si le système de lévitation est basé sur des recherches actuelles, il pourrait se heurter à des défis inattendus lors de son déploiement à grande échelle.

Disclaimer

The report presents a first-order estimate for one specific, envisioned type of vacuum transport system. It must be read in its entirety, and it is necessary for the readers to be aware of the underlying assumptions. Results might be inaccurate when not used in the full context of the work. It shall be clear that any significant development in technology or change of assumption can substantially alter the results of this study. It shall hereby be clearly stated that this work examines **one of many** potential vacuum transport-like systems and was done to the best of the authors' knowledge. It does not represent a design or recommendation, which was neither part of nor within the scope of the project. In practical applications, it is essential to understand that relying on a single number from this report may not yield accurate results. We recommend a comprehensive review and potential redesign for real-world implementation. To take decision of a construction more extensive feasibility on specific route would need to be realised.

1 Initial situation

Vacuum transport (VT) is a concept proposed first in the late 18th century [10] and made popular again at the beginning of the 2010s under the term 'hyperloop'. In this study, we use the terms 'hyperloop' and 'vacuum transport' interchangeably. While they refer to a system featuring reduced air pressure and magnetic levitation, it is important to note that these systems do not adhere to a fixed set of parameters. They can vary in aspects like speed, propulsion mechanisms, and other specifications, and are not confined to any specific benchmarks. The vision of hyperloop consists of vehicles levitating in a tube with reduced air pressure, which enables fully electric ground transport at a speed up to that of planes, opening a potential addition to the existing transport infrastructure. With hyperloop, the travelling distances between Zurich and Berlin would shrink to a mere 48 minutes.

1.1 Why hyperloop now?

Apart from the appealing, futuristic vision and reduction in travel time, there are strong reasons that advocate for the introduction of a hyperloop infrastructure now.

1.1.1 The predicted future of transport

The combination of population growth and economic expansion will inevitably lead to a higher demand for transport, i.e. more and faster passenger kilometres (pkm) will have to be served by some sort of infrastructure [11, 12]. At the same time, an even more rapid climate change is starting to show its alarming impact on human activity and the need to reduce emissions of the transport sector is as imperative as ever [13]. This reduction can either come from less movement or from smarter ways of transporting people and goods: plausibly, it will result from a combination of both. Among other goals, hyperloop aims at reducing the volume of short-haul or domestic flights as they entail much higher emissions per flown passenger-kilometre than long-distance flights or any other competitive mode (see section 5.3 for benchmarking).

1.1.2 Future options for transport

Short-haul and local transport has seen extensive innovation in recent years. Electric cars have started diffusing in the car fleets of all developed countries [14]. Even though further efforts are needed, the technological alternatives are proven. The situation is more complex for long-haul transport, where the physical characteristics of fossil fuels - energy and power densities and the ease of storage - prove to be more challenging to replace. The typical example is aviation, where the combined speed (hence power) and range (hence energy) requirements can only be met by chemical fuels combusted in gas turbines. This is why the major pathway pursued for its decarbonization entails the employment of sustainable aviation fuels (SAF), i.e. chemical energy carriers of biogenic, solar or synthetic origin [15]. But the situation is not easier on the ground, where the weight and range requirements of trucks represent indeed a challenge in their direct electrification [16]. Railway is often presented as the best alternative mode of ground transport and, depending on the electricity mix and ridership rate, it may carry goods and passengers with the minimum environmental footprint [17–19]. However, railway suffers from tight capacity constraints and the expansion of its throughput or the introduction of high-speed services often entail the construction of new lines [20] with significant landscape and environmental footprint. If additional capacity - at higher speeds - is required, the question is whether conventional modes of transport could provide it or whether alternatives should be considered.

1.1.3 The potential of hyperloop

Most likely, the aforementioned modes of transport will complement each other to build tomorrow's transport system: an extension of the current rail network in Europe is unavoidable, and intercontinental connections are unlikely to be connected on ground-based, sustainable and even moderately fast modes. However, hyperloop comes with certain characteristics that justify the inclusion of the hyperloop into the transport landscape of tomorrow.

- Speed regimes: A major limitation of the railway network is that it is used by trains of various speed regimes. To increase capacity, disentanglement of the infrastructure for fast (long-distance) and slow (local) modes of transport is necessary, as also mentioned in the *Perspektive Bahn 2050* report by the Federal Office of Transport (FOT) [22]. This means that

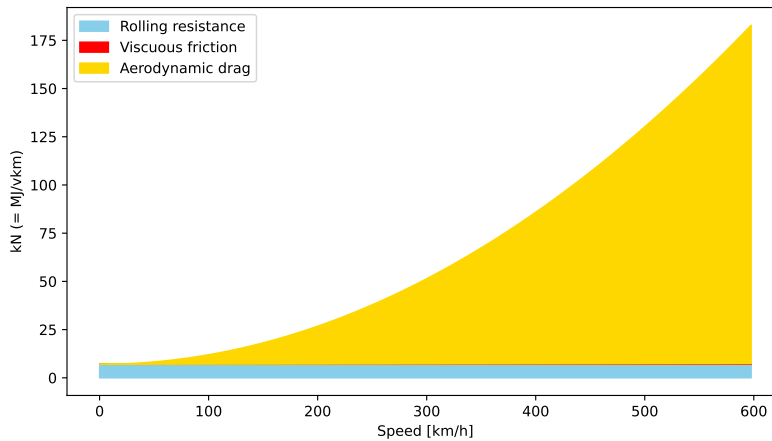


Figure 7: Breakdown of resistive forces acting on a train at constant speed. Based on TGV measurements [21].

new routes eventually have to be constructed to increase the volume of transported passengers. Compared to high-speed railway (HSR), hyperloop, however, has the potential to run at more than twice the speed of the most advanced HSR trains with a similar environmental footprint (see section 5.3).

- **Aerodynamic drag:** Magnetic levitation trains (such as the Transrapid) allow for much higher speeds and almost no wear and tear due to the absence of any contact between the vehicle and the track. However, as depicted in Fig. 7, the major share of the energy consumption for an HSR is aerodynamic drag, increasing with the square of the train speed [21]. A magnetically levitating train has the above-mentioned advantages but still has to overcome the substantial drag forces while requiring a fully dedicated track. Hyperloop addresses exactly this issue by mitigating to a high extent the remaining drag. Even though this comes at a certain cost both economically and in terms of power and energy management, the results in Chapter 4.4 show that the overall savings in energy and emissions are remarkable.
- **Saturation of current networks:** Airports are reaching their saturation point in terms of volume [23, 24]. Since an extension of the airport infrastructure in the context of climate change is somewhat inadequate in the near future, the addition of hyperloop to the aviation network could provide additional capacities. Furthermore, connecting cities at the speed of an aeroplane might therefore shift large parts of the short-haul flight volume to hyperloop, reducing emissions there and creating capacity for long-haul SAF flights.
- **Issues with sustainable alternatives:** Most of the SAFs planned to be blended in the short- and medium-term are of biogenic origin, but their larger employment is limited by the competition with other sectors for the available sustainable biomass feedstock, specifically with the current trends of farmable land reduction and population growth.[15]. As for power-to-liquid (PtL) synthetic fuels, there has been progress with the establishment of pilot plants and proof of concepts, but the overall production pathway remains at a prototypical phase [25] and the massive investments required to scale up this new fuel supply chain are still lacking [26]. In addition, the low well-to-tank efficiency of PtL fuels implies that the (renewable) electricity required to fly on SAFs will always highly exceed the direct use of electricity in a hyperloop system. Thus, even in fossil-free aviation, the energy consumption per passenger-kilometre on short-haul flights will be substantially larger than in hyperloop. Finally, non-CO2 climate forcers related to aviation (primarily contrail cirrus) would also not necessarily be abated with SAFs [27] and are generally estimated to contribute up to two thirds of the effective radiative forcing of aviation [28].

1.1.4 Financial situation

Hyperloop is a large-scale infrastructure and comes with a correspondingly high investment price tag. Even though reliable estimates for the construction cost of hyperloop lines are still to be confirmed (and if underground, they are strongly dependent on local geology), it is clear that cost figures for an entire European network will be in the three-digit billion range. However, already now the financial means invested in hyperloop on a European level are remarkable. In Northern

Italy, an 800 mill. EUR tender for the construction of a first freight hyperloop track has been published [29]. Similarly, both the private companies Hardt and Nevomo have raised money for their research and development activities in the double-digit million order. Furthermore, Europe is currently at a stage where substantial investments into transport infrastructure have to be made: Fig. 8 shows the split in billions of EUR of the forecasted investment needs for the time horizon of 2050. Investments in hyperloop in the order of a tenth of the share allocated for the rail would allow building of the first hyperloop network in Europe connecting ten cities, according to the most recent transport simulations conducted at EuroTube. According to a report by a consortium of the major hyperloop players in Europe [30], a full European network is supposed to be within reach for roughly one trillion EUR (not including any development cost). In short, this means that the financial volume needed to construct a hyperloop network is, in infrastructure dimensions, within the magnitude of already predicted investments.

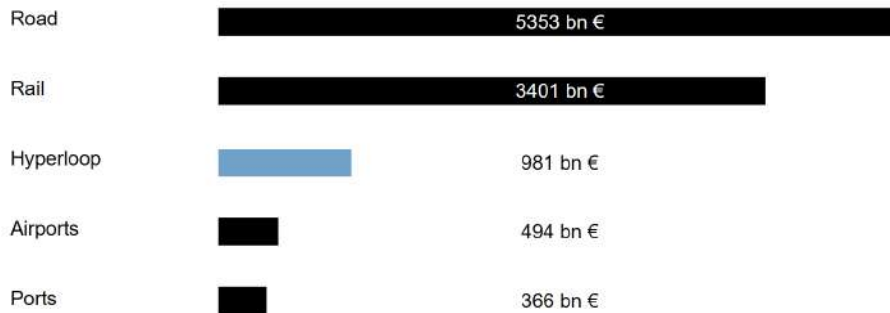


Figure 8: Total forecasted infrastructure investment needs by mode, from 2022 to 2050. Note: Estimates are based on a linear extrapolation of G20 investment requirement projections from 2017 to 2040 [31].

1.1.5 Switzerland’s role in pioneering transport technologies

- Swissmetro:** Switzerland has always been at the forefront of hyperloop-like developments, mainly through the Swissmetro project, which used many concepts of hyperloop, adapted to a network limited to Switzerland. Despite a rejection of the concession to build a Geneva-Lausanne line, it was clear within the FOT back in 1997 that the decision whether to build the first segment of Swissmetro does not decide on the future of the technology [32]. This means that there was no fundamental concern or political unwillingness toward the intrinsic idea of Swissmetro. Back in 1997, being a Swiss initiative with technology that was about to become ready, Swissmetro was primarily lacking a European business case and had to compete on a national level for funding with the AlpTransit and Bahn 2000. It is important to stress that Swissmetro therefore should not be considered a failure but a concept ahead of its time and unlucky in terms of timing since the spot of the next lighthouse project (AlpTransit) was already occupied. With the current Europe-wide hyperloop movement, the starting conditions and timing for an improved version of the idea are much more promising. The consideration of potential new visionary infrastructure projects is also arguably better timed in light of the ambitious climate targets urgently needed. It is therefore somewhat comprehensible that the completion of the large other infrastructure projects were prioritised at the time, and that now the concept of a high-speed underground transport system has reached the time to be reconsidered again.
- Cargo sous terrain (CST):** In the specific case of Switzerland, a large-scale underground cargo infrastructure is in planning. However, it is important to understand the differences between a system implemented in CST and a hyperloop. CST aims at distributing goods only and operates neither in a vacuum nor at high speeds, which is well sufficient for most goods in a domestic market (in the case of a comparatively small country like Switzerland). The benefit of the speed of the hyperloop is mainly created for passengers. In the Swiss case, a pure freight use case for hyperloop is indeed questionable. However, in light of the accelerated growth of e-commerce and the international cargo demand surge during COVID-19, transporting goods on a hyperloop can substantially improve the capacities of the already existing infrastructure and simplify the transport of urgent goods. Furthermore, on distances larger than several hundred kilometres, a system like CST can become unfeasible. Therefore, CST and hyperloop are neither comparable nor competing but complement each other in

the creation of tomorrow's transport infrastructure at both a transnational and continental level.

2 Objectives of the work

This study shall serve as a potential analysis of vacuum transport technologies in the public transport infrastructure of Switzerland, and give estimates for key performance indicators (KPIs) in life-cycle assessment and energy consumption of such a potential future infrastructure. An estimate for cost shall also be given.

It is apparent that in the context of climate change new infrastructure has to, on top of other substantial improvements, be able to compete with current standards in terms of environmental footprint. While various concepts and technical solutions are being introduced, the primary objective is to suggest one (of many possible) functional hyperloop system and evaluate its energy consumption and environmental impact. This means that in this work the main focus was set on investigating the features, technical components and characteristics of hyperloop that most strongly influence energy consumption and environmental impact. This means that some aspects were known *a priori* to be of large significance and have been thus refined; some others were identified along the way as key factors and, consequently, might be investigated in further technical studies.

The second criterion to determine the focus of the work was the achievability of results within the scope of the project: for example, drag is a major contribution of energy consumption and has been modelled accordingly. Nevertheless, possible aerodynamic effects such as shock waves have to be evaluated by highly specialised experts with access to extensive computation resources, which would entail an entirely independent research project.

3 Approach and current state of knowledge

3.1 Overview of the hyperloop system

Fig. 9 shows an overview of the different parts of a hyperloop system from a functional perspective, outlining the key elements that are contained, independent of the specific technical design. There are three main physical subsystems and a more abstract one related to the management of the whole system, as described below:

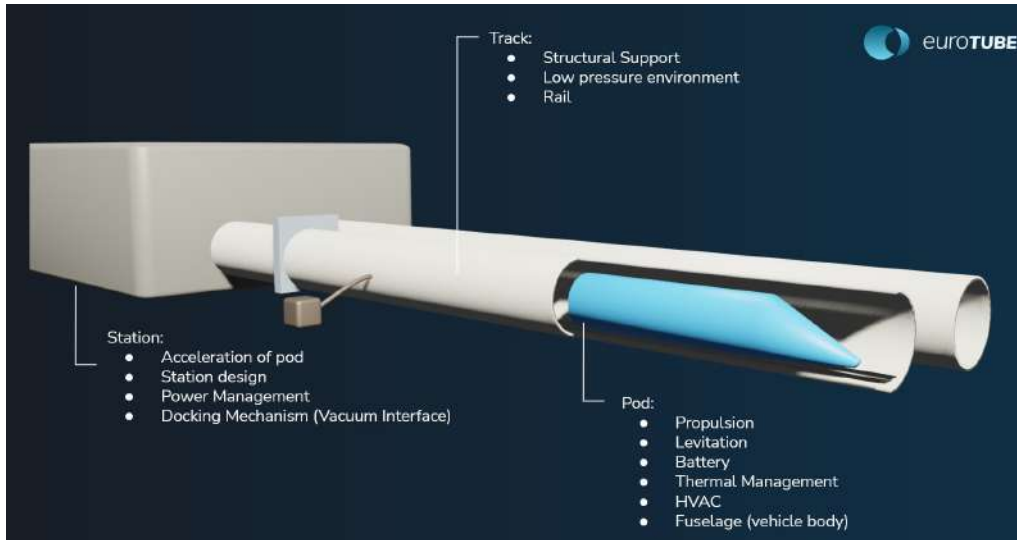


Figure 9: Essential subsystems with the corresponding components included in a hyperloop system.

Track

Since the hyperloop aims to achieve high cruise speed through reduced aerodynamic drag compared to conventional rail, the hyperloop vehicle (referred to as “pod”) travels in a tube that provides a low-pressure environment. The tube itself serves as the main structural component, which can be either above ground, supported by consecutive piles like a viaduct, or underground as a tunnel. The vehicle is guided along the tube by a rail, which can be mechanical or consist of magnetic systems. In this study, the rail is often referred to as the combination of levitation and guidance parts of the track. The low-pressure environment is commonly referred to as “vacuum”, although there is a residual pressure present (usually between 1 and 100 mbar, design-dependent). Achieving this pressure level involves a main pump-down procedure and then maintaining it via insulating materials in and around the tube, along with additional pumping for leakages. Fig. 10 shows the different pressure regimes at which key players in the hyperloop plan to operate.

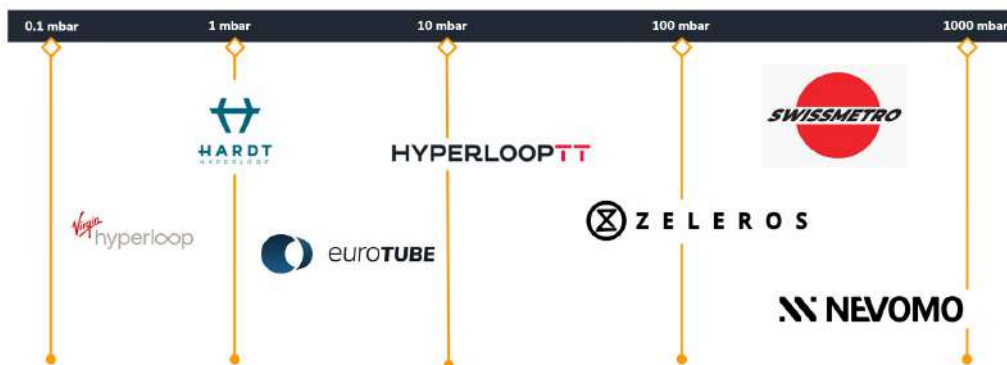


Figure 10: Envisaged pressure regimes of key players in the hyperloop field.

Pod

Since one of the main advantages of hyperloop is its high cruise speed, a mechanism needs to be provided to accelerate the vehicle to its maximum speed within a reasonable time. Even at top speed, propulsion is still needed to counteract resisting forces that slow down the pod. Another significant difference between hyperloop and conventional trains is that there is no contact

with the track, and the vehicle levitates, allowing for higher speed and minimal wear and tear of the guideway material. As a result, a cooling mechanism for various heat sources and an HVAC (Heating, Ventilation, and Air Conditioning) system to ensure passenger comfort and safety are necessary.

Station

Stations have two main functions:

- Like conventional railways, they serve as boarding points for passengers. However, unlike railways, they also serve as interfaces between the atmospheric environment where passengers wait to board the vehicles and the vacuum tubes where the pods travel at high speeds. Different technological options for stations are available and discussed in section 3.5.4.
- Depending on the propulsion strategy (track-side or vehicle-side), stations may also be responsible for refuelling or recharging the vehicles. The management of power flows for charging and/or accelerating the vehicles becomes crucial in such cases. Additionally, stations function as refuelling stations for heat removal systems and HVAC, providing additional oxygen, etc.

Traffic management and safety

In this study, we also look at hyperloop to be used in a network rather than only as point-to-point connection (i.e. only single lines). Therefore, a switch concept is required, which is different for levitating vehicles compared to conventional rail. A bypass and venting system is suggested to allow access in and out of the tube in cases of traffic disruption and emergencies. Maintenance access also needs to be ensured. It is however an ongoing discussion in the field, whether or not bypasses shall be a feature or not.

In section 3.5, we will qualitatively outline the technological concepts used in the model presented in this report. We will also briefly assess key concepts essential to the feasibility of hyperloop from a qualitative and technological point of view. Below is stated a brief distinction of what is considered crucial to be modelled within this study and what was either outside the scope of the project from an achievability point of view or since there are valid reasons to consider them non-crucial and solvable in the future.

Not in focus

- Pod:
 - Fuselage: Aeroplanes and aerospace have shown that fuselage for the most adverse conditions can be developed, and several hyperloop companies are already investing in fuselage development.
 - Exact shape of pod: Placement of components and the exact shape of the pod were not studied since they are determined by numerous successive optimisations and depend on the technology. The same holds for the placement of inner components to some extent.
 - HVAC: Providing breathable cabin air in a vacuum is a non-trivial challenge. However, concepts exist (such as in submarines) and the energy consumption, given that vacuum and heat for desorbing scrubbers are already onboard, is negligible. A device specifically designed for hyperloop can then later be developed in an industry project.
 - Magnetic lateral guidance: If a levitation mechanism can be provided, it is clear that, in the simplest case, the same physical concept can be used to guide the vehicle between lateral guidance structures. The required forces in bends are in the order of 0.1 g, so the guidance system weight and energy consumption will be significantly lower compared to levitation and are thus not modelled in detail.
- Station:
 - Layout: The size and space needed for a station are included in the LCA (Life Cycle Assessment), and exact designs and processes depend strongly on the final technology and mainly local conditions.
 - Switch: A proof of concept has to be provided since it is an integral part of any network to allow for switching at full speed. As it will turn out, for very small networks this might not be required after all. However, any detailed design is not important to the energy consumption and environmental footprint.

Essential

- Pod:
 - Power densities: For levitation and propulsion, it is critical to estimate how much power can be provided by how much weight.
 - Energy densities: Similarly, for batteries and cooling systems, a “weight runaway” (positive feedback loop in weight increase) has to be avoided.
 - Diameter: The blockage ratio of the pod (section area of pod compared to tube) strongly influences the aerodynamic drag, power needed, motor size, and weight.
 - Levitation: The weight of the vehicle strongly affects the size of the levitation system. The levitation system is critical in three technical parameters: how much power per lift is consumed, how heavy the system itself is (lift-to-weight ratio), and how much drag is created by the physical phenomenon used for levitation. If these three characteristics are known, the energy consumption and emission impact can be determined. A detailed design of the system is not within the scope or part of the project.
 - Propulsion: Similarly, to fulfil the feasibility analysis, a detailed motor design is unnecessary as long as the achievable power density and energy consumption can be estimated.
- Track:
 - Vacuum Assurance: This is the second key concept of hyperloop and includes a full pumping system layout. Therefore, it needs an accurate model and adequate planning. For this study, a value measured in the laboratories of EuroTube is used (see 6). Due to its importance, leakage values are another example of a quantity that is investigated in separate ongoing research projects to be refined.
- Station:
 - Track-side acceleration: Estimations of the motor’s efficiency and its material composition are necessary since, for moderate accelerations, the track-side acceleration will be several kilometres long and thus relatively emission-intensive during production.
 - Airlock: The detailed layout and number of airlocks are not critical to the feasibility. The energy consumption was evaluated as it directly influences the environmental footprint.
 - Time: Total dwell time in the station is of some significance since it determines the number of pods needed to serve a certain capacity.

3.2 Overview of methodology

This section presents the general methodological workflow employed in the study. The project encompasses multiple modules, which range from the prediction of passenger demand to the estimation of the system energy consumption. Fig. 11 details how the different modules are interconnected.

The first step is the high-level design of all parts of the system, from the vehicles to the track. This step is detailed in section 3.5 and is the prerequisite to all subsequent modules, as the size of the components is a pivotal information to derive the KPIs of the system such as costs and environmental impact (see sections 3.7 and 3.8). Part of the design definition is also the description of the system’s operation, including the overall speed profile of the vehicle journey. This directly affects the total travel time between the hyperloop destinations, which, as explained in section 3.3, is the main mode choice criterion used to estimate passenger demand flow. In turn, the total passenger flux is used in conjunction with other operational requirements such as the headway between vehicles to estimate the recommended pod size and thus the total fleet size (see section 3.4.1).

Ideally, all these modules would belong to the same top-down model where the system design would be optimised to maximise or minimise some of the KPIs. However, such a model would be extremely complex and computationally expensive due to the many non-linearities linking the different parts of the system. Furthermore, it would be cumbersome to investigate the dependencies of smaller parts of the system separately. The opposite alternative would be to perform a bottom-up construction of the system, where the various parts are individually designed. But the hyperloop technology is a highly complex and interconnected system and it would thus be impossible to freely set all aspects of the infrastructure without giving rise to design and physical conflicts [33].

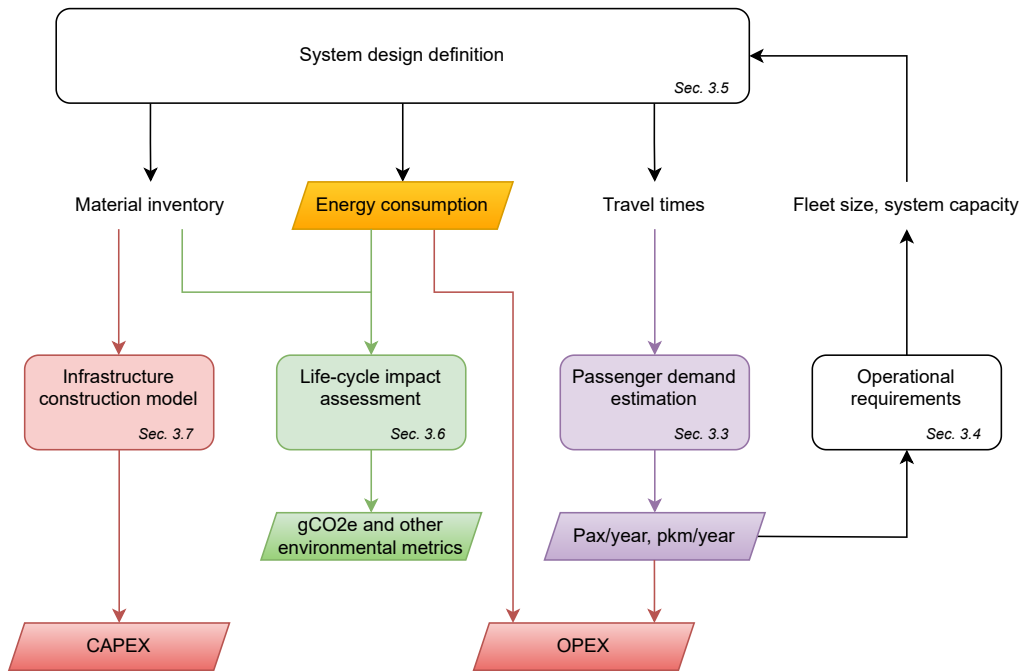


Figure 11: Schematic relations between the different modules of the study. Each module is explained in the given section and the quantities in the parallelograms are the main KPIs of this study.

This project follows a hybrid approach, where the number of modelled inter-dependencies has been reduced to the minimum necessary for a coherent design, but no overarching optimisation is automatically performed. To quantify the impact of a design or operational change, the input to the corresponding module is modified and the downstream flow of Fig. 11 is then followed to derive the KPIs. However, inside each module, the simulation is kept as implicit and coherent as possible. This is especially important for the vehicle design within the system definition and the actual modelling tool is explained in section 3.6. The overall approach allows for numerically efficient simulations and the possibility of exploring a large range of functional system designs.

This exploratory evaluation of KPIs for given input changes conflicts with the fleet sizing feedback introduced in Fig. 11. As section 5.2.1 will show, a few heuristic iterations have first been performed to circumscribe the likely size and specification of the fleet. Then, the fleet specifications have been frozen and the travel frequency has been used as the sole output feature to absorb changes in traffic volumes. In this way the feedback loop of Fig. 11 could be neglected when deriving KPIs for a wide range of inputs. Most of the results presented in section 5 employ the fleet and system specifications obtained after these fleet-sizing iterations¹.

3.3 Passenger demand model

3.3.1 Data declaration

The estimate of future hyperloop passengers in 2050 is based on comprehensive data that incorporates passengers' current travel patterns using various transport modes, such as public transport, private cars, and aviation.

The data utilised in this study originate from the NPVM 2017 (Nationales Personenverkehrsmodell) [34], an open-source data set published by the Swiss Office for Spatial Development (Bundesamt für Raumentwicklung ARE). The NPVM divides Switzerland into 8,000 zones (shown in Fig. 12) and provides information on approximately 60 million passenger origin-destination (OD) pairs. NPVM data also shows the average travel time for each OD by using public transport and private vehicles.

According to the NPVM data, there is an average of 4 million weekday passengers utilising public transport throughout Switzerland in 2017. As for private vehicles, the data indicate an average of 10.87 million weekday passengers.

¹Only a few results refer to systems that predate the implementation of these feedback loops and the detail specifications are provided when this is the case. But the associated learnings are nevertheless valuable and applicable to the actual final system.

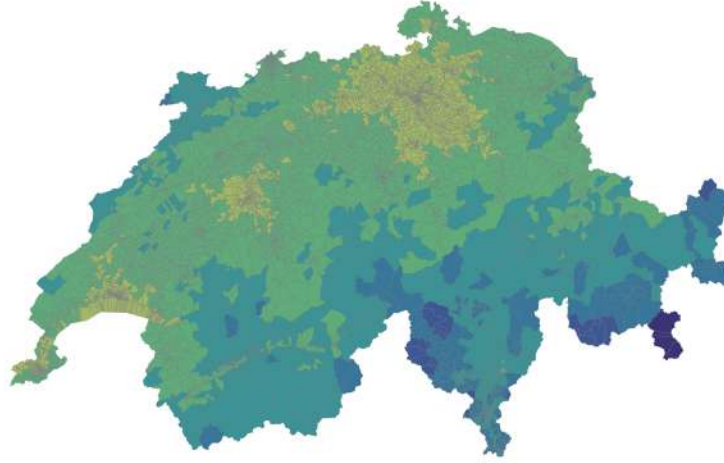


Figure 12: Zones of Switzerland in NPVM 2017.

To calibrate the number of car users, the study relies on the MZMV (Mikrozensus Mobilität und Verkehr) data [35] published by the Federal Statistical Office (Bundesamt für Statistik) in Switzerland. The MZMV data report 5.87 billion passengers in the year 2017, which is approximately 1.48 times higher than the corresponding data in NPVM. Consequently, the number of car users in each OD pair in NPVM is adjusted by a factor of 1.48 to match the MZMV calibration.

For the aviation data, Eurostat [36] is the primary source used in the study. This data specifically help estimate the number of passengers currently travelling between Zurich and Geneva by air. The intention is to assess how many of these air passengers might potentially shift to using the hyperloop system in the future.

3.3.2 Passenger simulation model

The passenger simulation model primarily relies on determining the fastest travel time from the passenger's origin to their destination. This involves comparing travel times on various routes for each OD pair, considering both current transport modes (public transport or private cars) and potential hyperloop routes, depending on the selected hyperloop stations.

The hyperloop route consists of five key components:

- Access to the hyperloop station: This part involves calculating the travel time from the passenger's origin to the entrance station of the hyperloop using public transport and private vehicles.
- Transit time at the entrance station: The model takes into account the time required for passengers to transit at the entrance station of the hyperloop before boarding the hyperloop pod.
- On-Route time of hyperloop: Once passengers are on board, the model calculates the time taken to travel between the selected hyperloop stations, representing the on-route time of the hyperloop journey.
- Transit time at the exit station: Upon reaching the destination hyperloop station, the model considers the time needed for passengers to transit and leave the hyperloop system.
- Final leg to destination: Finally, the model calculates the time from the destination hyperloop station to the passenger's actual destination using public transport or private cars.

By integrating these five components, the passenger simulation model can assess the total travel time for each potential route, whether it involves current transport modes or the hyperloop system. This enables a comprehensive comparison of travel times and allows passengers to make informed decisions about the most time-efficient route for their journey.

Once the fastest route for each OD pair is determined using the passenger simulation model, all passengers are assigned to this optimal route. This means that each OD pair's passenger demand is entirely allocated to the corresponding fastest route. By performing this assignment process, we can calculate the total number of passengers utilising specific hyperloop routes and aggregate

the passenger numbers for each hyperloop segment. This approach allows us to assess the demand and popularity of various hyperloop segments, understanding the distribution of passenger flow along the studied hyperloop line. More details of the calibration of this simulation model are in Appendix A.

3.3.3 Traffic extrapolation to 2050

To correctly size the hyperloop system the passenger flows derived in the previous section are extrapolated to 2050. This is done according to the Federal estimates of the “*Verkehrsperspektiven 2050*” [37]. According to the “Basis” scenario, between 2017 and 2050 the annual passenger kilometres by rail and road will increase by the following percentages:

| | |
|----------------------------------|--------|
| Relative pkm increase 2017–2050: | |
| Passenger cars | +2.9% |
| Railways | +33.0% |

These factors are used to scale the passenger flows respectively captured from road and railway.

In addition to the passenger traffic by road and rail modelled in the previous section, it is expected that the proposed Swiss hyperloop line would entirely absorb also the domestic flight demand between Zurich and Geneva. According to Eurostat, in 2019, 629’200 passengers flew between the two Swiss cities [36]. To extrapolate this traffic to 2050, the “Global Market Forecast” by Airbus is used, which predicts an annual compound growth of 1.5% until 2042 [38]. For this study the same growth is assumed until 2050, resulting in a total increase of +58.7% between 2019 and 2050.

3.4 Operational requirements and fleet sizing

3.4.1 Rush hour and fleet sizing

The model introduced in the previous section returns the expected daily traffic demand by hyperloop between all Swiss stops. This section uses this information to characterise how the system would operate and determine the optimal vehicle size. The following assumptions are made:

- In a first step, pods travel end-to-end without intermediate stops: this makes especially sense considering the high speeds that characterise the investigated transport system. With lower speeds the option with intermediate stops could also be investigated, as will be done in section 5. The end-to-end model is also enabled by the relatively short distances of the considered network: the range of hyperloop vehicles is not unlimited and with a larger hyperloop network a “hub” model would rather be envisioned, where major cities turning into necessary stops within the network.
- Passengers taking hyperloop would always opt for the direct connection, avoiding changing vehicle in an intermediate stop. This follows from the idea that the travel frequency on any route is high enough to never make the option with change convenient. As in the first assumption, this is possible thanks to the “small” Swiss network, but in a larger system, passengers would likely be forced to change vehicle in the central hub stations.
- Each pod is assigned to a single route, i.e. it travels back and forth between the same two destinations: This is a model simplification that follows from the first assumption, but that is also coherent with the end-to-end model as each route has different vehicle requirements, especially range and capacity.
- Each route is assigned a unique vehicle model: this follows from the fact that each route will have its own requirements, but for the sake of simplicity there is no need to introduce hybrid fleets within any route.

From these assumptions the traffic flow on each route can be directly related to a certain vehicle size and a frequency of travel. However, the traffic flow is not constant during the day and the rush hour demand should be used to determine the correct vehicle size. To derive the rush hour traffic on hyperloop we derive what would have been the rush hour by rail and car, and then determined the share of passenger traffic that shifted mode to hyperloop. In addition, while the traffic values from section 5.1 refer to the *average daily* demand, the rush hour traffic should be evaluated on a *working day*.

Fig. 13 shows the hourly distributions of passenger traffic by car and rail on an *average working day* (Mon-Fri), normalised to the total traffic during an *average day* of the year (being this the output from the passenger demand model). This means that the sum of the columns exceeds 100% (as weekdays typically entail more movements than weekends), but the highest values can be used to directly derive the maximum hourly traffic from the average daily traffic. In the figure railway displays a profile concentrated around commuting hours, while car mobility is more evenly distributed during the day; however, in both cases, the rush hour traffic occurs at 5 p.m. The rush hour passenger demand on hyperloop can thus be taken as about 12% of the daily traffic captured from railway plus 9% of the daily traffic shifted from cars.

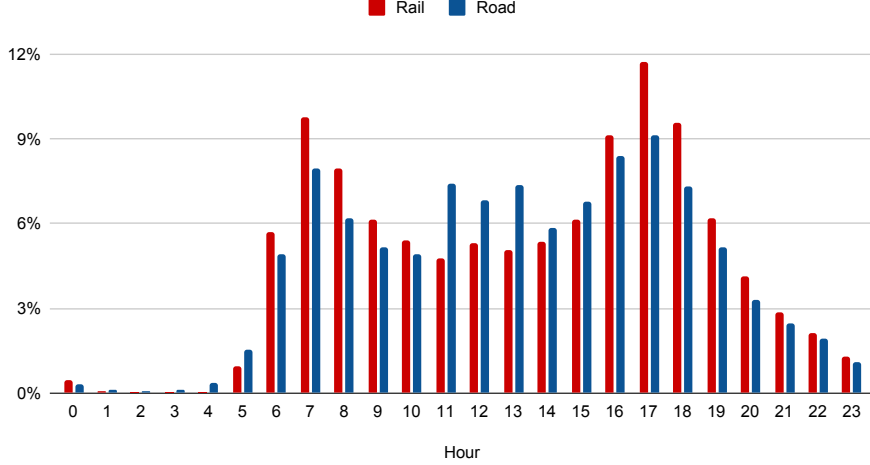


Figure 13: Hourly distribution of passenger traffic by car and by train. The distributions refer to an *average working day* but are normalised with respect to the total traffic of an *average day* of the year. The sum of the columns thus slightly exceeds 100%.

For a given hourly passenger demand Q , the recommended vehicle size S_{pod} can be simply estimated as a function of the desired headway (time between vehicles) $\Delta t_{headway}$:

$$Q_{max} [\text{pax/h}] = \frac{3600 \cdot S_{pod} [\text{seats}]}{\Delta t_{headway} [\text{s}]} \quad (1)$$

where $\Delta t_{headway}$ is the time gap between the fronts of two consecutive vehicles travelling in the same direction. Headway is typically sized based on emergency braking considerations. Considering a simple safety factor k and a latency time $\Delta t_{latency}$ between first signal of intervention and brakes activation, headway and braking rate $a_{em. brake}$ are related through the following equation:

$$\Delta t_{headway} = \Delta t_{latency} + \frac{L_{pod}}{v_{cruise}} + k \cdot \frac{v_{cruise}}{2 \cdot a_{em. brake}} \quad (2)$$

Fig. 14 shows the typical relationship between headway, passenger flow and braking rate based on equations 1,2 for typical system settings².

For reference, emergency braking rates of 2.5 – 5 m/s² are common in railways [39] as well as in aviation [40]. This means that pods with a capacity of 70 passengers can unlock throughput capacities of 3'000 - 6'000 pax/h per direction and with 200 passengers per vehicle the maximum capacity stretches to 17'000 pax/h per direction. These transport capacities are well-aligned with conventional modes of transport and can strongly support the relief of congested segments of the transport network. In addition, the inclusion of virtual coupling³, which is slowly being introduced for conventional railway and seen as one of the key technological improvements in railway technology, could add further capacity [41, 42].

However, this study adopts a more conservative approach and the vehicles are heuristically sized in order to fulfil the rush hour demand of the system while ensuring a headway of 90 – 120 seconds. This translates to about 1 and 2 m/s² of braking rate for cruising speeds of 500 km/h

²It is assumed a cruising speed of 250 m/s, 5 s of latency between first accident notification and brakes activation, and a safety factor of 1.5.

³Virtual coupling in railways is a technology that allows trains to operate closely together, like connected cars, but without physical couplings

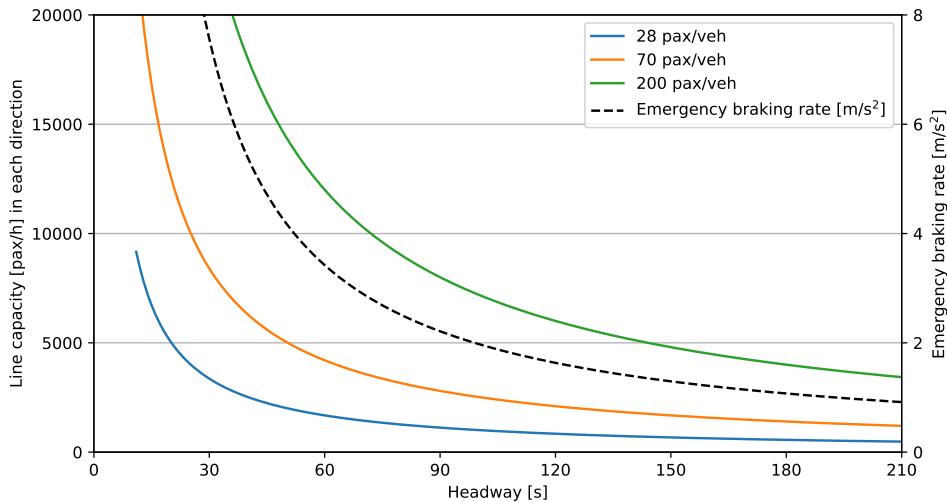


Figure 14: Passenger capacity of a hyperloop line (left y-axis) achievable for a given headway between travelling vehicles (x-axis) and seat capacity of the pods (different colours). The right x-axis shows the minimum emergency braking rate required to safely operate at a given headway.

and 900 km/h respectively. The resulting vehicle dimensions for the Swiss network are presented in section 5.2.1.

It is worth mentioning that, beyond safety concerns, high usage of hyperloop lines would also lead to higher energy consumption of the system. This power demand will be concentrated at the stations in both track-side- and pod-side-acceleration systems. The possibility to locally supply high power to the stations may ultimately one of the most constraining criterion while sizing the line capacity.

3.5 System design

This section presents a description of all the parts of the hyperloop system as exemplary displayed in this study. Specifically, for each component it provides:

- an overview of the possible technological options,
- the selection made for this study
- how the component is modelled for the energy calculations, the environmental and economic assessments.

Table 1 provides an overview of the main functionalities that a hyperloop system must provide, the technological options available and the selection made in this study. The following sections deepen the introduced concepts and outline the respective technical solutions in more detail. At the current stage of hyperloop development, it is clear that these choices are not yet definitive answers and are subject to change as data is collected and the model is expanded in the future, i.e. as the level of modelling detail increases. We briefly explain the choice and its modelling process, with a reasoning. More detailed description of alternatives can be found in the appendix, additional explicit values also in Table 6.

The choices to assume a certain design for the model are determined by the current best guess but also data availability: in fact, certain technologies are very promising but only very sparse testing data is available. The results here shall be seen as an example of one system designed similar to the assumptions made in this report, and only understood as an order of magnitude estimate.

3.5.1 Vehicle systems and energy consumption

This section focuses on all live systems, which are mostly located on the vehicles or at the interfaces with them. The only source of energy consumption that is not directly related to vehicle propulsion or suspension is the vacuum assurance, which is explained in detail in section 3.5.2. Fig. 15 shows all the energy and mass flows modelled in the system. The multiple interconnections highlight the

| System | Functionality | Chosen option |
|---------|------------------------------------------|--------------------------------------------------------------------------------------------------------------------------------------------------|
| Pod | Propulsion during cruise | Pod-side (various motor designs) Track-side |
| | Levitation technology | Electrodynamic Suspension (EDS) Electromagnetic suspension (EMS) Magnetic reluctance Various technologies requiring active track |
| | HVAC | Onboard oxygen tanks and CO₂ removal Carry-on breathing air Filtering of air in tube |
| | Thermal management | Phase-change thermal storage (ice-water) Salt-based thermal batteries Heating of fuselage + cooling |
| | Fuselage | Mostly carbon-fibre-reinforced polymers (CFRP) |
| | Lateral stability/Turning | attractive repulsive |
| Tube | Structural part | Concrete Steel |
| | Vacuum assurance | Concrete + Liner |
| | Rail | Determined by Levitation |
| | Vacuum generation | Pumping system |
| | Segments connections | Silicone joints |
| | Safety and reliability | Bypasses and valves |
| Station | Low pressure interface | Airlock (Valves + Pumps) Vacuum fingers |
| | Acceleration of pod | Track-side acceleration through Launcher Pod-side acceleration through onboard motor |
| | Braking energy recuperation ⁴ | Pod-side with motor analogous to acceleration Track-side with motor analogous to launcher |

Table 1: Functionalities of a hyperloop system and technological concepts assumed in this study. Bold represents the chosen concept, where sometimes several were investigated and some omitted in the modelling process.

complexity of the system and the impossibility to design a coherent vehicle without simultaneously solving all mass and energy balances.

Already at this point a fundamental choice arises: Is the track passive or active, i.e. is propulsion, levitation and guidance of the vehicle provided by a track that then has to be a working complex part for thousands of kilometres? This most likely would increase cost significantly compared to a passive track (as in e.g. railway). However, active parts on the pod increase weight and lead to challenges related to heat management on the vehicle. In this exemplary study, a system with a passive track was modelled, with the exception of acceleration phases (which are shown in section 5).

The next pages detail how each component works and how it has been modelled for the study, while section 3.6 introduces the implicit numerical solver used to perform their simultaneous design.

Propulsion As mentioned before, in this study we assume a passive track. As mentioned later, this might include initial active segments around the stations that help with the initial acceleration of the vehicle. Once at speed, we model it to be self-propelling.

There are various types of motors that are able to propel the vehicle without contact with the rail. EuroTube’s main focus is currently on infrastructure development, which contains both the highest risks but also levers since it is the major cost factor for hyperloop development. For the propulsion system information has been provided by Swissloop, the ETH Zürich university team in the hyperloop ecosystem and a regular participant to the SpaceX hyperloop competition. More details can be found in [43].

Depending whether or not a launcher is included, the propulsion is sized to either accelerate the pod to full speed or only to overcome the combined drag of electromagnetic and aerodynamic contributions. The power density of the onboard propulsion was taken from [43]. However, since this particular propulsion was not specifically designed for a multi-ton vehicle as the eventual commercial hyperloop pods, propulsion engineers of EuroTube re-scaled the power density to a lower motor frequency, approaching a more realistic value for eventual large scale vehicles. Data sources from other players like Hardt were incomplete for our modeling process, but will be included in iterations of the model.

Levitation Similar to propulsion, there are various levitation types worth considering. A well known concept is the one of the SC Maglev in Japan, which however requires an active track. In this study, electrodynamic suspension was modelled. This principle was also used in the first passenger test of Virgin hyperloop (website and therefore source not available anymore at the time of publication), although in a slightly different realisation. The pod is equipped with magnets gliding over a conductive (and not primarily magnetic) rail on the track side. When the rail is exposed to a change in magnetic field it will create eddy currents to oppose this change and therefore create a field opposite to the one of the pod, repelling the vehicle and making it levitate. This technology, however, requires some landing wheels, since a minimum speed is required to levitate. The two main advantages of this are: 1) the system is intrinsically stable, i.e. the force acting on the vehicle when pushed out of the equilibrium height is opposing the change; 2) the track can be built on the bottom of the tube, which allows for cheaper and easier construction, while still allowing for a completely passive switching system, at least on a conceptual level.

To model a fully functional pod, the following key characteristics of a levitation system need to be known: power consumption per lift created, lift-to-weight ratio (since the weight of the levitation system influences the weight of the pod and in return the lift needed) as well as the lift-to-drag ratio. In any magnetic levitation technology, there are boundary effects (although coming from different physical phenomena, depending on the levitation technology), which create force components not purely orthogonal to the direction of travel, therefore slowing the pod down. At the current stage of development of magnetic levitation, only very few complete data sets are available, and many of the technologies do not yet have sound experimental values with respect to each of the characteristics. For the model in this work, an electrodynamic suspension system (EDS) was chosen, based on a series of papers by Hao [44, 45] with whom intensive exchange about a possible design was established.

The series of publications by Hao also provides data on lift-to-drag ratios [44]. The data had to be extrapolated for speeds between 200 m/s and 250 m/s. It should be noted that the electromagnetic drag force for this levitation technology is speed dependent and decreases with increasing velocity. However, the power used to overcome it is the product of force and speed, and thus non-negligible even at high speeds.

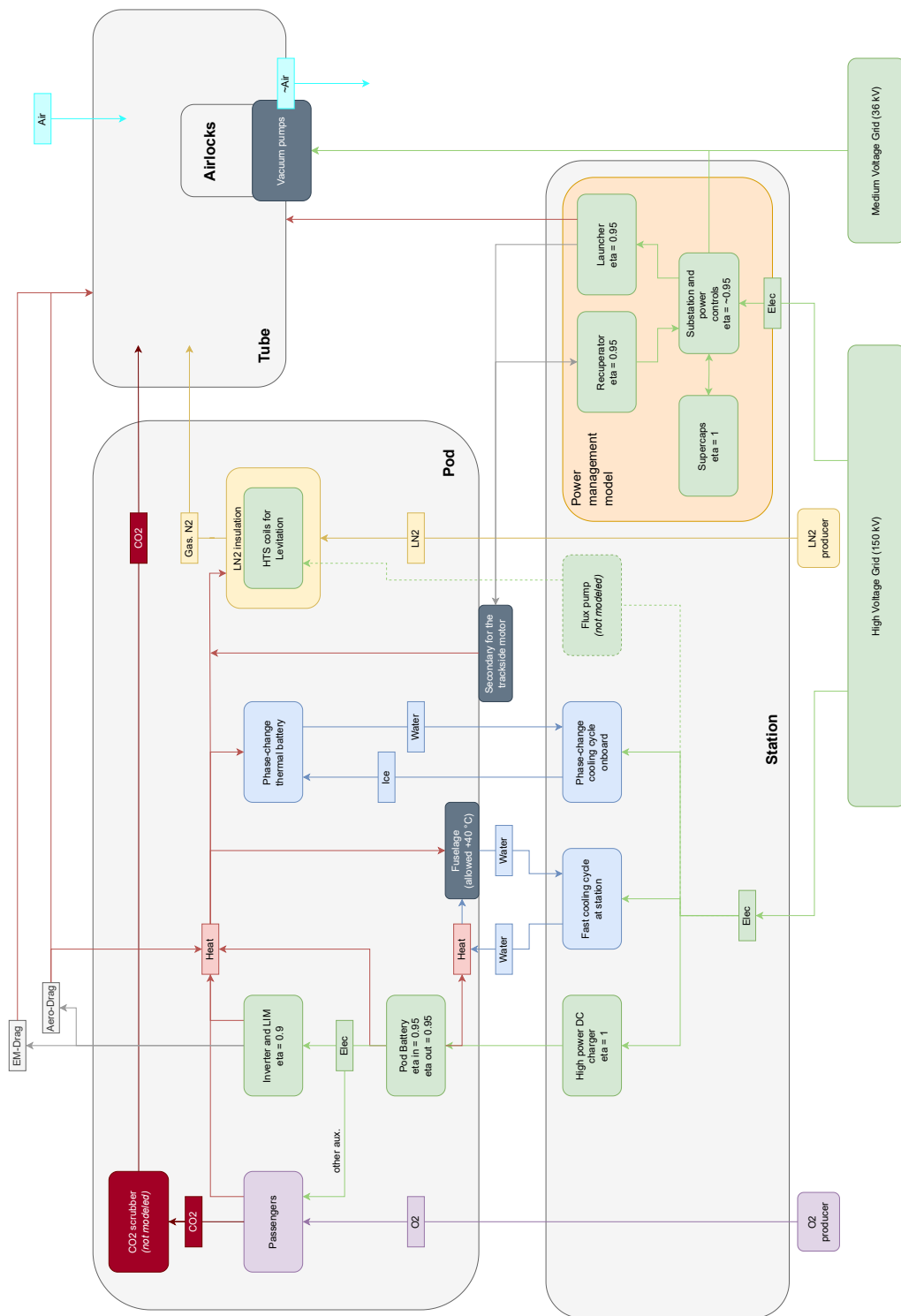


Figure 15: Energy and mass flows modelled within the simulation.

Rail The rail is based on the chosen levitation principle. The thickness of the rail is chosen conservatively with respect to Hao [44].

Pod dimensions and fuselage A fundamental design feature in hyperloop systems is the “blockage ratio” (BR), i.e. the share of the tube’s inner cross-section that is occupied by the pod. This characteristic strongly affects the aerodynamic drag, hence the energy consumption, the size of the propulsion motor etc. Fig. 16 gives an intuition of different blockage ratios. The exact cross-section of the pod depend on the precise space requirements of the propulsion and levitation systems, as well as the intended payload to be carried. For instance, container pods could potentially have a rectangular cross-section. Aerodynamic simulations [46] show that the pod shape does not have a particularly strong impact on the aerodynamic drag and this is due to the front-tail pressure difference being the largest component to the total drag. For simplicity a standard circular and axisymmetric shape has been assumed in the calculations. Nevertheless, further investigations on the impact of different shapes and vertical alignments are necessary for better estimates of the energy consumption.

The vehicle can either be centred in the tube or not, depending on the necessity to allow for the installation of a lateral walkway, which can be used for maintenance or emergency services. The aerodynamic stability of this configuration has been checked by an engineer of EuroTube.

The minimum cabin configuration where 4 abreast could be fitted has a pod diameter of 2.64 metres. Depending on the level of comfort, for a blockage ratio of 0.6, four to six people abreast could fit. This is also the blockage ratio used within this work, to allow for a reasonable balance between tube size and aerodynamic drag.



Figure 16: Left to right: Blockage ratios of 0.36, 0.6 and 0.83: Ratio of the inner area of the tube that pod and sleeper occupy together.

For a fixed number of passengers and blockage ratio, the length of the pod is given by the necessary cabin length plus some additional space for machinery and auxiliaries.

For the fuselage modelling the weight and compositions typically employed in aircrafts are chosen due to the similar performance requirements. Markish [47] shows that the fuselage and other systems make up about 50% of the operating empty weight (OEW) of aircrafts. By comparing the OEW of many narrow-body aircrafts with their passenger capacity an average of 140 kg fuselage/seat can be estimated. As for the fuselage composition, the most advanced material composition used by Boeing [48] for the B787 is adopted: 50% carbon fibre reinforced polymer (CFRP), 20% aluminium, 15% titanium, 10% steel and 5% other (neglected).

Aerodynamic drag The modelling of the aerodynamic drag in an enclosed system at very high speeds is a highly complex and computationally exhaustive task. Problematically, the modelling and estimation of power needed to overcome the remaining drag generated at high speeds is only vaguely known within the hyperloop community. However, it is of great importance, as can be seen in section 4.3.

Generally, the aerodynamic drag force is given by $F_D = \frac{1}{2}v^2 \cdot c_d \cdot A$, where c_d is the drag coefficient. In traditional applications, c_d is only a function of the geometry of the frontal area (hence of the blockage ratio), but in a hyperloop setup c_d becomes also a function of the speed. This occurs because at very high speeds the airflow around the vehicle “chokes” at the throat (minimum cross-sectional area between vehicle and tube) to sonic conditions (Kantrowitz Limit). This leads to the propagation of a leading shock wave (LSW) ahead of the vehicle and results in pressure build-up in front of the vehicle. Furthermore, a low pressure region is developed in the back-end of the vehicle due to a rarefaction wave in the tail-end of the vehicle. This is further

contributed by the generation of an oblique shock in the vehicle tail-end, which leads to further decrease in back-pressure compared to tube base-pressure. The pressure difference between the front and the back-end results in pressure drag. This pressure drag adds to the traditional skin friction drag, hence changing the drag coefficient c_d experienced by the vehicle. This phenomenon is thus simultaneously important but extremely complicated and costly to investigate: analytical models are necessarily simplified and custom made wind tunnels for hyperloop are not available yet, hence the only estimates can come from numerical models. But even numerical models are complex and resource intensive, since drag investigations of hyperloop combine acoustic and non-isentropic (e.g. shock waves) phenomena with the need to resolve thermal and momentum boundary layers. This requires numerical setups with large meshes and small time steps, which make the simulations computationally expensive.

For this study, a 2D numerical simulation is built and run on a commercial software for a reference case. To capture the c_d dependency on different parameters, the methodologies described in Table 2 are used. The vertical forces created by the airflow around the vehicle are not modelled. However, the drag force experienced by the vehicle is not the only aerodynamic concern. Travelling at high speeds in a closed environment, the pod generates both front and rear shock waves, which may travel the tube for long distances and interact with preceding or trailing vehicles. Importantly, the aerodynamic drag does not depend on the vehicle weight and it can thus be computed outside of the pod solver.

| Change in... | Modelling technique |
|----------------|--------------------------------------------------------------------------------------------------------------------------|
| Pressure | c_d stays constant (hence drag varies linearly with pressure). Confirmed by sensitivities on the above reference setup |
| Speed | c_d scales with respect to the reference simulation according to Table 2 from Bizzozero [49] |
| Blockage ratio | c_d scales with respect to the reference simulation according to Table 2 from Bizzozero [49] |
| Vehicle length | c_d slightly increases with vehicle length. Weak dependency confirmed by the literature [50] |

Table 2: Modelling of drag coefficient dependencies on key system design parameters.

Thermal management This is considered to be a critical technological aspect that might substantially change the key metrics of any hyperloop system. Therefore, EuroTube will conduct an InnoSuisse project in 2024 to further investigate the technology. Due to the vacuum environment, any thermal exchange with the tube or partial vacuum is highly dampened. There are considerable heat sources onboard the vehicle that have to be compensated. The most promising technologies currently available are phase-change materials (PCM), i.e. water-ice or salt hydrates. A part of the electrical energy fed to the propulsion, which is needed to overcome the aerodynamic drag, is accumulating on the pod fuselage as air friction heat. The fuselage is only allowed to heat up to a certain temperature difference, and any excess heat has to be captured by the thermal battery. The fin of the pod (which is the passive part on the pod) which is used by the track-side accelerator (launcher) during acceleration has to be cooled as well, even though this delivers only marginal additional cooling requirements. No power consumption for the HVAC is included (included in auxiliaries, but not a potential CO₂ scrubbing device). No power for the maintenance of any cooling circuit or similar is included and considered to be negligible.

Onboard battery Currently, the model assumes state-of-the-art Li-ion batteries. The sensitivity analysis in section 4.3 will explore how the future development of battery technology may influence the energy consumption of hyperloop systems. The batteries however, according to the results of the LCA, are not the main contributor to the environmental impact of hyperloop systems. In addition, the lower tank-to-rail efficiency of fuel-cells entails additional heat sources that have to be absorbed by the already critical thermal management system. New fuel cells such as hydrogen based ones are therefore no viable option.

3.5.2 Overground infrastructure

Material choice From a structural point of view, the two viable material candidates for overground systems are steel and concrete. In this work, a modular concrete tube has been modelled. Concepts for casting small segments on site that allow for local production, mobile factories and reduction in cost have been developed for half-scale versions by EuroTube in the past. In case of an overground structure, improving the speed of the construction process while reducing the cost and the environmental impact is a key factor for the introduction of a new transport system in the existing network.

Also, concrete has the potential to be produced from fully recycled composite materials in the future. The tube has an inner diameter of 4.6 m with a thickness of 20 cm of steel fibre reinforced concrete (SFRC). The tube thickness and material composition is based on the upscale of the so-called GammaShellPipe (GSP), which is a fully developed product for EuroTube’s first test track in 2023 which was developed with i.a. Eberhard, Vigier and VSL. The upscaled version consists of 10 Elements of 4 metre length each, post-tensioned to make one segment, which is placed on pillars of equal spacing. Post-tensioning is a technique in construction where high-strength steel tendons are installed and stressed to strengthen concrete, enhancing its load-carrying capacity. One pillar is six metres high to allow for crossings with highway and train lines. Foundations are for simplicity chosen to be of equal size as the pillars.

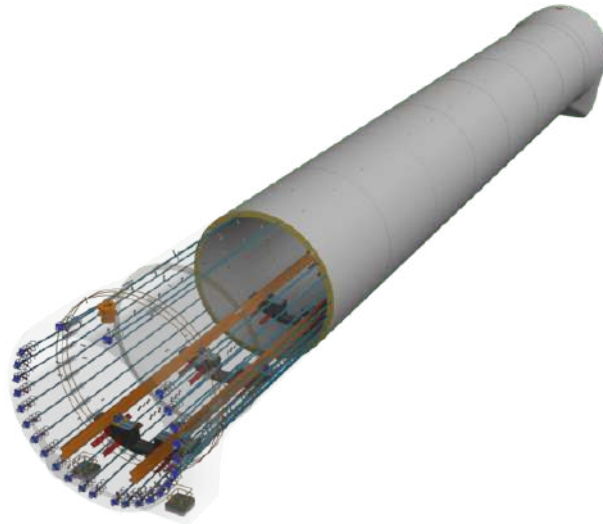


Figure 17: EuroTube’s concept of the *GammaShellPipe*, for which the design is completed and first pipes will be produced in 2024. For this study, an upscaled version was used (doubling of diameter and span). Pillars are placed at the interface of two tubes.

Vacuum assurance While steel provides air tightness intrinsically, in a standard concrete solution a vacuum-proof liner has to be applied to the concrete tube. The liner could consist of polymer materials such as polypropylene. EuroTube is currently conducting leakage measurements, having already provided a proof of concept for the application and welding of such a hybrid material system. The liner thickness has been determined in collaboration with the corresponding supplier.

EuroTube engineers designed a pumping design both for pump down and maintenance of the vacuum together with a pump manufacturer. This system foresees pumping stations along the track at a regular distance of 8 km. The energy consumption is estimated from the leakage calculation, pump output and power profiles provided by the manufacturer. These were initially designed for EuroTube’s planned test track of 3 km, *AlphaTube*, meaning that in a large-scale system the efficiency could most likely be improved. In the energy consumption estimates in Section 4, one complete re-pump down per year is included.

3.5.3 Underground infrastructure

Of higher interest than an elevated structures is, especially for the Swiss case, a tunnelling solution. It is however not obvious how a tunnel can provide vacuum, and in-depth research on this topic is urgently needed to realise any hyperloop route. Our modelled solution includes the following layers: Outer Tubblings, which are placed by a Tunnel Boring Machine (TBM) and secure initial stability of the tunnel. The outer liner, which is usually placed in tunnels for waterproofing can be replaced by a double-layer airtight liner, e.g. the one used for the overground solution. Then, the inner finishing is constructed, including the continuous sleeper on which the rail is installed. For reasons of conservative modelling and maintenance options, a sprayable second layer is applied to the inside of the tunnel for vacuum proofing. Sprayable layer solutions are currently investigated by EuroTube in cooperation with experts in the field.

In the underground case, there is an additional safety cavern placed above the two opposite tunnels. It could be used for evacuation as well as utilities. This cavern is included both in the cost estimate and the LCA in the results section.

The LCA for tunnelling was obtained with the help of an expert group at FOT that provided a tool developed by *EBP*, which was then modified to fit the hyperloop case [51]. Additionally, hyperloop specific elements had to be modelled (similar to the overground case).

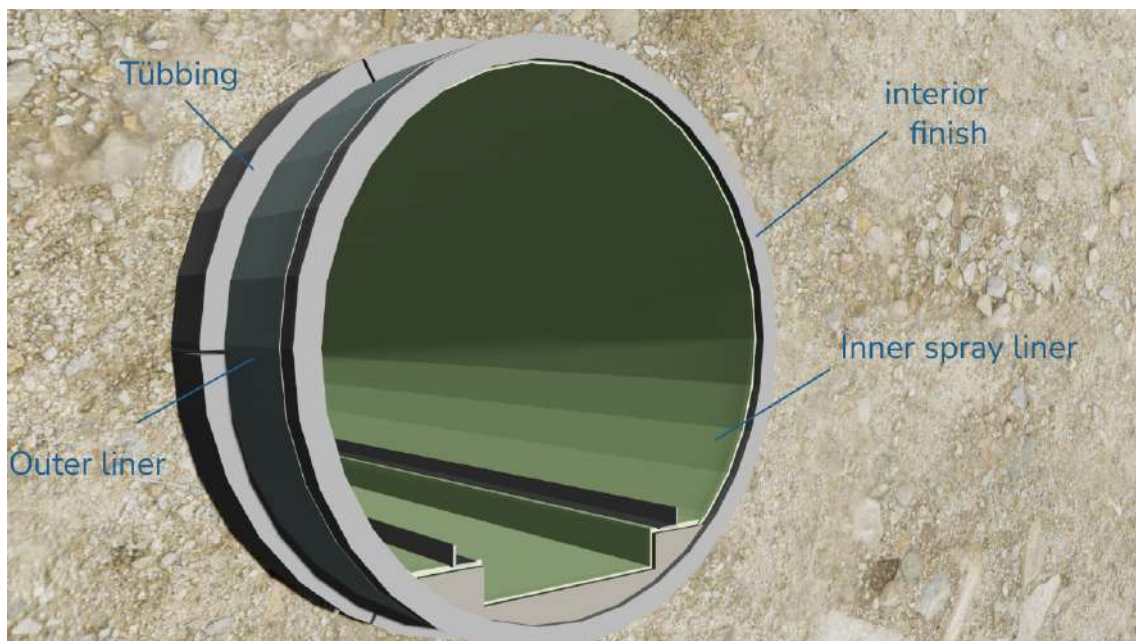


Figure 18: Overview of layers included in tunnelling solution.

3.5.4 Additional infrastructure

Vacuum Interface: Together with partners, EuroTube has developed a valve that is capable of isolating vacuumed sections even with tubes several metres in diameter as needed in a hyperloop system. In this scenario, pods arriving at the station stop between two valves and the section is ventilated. When leaving the station, they again stop between two valves and the airlock is either vented into the tube or pumped down. The former allows for almost no time delay in the station. In case of a cargo use case, airlocks are technologically more feasible than docking ports for the size of a full shipping container. In terms of modelling, the energy needed for pump-down of the airlocks is included.

Launcher (Initial acceleration): Both track-side acceleration and on-board motor options are modelled, as well as combinations. Whether or not a track-side acceleration is favourable depends strongly on the vehicle weight and range, as well as future development of the launcher and propulsion technology. A launcher is an active segment of the track that extends from the station to the point where the pod has reached its maximum speed. The advantage of this solution consists in the fact that all the energy required to accelerate the vehicle can be provided from the infrastructure side, allowing for a smaller battery. On the other hand, the cost and environmental impact of such a device is considerable. On the contrary, in self-acceleration the pod has to be

equipped with a much larger motor to accelerate within reasonable time. This again increases the weight of the pod and, in turn, the size of the motor for acceleration: therefore this proves to be a mathematical limit for the pod size since also larger thermal and electrical batteries are required. The detailed engineering of a launcher suitable to accelerate the pods at the desired speed is outside the scope of this project. However, a launcher consists mainly of high-emission-impact metals such as copper and steel, thus some estimates are nevertheless necessary to be made. The material bill needed for a full-scale launcher is based on the design of a test track launcher with corresponding scale up. Being far from optimised for the real-world application, the numbers estimated by the scale-up of this design constitute a conservative upper limit on the materials needed for the construction of a launcher. The tube and launcher are assumed to be passively cooled with a heat sink mechanism.

A recuperator is a machine with the main objective of recovering electrical energy from the kinetic one of the pod which, as a result, is slowed down. While this system is structurally identical to the one of the launcher, its beneficial effect depends again on the system configuration. However, first results of LCA show that a track-side recuperation cannot be justified compared to its impact.

Battery charging: From a weight and efficiency point of view, it appears clearly that the thermal and electrical batteries should not be designed to have capacities able to support a full day of uninterrupted use. Instead they should be designed for a single trip (with possible intermediate stops) and to be recharged at the end of the line before continuing. Whether batteries are charged directly while inside the pod or are swapped is determined by the trade-off between dwell-time at the station (and therefore higher number of needed pods to run the network) and the power management for charging all the batteries during rush hour.

Station logistics: With the proposed levitation technology, vehicles will stop levitating at low speeds (approximately 8 m/s [44]). This will require the presence of wheels onboard. Between the airlock and platform, there are different ways for the vehicles to move because there no longer are the constraints of vacuum and very tight air gaps (distance vehicle to track): vehicles can move either rail-guided (e.g. switches, turntables) or autonomously (i.e. zero turning radius) on wheels to the platform. Both solutions with one pod per platform (very broad but short stations) or few tracks with many pods are feasible (for the latter one a spare track is additionally needed for smooth traffic flow).

The specific design of each station would be subject to numerous local conditions and it is beyond the scope of this study (and not considered to be critical). However, to complete the life-cycle assessment the station size has been estimated based on the experienced passenger traffic. By analysing the traffic in the main Swiss railway stations in 2022 [52] and correlating it to their approximate footprint (considering their multiple floors) we obtain an average surface area of 0.6 m² per passenger a day either departing or arriving at the station. This factor has been used to estimate the size of the hyperloop stations in the modelled network and to compute the CO₂ emissions associated to the construction of the station halls and platforms.

Bypass system and emergency exits and ramps: Apart from continuous travel, vehicles will eventually have to take switches to change direction or move to stations. As mentioned below, it is a question of the applied safety concept whether or not an evacuation mechanism should exist or not. However, we estimated the economic and ecologic impact assuming a needed construction of a more complex layout than just two parallel tubes, as shown below.

Fig. 19 shows a possible underground infrastructure layout of a hyperloop system, highly scaled along the direction of travel (i.e. the distances in direction of travel are not true to scale). On- and off-ramps are exiting from the main high speed line into an intermediate station. On these ramps, the acceleration and deceleration will take place and the vehicles will only enter the main tube at full speed. A bypass system with suitable placement of vacuum valves allows closing down single sectors and venting of only specific sections in case of disruption. Having smaller sections allows for quicker venting in case passengers need to leave the vehicle. The vehicle will be designed in a way such that the emergency exit is at the rear, to avoid impediments in case of an obstacle in the front. The emergency exits are placed accordingly, such that in every section the path from the vehicle to the emergency exit is free. Light violet indicates the corresponding safety cavern.

Switch: Switches are inevitable for the build up of any network that has nodes at high speeds. For small networks, low-speed switches might provide the necessary service though. Additionally, without a switch concept, no bypass system is realisable. However, switching in magnetic levitation



Figure 19: Underground system for a hyperloop with bypass system, valves, on-/off-ramps and safety tunnel above the main line

is a highly non-trivial topic and depends strongly on the levitation technology. Since the lateral acceleration is limited by the passenger comfort, a switch at full speed of a hyperloop will extend over several hundred metres. At full speed, an element of several hundred metres length would have to be moved, possibly with a frequency of the order of minutes, not only being operationally intensive but reducing the lifespan of the components significantly. Therefore, a switch that itself contains active moving elements should be avoided to reduce construction and maintenance cost as well as line availability. The levitation technology modelled in this project allows for a fully passive switch. Patents for passive switches have been submitted, i.a. by Hyperloop Transportation Technologies (HTT)^{5 6}. A detailed engineering of a passive switch succeeding the identification of the ideal levitation system has to be done, but the proof of concept can be considered as given.

3.6 Numerical simulation and interfaces with other modules

The system design module introduced in Fig. 11 is at the core of the simulation tool and it interacts with all other modelling parts. It consists in a software written in Python, which was chosen for its simplicity, for the easy interaction with e.g. excel data sheets or folder structures. The hierarchical structure of the tool contains implicit parts as well as deterministic parts, as explained in Fig. 20. This means, most parameters are chosen *a priori* by the user. However, there are some properties of the pod, which cannot be chosen independently (i.e. weight of vehicle, levitation system, onboard propulsion, amount of cooling needed etc) since they influence each other. These are determined by the numerical solver. By solver it is meant that it is not an optimisation process but finding the only physical solution possible (apart from over-sizing the pod). Of course, some choice was made by the developers which variables are input and which are determined by the solver (i.e. it was chosen to fix the passenger number and not the total pod weight). Even though coding the full hyperloop model in implicit dependencies would certainly allow for the automated optimisation of the whole system, it was decided to follow a more pragmatic approach of a (mostly) deterministic model. Also, sensitivity analysis on specific parameters is of higher interest than a full optimisation. Depending on the size of the sub-parameter space size which shall be explored, it is feasible to perform an extensive grid search, with the computational time for the evaluation of one parameter set varying between four and eight seconds on a standard i5-1135G7, 16 GB RAM laptop. To investigate network effects, the load factor (ratio of occupied seats on a vehicle), trip distance, acceleration profiles and similar kinetic factors were investigated for a given "solved" pod when choosing the network parameters.

Fig. 20 shows a schematic of the software structure of the hyperloop modelling tool. All inputs are specified in a csv-file and read by the tool. The information is first given to the module which calculates the specifications of the pod. This has several reasons: First of all, the pod design influences most other aspects, e.g. its weight determines the size of the launcher needed to accelerate it at a certain rate. Secondly, the pod is the only hyperloop subsystem that has to be solved implicitly for each parameter combination: one cannot specify a certain passenger number, weight and top speed arbitrarily, since the combination is most likely physically inconsistent when chosen by the operator. For example, the weight of the pod influences how much levitation power

⁵This topological concept would allow for passive switches in an electromagnetic suspension system (such as in the Transrapid). Hardt Hyperloop is developing a switch for electromagnetic suspension systems from the top, which is conceptually easier.

⁶Patent of HTT: <https://patentimages.storage.googleapis.com/bc/f2/c4/b03ff4e26bc03b/US20190023285A1.pdf>

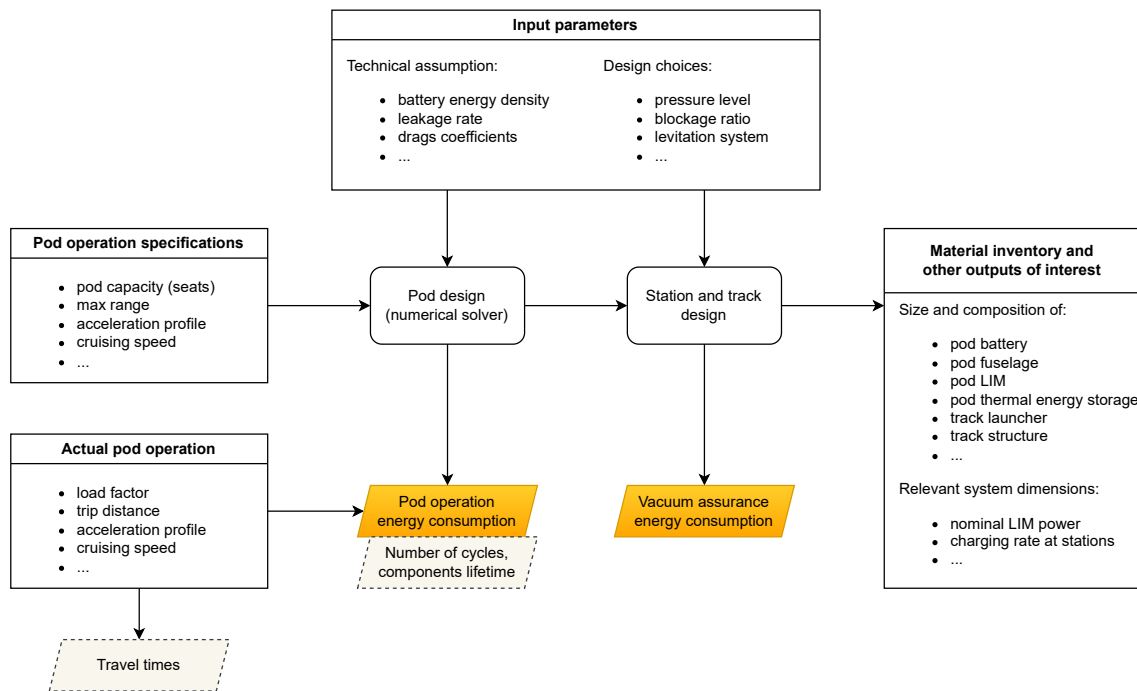


Figure 20: Internal structure of the design module.

(and therefore the weight of the levitation system) is needed, which again influences the pod weight. In total, the model contains eight connected equations that have to be solved simultaneously to determine the pod. Then, the outputs of the pod module are fed to the track and station module. Furthermore, any quantity of interest that is calculated during the estimation of the KPI is logged.

3.7 Life-cycle assessment (LCA)

An LCA is divided into four phases (see Fig. 21). In the first phase, the *goal and scope definition* of the investigation are set and various basic definitions are made with regards to the form and content of further work. The second phase, the so-called *life-cycle inventory (LCI) analysis*, is used to determine all mass and energy flows of the so-called product system. In the third phase, the *life-cycle impact assessment (LCIA)*, environmental effects are allocated to the identified mass and energy flows. The fourth and final phase, the *interpretation*, involves the results to be reviewed and organised into an understandable presentation for the recipient of the investigation.

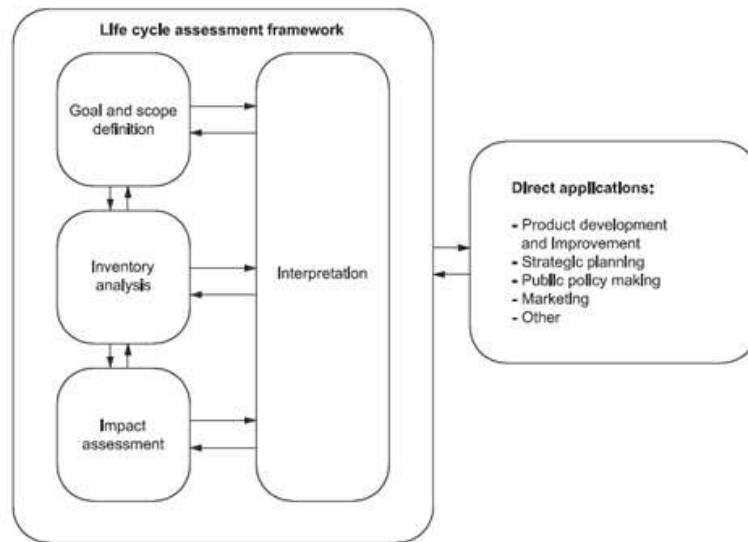


Figure 21: Phases of an LCA [53]

3.7.1 Goal and scope definition

The goal and scope definition forms the basis for defining the physical and temporal system boundaries and the delimitation of the product system.

Functional unit.

Comparing different products or services requires that their function be clearly defined and identical in terms of their usefulness. The benefits of the product or service must therefore be described quantitatively since the ecological balance records the environmental impacts quantitatively. This requirement is implemented by defining a so-called *functional unit*. The functional unit defines the quantification of the identified functions of the product. The main purpose of the functional unit is to provide a reference to which the inputs and outputs are allocated. This reference is necessary to ensure comparability of LCA results [53]. Therefore, all the results of an LCA are expressed in relation to the functional unit. For each functional unit, a so-called reference flow is defined, which indicates the amount of product required to perform the function [53].

System boundaries.

The definition of the scope of the investigation includes the definition of the system boundary for the LCI. It is given by emphasising the life-cycle of a product, which is referred to as a life-cycle in contrast to the business product life-cycle [53, 54]. Basically, it is necessary to record the complete life-cycle; in the case of certain questions, however, it may be sufficient to cover only parts of it. Such studies are explicitly not referred to as LCA within the meaning of the standards and are classified as follows [53]:

- from cradle to factory gate (cradle-to-gate),
- from the factory gate to the factory gate (gate-to-gate),
- specific phases of the life-cycle (e.g. waste management, parts of a product).

Data and data quality. In addition, requirements for data and data quality must be stated and the categories of impact to be considered must be selected [53]. The categories of effects must

therefore be selected at the beginning of an investigation since the information to be identified in the LCI depends on it. If, for example, only the scope of action anthropogenic global warming (climate change) is to be considered in the LCIA, the LCI of the material may be limited to the coverage of mass flows with climate impact [54].

3.7.2 Life-cycle inventory (LCI) analysis

The aim of the LCI is to identify all mass and energy flows that stream from the ecosphere into the technosphere as defined by the scope and are then released back into the ecosphere. To this end, an understanding of this technosphere must first be developed, i.e. the individual processes within the system and their connection via intermediates or even waste must be identified and described [53]. Subsequently, the necessary data and information on processes and material flows must be collected.

Cut-off criteria. In a complex product system, it is usually not possible to track all mass and energy flows. This is also not necessary for the purpose of an LCA. However, the system must be described completely in the sense that all relevant information and the data required for the assessment is available and complete [54].

Data gaps. Data gaps can arise during data research, for example some possibilities include data on relevant material flows cannot be determined, no knowledge is available or if the measured data is not accessible. This can represent a substantial problem in the results of an LCA and must therefore be clearly indicated [54].

Multi-product processes. A methodological problem occurs in so-called multi-product processes. These are technical plants or processes that generate more than one product. Typical examples of these are chemical processes that produce main products as well as by-products, combined heat and power plants that supply electricity and heat, or transport systems that serve both passenger and freight demand. For the calculation of the product system, it is necessary to refer to the input and output flows of each process to exactly one reference flow. To make this possible for multi-product processes, input and output flows must be allocated proportionally to the products involved. This approach is called allocation. Such allocation can be carried out in different ways. The preference is determined by an underlying physical relationship between the products [54]. In practice, this means that the inputs and outputs of the process are divided in proportion to the masses or the energy contents of the products. If this is not possible the inputs between the products and functions should be mapped in such a way that they reflect other relationships between them [53]. As such a relationship, the economic value of the products or services is usually considered. The result of an LCI may depend on the allocation approach chosen. Accordingly, the different approaches have been and will be discussed extensively and controversially. This is another reason why the standards recommend avoiding allocations as far as possible [53].

An often-used method (also for this LCA) is the *cut-off* allocation (see Fig. 22), in which by-products (or waste) leave the system without being allocated any of the environmental burdens. On the other hand, it implies that recyclable materials are available to the recycling processes and secondary (recycled) materials only carry the effects of the recycling processes.

Software and database. Differences can occur, especially with different databases. This should be considered when comparing with other LCAs. Widely used software programs include: GaBi, SimaPro, openLCA and Umberto. Ecoinvent and GaBi are often used as databases.

Brightway is an open-source framework for LCA modelling in Python and is used for this study [55]. The mix of a modular design, the expressiveness and interactivity of Python and Jupyter notebooks, and the coordinated calculation paths enables new research directions in LCA. Building on this is the Activity Browser, also an open-source software for advanced LCA, which is also used for this study [56]. This software provides a Graphical User Interface (GUI) for Brightway and therefore serves as a productivity tool for sensitivity analyses, parametric LCAs or scenario LCAs.

With the use of *ecoinvent* (version 3.8) as the master database, an extensive data collection is available. With around 19,000 LCI data sets in many sectors such as energy supply, agriculture, transport, bio-fuels and bio materials, and specialty chemicals, construction materials, wood, and waste treatment, ecoinvent is a comprehensive, transparent, and international LCI database [57]. However, even ecoinvent reaches its limits for prospective LCAs (pLCA) like this, which is why the “premise” database is additionally used here [58]. “Premise” allows the LCIs contained in the ecoinvent database to be matched with the results of Integrated Assessment Models (IAM) —

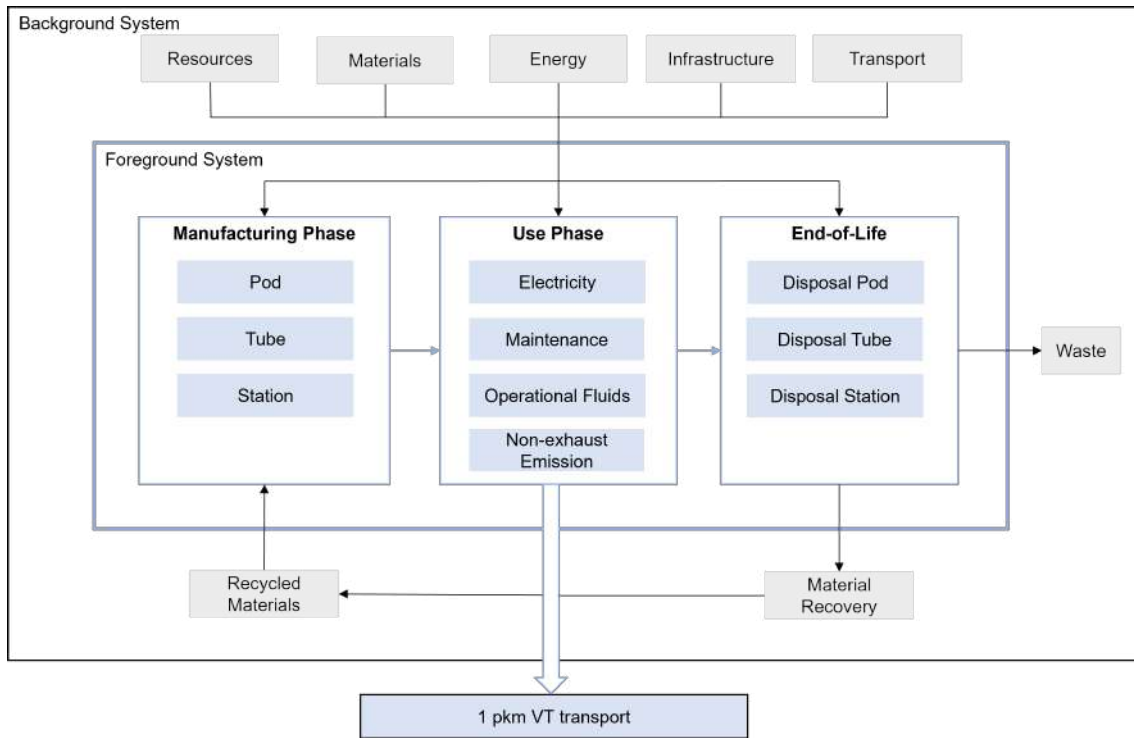


Figure 22: Scheme of the cut-off allocation used for the LCI of the hyperloop system. The diagram serves as a simplified illustration and does not represent all connections between the system components.

such as REMIND [59] or IMAGE [60] — to create LCI databases under future policy scenarios for each year between 2005 and 2100. In addition to the global IAM scenarios, specific projections for Switzerland (according to Energy Perspective 2050+ [61]) have been employed and coupled with the global scenarios. Table 3 displays the scenarios explored in this study and the alignment employed to match Swiss and global perspectives.

| IAM IMAGE | | | Swiss Energy Perspectives 2050+ | |
|-----------|---------------------------------------|---|---------------------------------|-----------------------------------------|
| Scenario | Explanation | | Scenario | Explanation |
| RCP6.0 | Global temperature increase to 3–4 °C | ↔ | WWB | «Weiter wie bisher» (Business as usual) |
| RCP2.6 | Global temperature increase to < 2 °C | ↔ | ZERO Basis | Net zero GHG by 2050 |
| RCP1.9 | Global temperature increase to 1.5 °C | ↔ | ZERO Basis | Net zero GHG by 2050 |

Table 3: Alignment of climate and techno-economic scenarios between global and Swiss perspectives.

3.7.3 Life-cycle impact assessment (LCIA)

The phase of the LCIA is a fundamental requirement for the completion of an LCA, beyond the quantitative recording of material flows, it also plays a part in recording their effects on the environment. The aim is to enable a comprehensive assessment of all environmental impacts and to make different effects on the environment comparable.

The mandatory elements of the LCIA include three steps: selection of impact categories, classification, and characterisation. The first mandatory element in the LCIA is the *selection of impact categories*: each impact category represents a specific environmental problem (e.g. climate change). The selection of impact categories is part of the first phase of the LCA (i.e. goal and scope), but it is also checked here based on findings from the LCI, and modified if necessary.

In the second step of the LCIA, the *classification*, each elementary flow determined in the LCI

is assigned to an impact category. In general, several flows contribute to an impact category. However, an elementary flow can also contribute to several impact categories.

The third step, the *characterisation*, entails the quantification of the selected impact indicator (category indicator result) for each elementary flow associated with a category. For each elementary flow, the result of the LCI is multiplied by the characterisation factor of this substance for the respective impact category. As a result, all elementary flows associated with an impact category are converted into a common unit. The sum of all the partial contributions of the individual elementary flows gives the result for the effect category.

Impact indicators Table 4 summarises the impact assessment methods and categories used in this study, with respective indicators and units. The Global Warming Potential (GWP) was introduced in the IPCC First Assessment Report, where it was also used to illustrate the difficulties in comparing components with differing physical properties using a single metric [62]. There are different time horizons, the most common is 100 years⁷. Table 5 presents an example of the calculation of the impact indicator for the category “climate change” starting from the emission results of the LCI.

The Environmental Footprint (EF 3.0) method is an initiative of the European Commission. It is a new and improved method that companies should use to measure the environmental performance of a product throughout its life-cycle and includes many different impact categories [63]: impacts of land use on soil quality, resource depletion due to extraction of metals and minerals, water use in terms of potential deprivation, and impact of particulate matter formation on human health. Finally, the Cumulative Energy Demand (CED) method is a consistent approach that quantifies the primary energy content of all different (renewable and non-renewable) energy resources [57].

| Method | Category | Indicator | Unit |
|----------------------------------|--------------------------------------------------------------------------|----------------------------------------------|-------------------------|
| IPCC 2013 | Climate change | GWP100a | kg CO ₂ -eq. |
| Environmental Footprint (EF 3.0) | Land use | Soil quality index | dimensionless |
| EF 3.0 | Resource use, minerals and metals | Abiotic resource depletion (ADP) | kg Sb-eq. |
| EF 3.0 | Water use | User deprivation potential | kg world-eq. deprived |
| EF 3.0 | Particulate matter formation (PMF) | Impact on human health | Disease incidence |
| Cumulative energy demand (CED) | Biomass, fossil, geothermal, nuclear, primary forest, solar, water, wind | Renewable and non-renewable energy resources | MJ-eq. |

Table 4: List of impact assessment methods, categories, indicators and units that are used in this study to evaluate the hyperloop system.

3.7.4 Interpretation

The interpretation, the fourth and final phase of an LCA, is used to derive conclusions, to explain limitations and to make recommendations [53]. The detailed and mostly complex results of the LCAs therefore need to be prepared, commented on, and summarised in such a way so that it is comprehensible to the target group of the respective study and support for decision-makers can be derived. The main components of the assessment phase are:

- identification of the significant parameters based on the results of the LCI and the LCIA,
- review that considers the sensitivity, completeness, and consistency analysis,
- conclusions, limitations, and recommendations [54].

⁷It should be noted that the Intergovernmental Panel on Climate Change (IPCC) has started to publish its Sixth Assessment Report (AR6) in 2021. However, the updates to the characterisation factors do not result in any significant changes and IPCC AR5 from 2013 is still currently used in GHG accounting.

| Impact category | Climate change | | | |
|----------------------------------------------------------------|-----------------------------------------------------------------------|--------------------------------|-----------------------------------------------------------------------------------|-----------------------------------------------------------------------|
| Impact model and indicator | GWP100a as proxy of increase in radiative forcing (W/m ²) | | | |
| Elementary flow | Results kg _{emission} / func- tional unit | LCI in func- tional unit | Characterising fac- tor in kg CO ₂ -eq. / kg _{emission} | Indicator result in kg CO ₂ -eq. / func- tional unit |
| CO ₂ | 5 | | 1 | 5 |
| CH ₄ | 0.5 | | 28 | 14 |
| N ₂ O | 0.01 | | 265 | 2.65 |
| Result of the characterisation for the category climate change | | | | 21.65 |

Table 5: Examples for characterising the results of the LCI (impact category climate change from the IPCC 2013).

3.8 Economic assessment

This section provides a brief overview of the cost modelling and the corresponding sources for the estimates. Results are shown in section 5.4. To the extent possible, the modelling of cost was in agreement with the modelling/assumptions used in the LCA. It shall be clear that there is no development cost included in these estimates.

Pods: Delft hyperloop estimate the cost of a 90-seat vehicle to be around 15 mill. CHF [64]. Given that their expertise in vehicle development is among the best in Europe, using this estimate was considered to be favourable compared to an in-house estimate. However, this estimate is for a Maglev train, which means that it includes a levitation system, a linear motor but no battery compared to the system modelled in this work. The cost of the needed battery (several of them as their lifetime is relatively short compared to the one of the vehicle) is added accordingly. Although the levitation system is different, the cost difference was assumed to be within the acceptable margin, especially when the vehicle cost is compared to the cost per meter linear infrastructure. As seen later, this work mainly considers two vehicle sizes of 70 and 200 passengers respectively. The cost was scaled linearly with passenger capacity.

Linear infrastructure overground: This cost is given per kilometre per direction.

- **Tube:** As an upper limit, the cost estimate done for AlphaTube, a planned 3 km test track in Valais, was scaled up to a full-sized system. This includes material cost as well as the complexity of the components.
- **Post-Tensioning:** The cost of post-tensioning such a system was estimated in cooperation with VSL Schweiz AG. This is the cost of stressing the single cylindrical concrete elements into one tube as in Fig. 17.
- **Pillar, Foundation, Groundworks:** An approximate estimate for the cost of these components combined was derived together with Implenia Schweiz AG.
- **Liner:** Material cost were given by Sika Schweiz AG. An estimate for the application of liquid liners was given, although the application of a liner that has to be welded might be costlier.
- **Rail:** Instead of only taking the raw material price, online prices for simple profile shapes were taken and scaled up with weight.
- **Land acquisition:** A reasonable average for land cost in Switzerland was composed based on data by *hausinfo.ch* [65] and Canton of Zurich [66].
- **Electrical components in tube:** A cost breakdown from railway tunnels [67] was taken as a basis to account for electrical systems in the tube (apart from the separately estimated launcher).
- **Joint Silicone:** The offer made to EuroTube for a joint for half-scale was adjusted to fit the full size.

- **Pumping system:** The cost of the pumping system has been estimated based on a quote made by Leybold for the pumping setup of a 120 m hyperloop test-track (*DemoTube*) and scaled up to meet the pumping requirements of the large-scale system.
- **Valve:** Cost was upscaled from an offer for a half-scale valve in the context of an offer for the *DemoTube* test track.

Linear infrastructure underground: This cost is given per kilometre per direction. More details are given in section 5.4.

- **Tunnel:** Together with Implenia Schweiz AG, a simple model for a tunnel of the same size as the overground tube (such to not change any parameters in the vehicle or energy consumption) was developed and the cost estimated by a senior calculator within their tunnelling department. This was determined for three geologies that are common in “Mittelland”. These geology types also fit the ones used by the developers of the tool that was used to estimate the environmental impact of tunnelling. The modelling of tunnels has so far been avoided by the hyperloop community. Therefore, considerable effort was put into this estimate, including shafts to access TBMs, TBMs themselves, a safety cavern for maintenance etc.
- **Liners:** As mentioned in section 3.5.3, the tunnel includes two layers of lining: firstly, an outer one between Tübbing and inner vault, which is assumed to be identical to the one that would be applied to an overground tube (and replace the regular waterproofing in tunnels). Secondly, an inner one that is still in development to be sprayable and therefore could be applied to the inside of the inner vault.
- **Electrical components in tube, Pumping system, Valves, Rail, Liner (outer):** Analogous to overground.

Further CAPEX in infrastructure:

- **Stations:** There has been done very little work in the community about the exact cost of construction of such a station, mainly due to dependencies on location that prevent precise estimates for a generic station. For a Swiss case, we assume the stations to be underground. Furthermore, the cost should be comparable to railway: although there are a few more complex elements such as battery charging and safety checks, the tunnelling and caverns size needed will be significantly smaller.
In this work we scaled the cost of the planned underground station in Luzern and the cost of Bahnhof Löwenstrasse in Zürich HB with respect to the passenger flow (Swiss Francs per passenger per year). This metric was then extrapolated to forecast the financial implications for our network by applying it to the anticipated passenger flow. This approach, while not without its limitations, offers a reasonable estimate based on available data and analogous project costs.
- **Launcher:** This device has never been built in an even remotely related size so far. Knowing an upper bound for the material cost of this device, an assumption about the share of material cost to total cost was made based on voltage transformers, which are of similar complexity.
- **Substation:** The substation comprises the MV–HV (Medium Voltage - High Voltage) transformer connecting the station to the grid and a high-power supercapacitor to smoothen the power consumption profile from the grid, hence reduce the power connection bill (see OPEX). The prices per MW have been estimated based on existing commercial products and then scaled up based on the peak power consumption of each station at rush-hour (see Appendix F): this comprises all energy consumption at the station, from pod charging to vacuum pumping the pipe segments around the station.

Rough estimate of OPEX: For the OPEX, several factors had to be taken account and several approaches to modelling can be taken.

- **Personnel:** Simultaneously there are four station and 70 pods in operation. If we assume two shifts per day, three people of crew per pod, 100 people per station (due to potential

safety checks) and 200 overhead, then the system could run with 213 mill. CHF annually ⁸.

- **Energy:** Is given through section 4.3. If we assume a price of 0.12 CHF/kWh [70], then the yearly energy cost amount to roughly 70 mill. CHF, not including energy in the stations (such as lighting etc.)
- **Insurance:** An estimate per pkm was taken from [71] and scaled accordingly.
- **Infrastructure Maintenance cost:** An estimate per pkm was taken from [71] and scaled accordingly. This is for infrastructure maintenance. Vehicles do have a life-time of less than 10 years (assuming the same number of trips per life as airplanes, even though the motors will be able to run longer). Therefore the maintenance is modelled through depreciation of the vehicles.
- **Power tariff:** in a worst case scenario we assume a direct connection to the transmission grid of Swissgrid, which results in conservative high estimate. The cost includes a fixed annual connection fee and a variable monthly peak power tariff [72].

⁸As a very rough comparison: Lufthansa German Airlines had 119 bill. pkm in 2022 with ca. 34'000 employees [68]. This amounts to 35 mill pkm per one employee. The above for estimate for hyperloop in Switzerland yields 2.8 mill pkm per one employee, suggesting a conservative estimate compared to aviation. For SBB, one employee equaled roughly 0.5 mill pkm [69].

4 General hyperloop energy assessment

4.1 Overview of simulated scenarios

The objective of this work was to establish ballpark figures for the following quantities in a Swiss network, given a certain hyperloop system : Passenger throughput, energy consumption, environmental impact (LCA) and cost. The results of this work were established in two stages.

Firstly, a generic point-to-point hyperloop route was investigated from a technical point of view, meaning: In the model established and described in section (reference technical description), many so-called "design parameters" are still to be determined, such as operating pressure, cruise speed, acceleration rate, passenger per vehicle etc. Even though the energy consumption is not the main impact for the environment (but the construction), the energy consumption is the key metric most suitable to determine the mentioned system parameters. The so-called "reference case" is therefore a reasonable, through iteration established default case from which sensitivities of the system are explored.

In a second step, a network was investigated, in this case the Line Zurich-Bern-Lausanne-Geneva. Metrics of the LCA such as $\frac{gCO_2}{pkm}$ strongly depend on the demand and therefore the network, the same reasoning holds for cost. Energy-wise, only the vacuum assurance is network dependent, while every other contribution is per vehicle, therefore not network dependent. It also turns out that kinematics are of greater influence when investigating a network than e.g. pressure, therefore sensitivities are performed on those parameters again. Especially in a small network like Switzerland, top speeds of 250 m/s might be unfeasible.

4.2 Reference case parameters

The main technical and scenario parameters employed in the study are summarised in Table 6. They are either from in-house scale-up of values acquired in modelling test tracks or from literature and in cooperation with experts.

4.3 Energy consumption

This section summarises the results for the reference case from which sensitivities are explored. As a first result, the energy consumption breakdown is shown as well as the weight breakdown of a vehicle corresponding to the chosen parameters.

4.3.1 Track-side vs pod-side acceleration

Beyond the parametric sensitivities shown above, different fundamental design choices have also been investigated. A typical key question is whether pod-side or track-side acceleration is superior. Fig. 23 presents the comparison between these two solutions for the energy consumption breakdown and the pod weight distribution. The self-propelling pod has to be equipped with both a more powerful motor in order to accelerate the vehicle to its top speed as well as a larger battery to provide the needed energy. This results in a heavier pod that consumes additional energy, especially for the acceleration as well as levitation (due to the larger inertia and mass respectively). Other sources of additional energy consumption are the larger electromagnetic drag due to the need for more lift and the thermal management due to the heat losses linked to any additional energy flow.

Therefore, it is clear that from an operational energy point of view the track-side solution is more efficient. However, it requires a large track-side motor that must cover the entire distance travelled by the pod during its acceleration - contrary to the pod-side motor that is simply onboard. It is thus important to evaluate if the material investment in the track-side motor is justified by the displayed higher efficiency of the pod. Section 5.3 investigates this question from a life-cycle perspective. It will also show, that the answer to this trade-off is dependent on the network, the acceleration profile and travelled distances. In some cases, a combination might be optimal.

Remarkably, aerodynamic drag is still the major contribution, along with electromagnetic drag and the launching (i.e. the acceleration of the pod). Airlocks are optional in a hyperloop design, but can already be identified as no major problem in terms of energy consumption. With these results, it seems clear that the major improvements in hyperloop in terms of operational energy consumption can be made with more detailed knowledge of the aerodynamic behaviour of the vehicles and reduced pressure. The massive influence of the remaining aerodynamic drag is investigated in more detail in the following section. In terms of weight, the major contributions are the vehicle body and the passengers themselves. As the weight was estimated in the tool from an aircraft, potential to reduce this contribution is expected.

| Parameter | Value | Source |
|------------------------------------------------|---------------------------------|------------------------------------------------------------------|
| Traffic and Kinematics | | |
| Cruise speed | 250 m/s | own ass. |
| Acceleration / deceleration | 1 m/s ² | own ass. |
| Minimum headway | 25 s | emergency deceleration of 5 m/s ² |
| Traffic capacity (in one direction) | 10'000 pax/h | derived from headway and pod size |
| Traffic demand (in one direction) | 84'330 pax/day | daily road and rail traffic between Zurich and Bern |
| Load factor | 80% | as airplanes [73] |
| Line length | 300 km | own ass. |
| Time to manoeuvre in stations (incl. airlocks) | 300 s | own ass. |
| Pod | | |
| Fuselage mass | 140 kg/seat | average from narrow-body airliners |
| Fuselage lifetime | 110'000 cycles | common lifetime of aircrafts [74, 75] |
| Outer diameter | 3.4 m | own ass. |
| Blockage ratio | 0.6 | derived from pod and tube diameters |
| Passenger capacity | 70 seats/pod | own ass. |
| Share of drag energy heating up the pod | 50% | fluid-dynamic simulations |
| Efficiency of onboard propulsion motor | 90% | own ass. |
| Lift-to-weight ratio of levitation system | 62 | derived by the authors based on [44, 45] |
| Lift-to-drag ratio of levitation system | speed-dependent, up to 60 | derived by the authors based on [44] |
| Heat capacity thermal battery | 334 kJ/kg | latent heat of ice to water |
| Heat capacity fuselage | 1 kJ/(kg K) | average heat capacity of aluminium and CFRP |
| Allowed fuselage temperature increase | 30 K | own ass. |
| Battery cell energy density | 500 Wh/kg | [76] |
| Cell-to-pack mass ratio | 0.75 | [76] |
| Depth of discharge | 85% | [76] |
| Charging efficiency | 95% | [76] |
| Discharging efficiency | 95% | [76] |
| Additional backup capacity | 20% | own ass. |
| Battery lifetime | 5'000 cycles | expected battery lifetime in 2040 [77] |
| Tube and track | | |
| Tube pressure | 10 mbar | ongoing experimental campaign |
| Inner tube diameter | 4.6 m | own ass. (to potentially transport standard shipping containers) |
| Outer tube diameter | 5.0 m | based on structural requirements |
| Leakage rate | 0.0113 slm/m ² | ongoing experimental campaign |
| Efficiency of track-side launcher | 90% | own ass. |
| Efficiency of track-side recuperator | 90% | own ass. |
| Background system | | |
| Electricity mix | 7.79 gCO ₂ -eq./kWh. | Swiss Federal Railways electricity mix |

Table 6: Main technical and scenario parameters assumed for the hyperloop system.

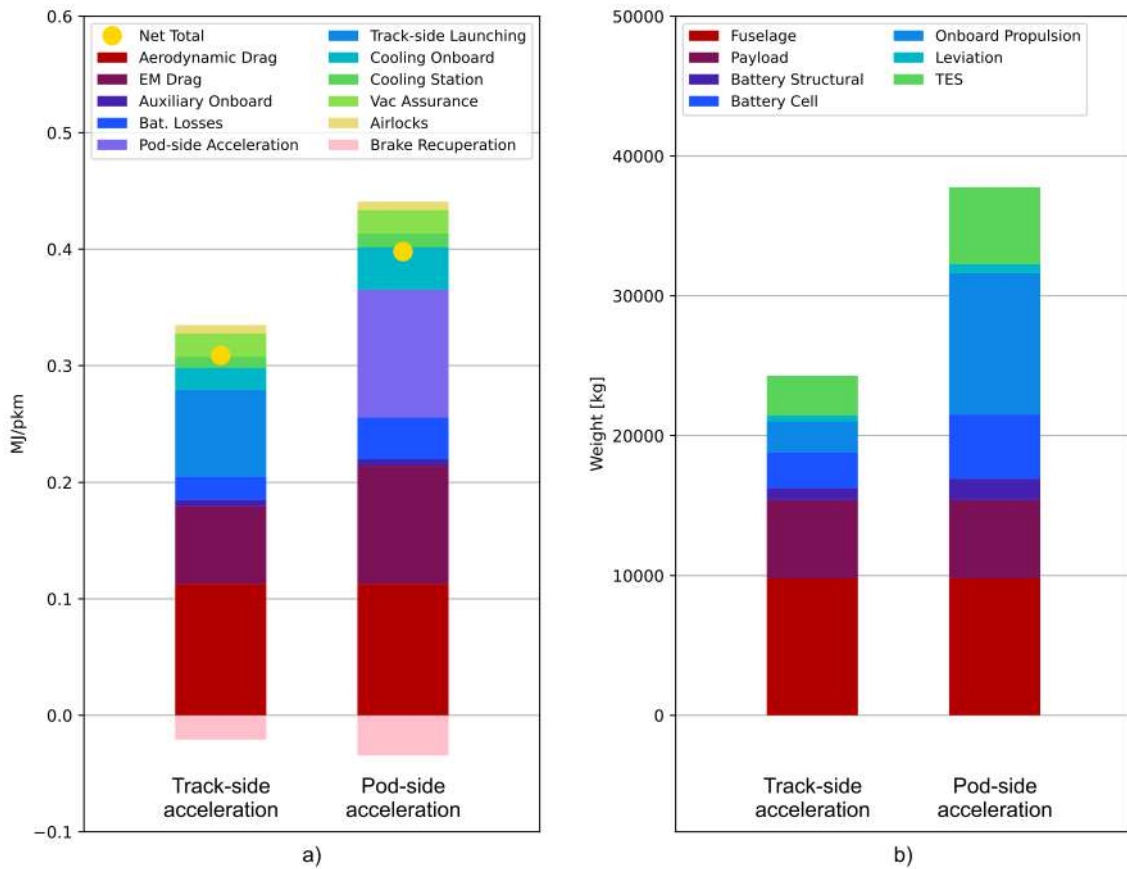


Figure 23: Breakdown of specific energy consumption (left, a) and pod weight (right, b) for the track-side and pod-side acceleration systems. In a) also the recuperation energy is shown as negative and the resulting net energy consumption is depicted by the yellow dots. The payload is for 100% load factor, which is the scenario the system is designed for.

4.3.2 Sensitivity Analysis

The numerical setup allows to explore the impact of the many degrees of freedom on the performance of the system. Fig. 24 shows the specific energy consumption during operation for different system designs. In order to keep the results traceable, only a single input parameter at a time is changed compared to the reference scenario and each row displays the energy consumption resulting by varying this parameter between two extreme values. The three written values refer to the left-centre-right results in this order, with the centre one belonging to the reference scenario and identified by the dashed line. The only exception is the sensitivity on the pod acceleration design, where only two options are possible: track-side (which belongs to the reference scenario) and pod-side, both with recuperation.

The sensitivity explores both changes in technical properties whose exact estimate is difficult due to uncertainties in the development of the technology (first four dimensions) as well as changes in design options that can more freely be set by the system constructor and operator based on the use case (next seven dimensions).

It is visible that, although many uncertainties in the technical understanding of some components persist, the choice of sub-optimal designs is what mostly penalises the system. Meaning: The selection of small pods (28 passengers) or high blockage ratios (0.83) has a much worse impact than if the forecast of LIM (Linear Induction Motor) or battery developments has been overestimated by a factor of 2. However, on the technical side the lift-to-drag ratio of the levitation system displays the largest impact on the energy consumption due to its strong reinforcing feedback (more drag for the same lift leads to more energy consumption, hence higher LIM and battery weights, hence the need for more lift). Accurate estimates of its magnitude are thus of primary importance. On the design side, the sensitivity confirms the paramount role that the aerodynamic drag has on the energy consumption, with both pressure level and the blockage ratio having the largest influence on the outcome. This however highlights not only the need to carefully calibrate these two dimensions, but also to model and test the aerodynamic drag of the vehicles in general: factors like vehicle shape, turbulences and shocks may have a comparably marginal impact on the aerodynamic drag but they would still strongly affect the system performance due to the large role that the drag has in it.

Due to their criticality, Fig. 25a breaks down the combined impact that pressure levels and blockage ratios have on the vehicle design and the operational energy consumption.

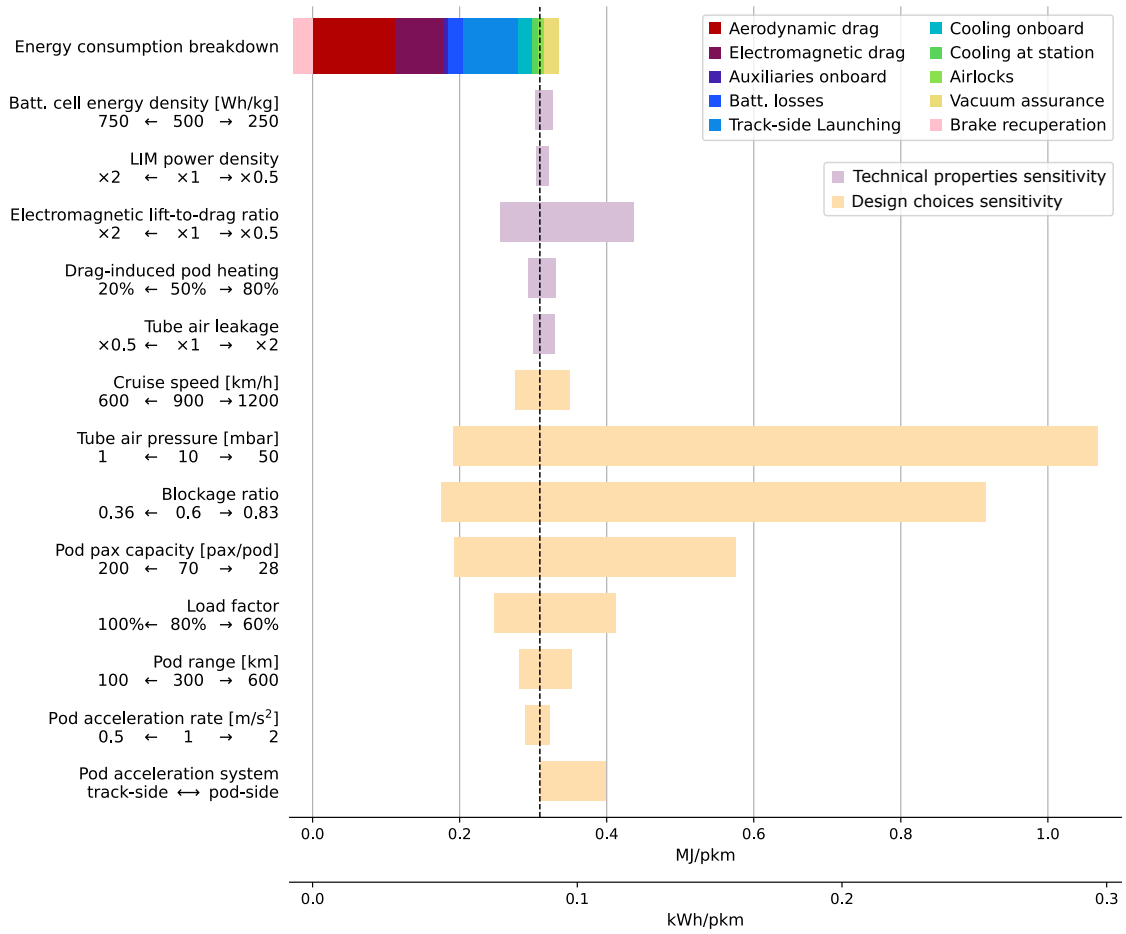
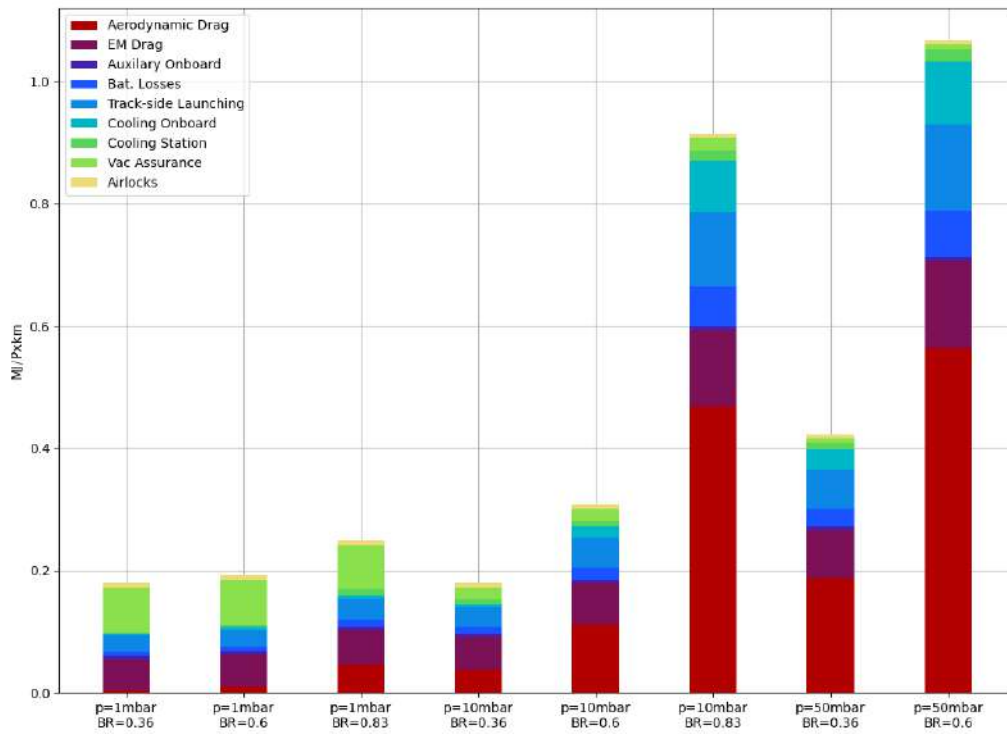


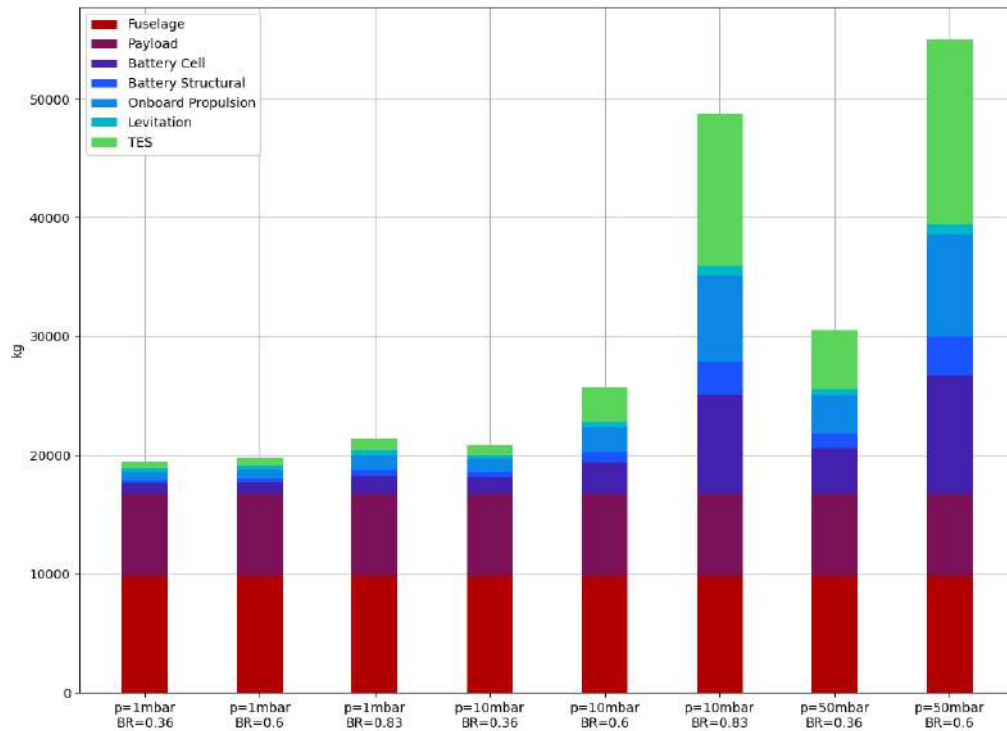
Figure 24: Specific energy consumption of the hyperloop system (in MJ/pkm) for various input designs settings. Each row explores a different dimension: first and third values correspond to the left and right margins of the bars; the second value is captured by the dashed line and indicates the reference case.

4.3.3 Role of aerodynamics

As mentioned above, the energy consumption of a hyperloop system in operation strongly depends on the reduced, but still significant aerodynamic drag. Therefore we investigated three pressure levels (1 mbar, 10 mbar and 50 mbar) combined with three blockage ratios (0.36, 0.6, 0.83) which are commonly used for discussions within the hyperloop community. The split into contributions to the overall operational energy by usage can be seen in Fig. 25a for all the combinations. However, the maximum pressure combined with maximal blockage ratio is not shown, since it becomes physically impossible with the chosen parameters. Specifically, this means that the solver for the pod does not find any valid solution within the boundary of physical solutions (e.g. mass values becoming smaller than zero). The problem occurring is conceptually similar to a thermal runaway: the high power needed means increased cooling and in turn more weight, which recursively enhances the need for cooling etc. This illustrates nicely that the feasibility (in terms of operational energy) strongly depends on the design of the hyperloop pod and the reachable pressure in the tube. Therefore, enhanced research in this area is inevitable.



(a) Operational energy breakdown for different combinations of blockage ratios and powers. The combination 10 mbar, BR=0.6 corresponds to the reference case.



(b) Mass breakdown of the pods shown in Fig. 25a. For combinations of both large blockage ratios and pressure, the majority of the pod weight becomes functional units compared to payload. The combination 10 mbar, BR=0.6 corresponds to the reference case. Design for maximal payload.

Figure 25: Aerodynamic sensitivities

4.4 LCA for linear infrastructure

The LCA evaluates the total cradle-to-grave environmental footprint. In a first step, we compared discrete design choices for what is called “linear infrastructure”, meaning per km of tube/tunnel, not considering stations or vehicle - which are highly dependent on the network. Three cases are thus defined:

- Underground case: Tunnelling through an average geology of the three types defined with *Implenia Schweiz AG*
- Overground case concrete: A post-tensioned concrete pipe based on the scale up of the test-tube of EuroTube elevated on concrete pillars
- Overground case steel: Steel tubes based on a the design by *Hardt Hyperloop* elevated on concrete pillars

Fig. 26 shows the overall environmental impact over the whole life-cycle per meter and direction of linear infrastructure, for a lifetime of 100 years (this means there are e.g. several linings included, which have an assumed lifetime of 40 years only). It is important to highlight that the absolute number of GHG emissions will change with network effects. However, the comparison between the cases described above is still valid.

While the significant contribution of the rail (i.e. guidance system) is equal for all designs, there are fundamental differences in the tube construction between concrete and steel, with the latter contributing more than half of the entire GWP of the steel case. Concrete has a much lower energy consumption involved in the manufacturing process. However, stronger conclusions on the relative assessment of concrete and steel should only stem from detailed dynamic analyses of the material performance under the specific stresses that they will undergo during hyperloop operation. Although tunnelling needs substantially more material, it only increases the GWP by roughly a third compared to the overground case. Fig. 26 also shows a rough comparison with railway, both overground and underground. The overground value is taken from *Ecoinvent* and therefore not split by contribution. As expected, building railway overground is the most environmentally friendly option in terms of construction by far. Knowing this, it seems unrealistic to build too large of an additional infrastructure in Switzerland, especially if it is not even elevated on bridges. The underground estimate for railway was taken as close as possible to the modelling of the hyperloop scenario: In order to obtain a somewhat fair comparison we assumed all the same parameters and methods of construction, but increasing the diameter to 8.5 m (where the Zimmerberg-Basistunnel acts as a reference) and scaling the thickness of the Tübbings and inner vault linearly with the diameter. Apart from much more GHG contributions due to the larger tunnel, railway underground has a more environmentally friendly guideway and no emissions in liner and vacuum system (the liner to waterproof the tunnel is in the main structure material, but hyperloop does have an additional one sprayed on the inner vault).

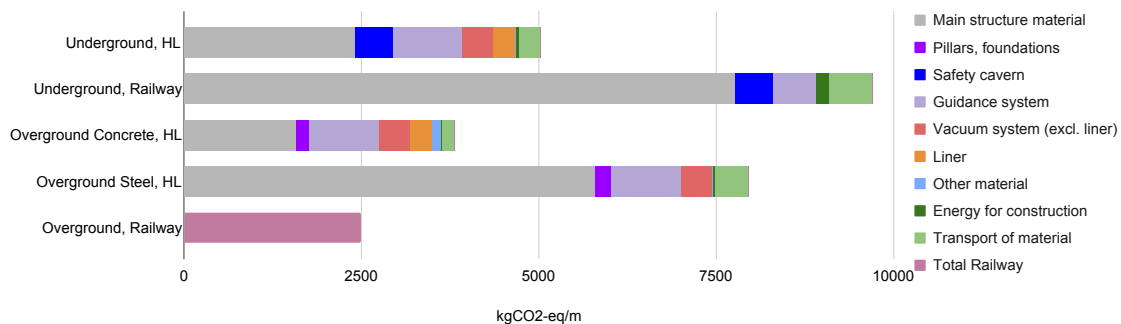


Figure 26: GWP per meter of infrastructure for a lifetime of 100 years. This does not include stations, launching devices or vehicles but is used to illustrate the breakdown into subsystem contributions as well as comparison between ways of construction.

4.5 Cost of linear infrastructure

Fig. 27 shows a first estimate of the cost per kilometre and direction depending on the construction types mentioned above. Although tunnelling is more expensive than an overground construction,

the difference is surprisingly small according to the authors estimate. Land cost in Switzerland, the construction of foundations and pillars as well as post-tensioning and erection are quite costly as well. It can be assumed that the land cost especially in Switzerland would be much higher for extension of railway lines, not even mentioning the legal procedures that might factually prevent any construction of new high-speed lines in Switzerland. It can therefore be expected that, although the construction cost of a hyperloop line is considerable, it is comparable to the costs of a new underground high-speed line (due to the small diameters required by hyperloop) and in some cases even to the construction of an overground line.

The increased cost in the vacuum system underground compared to the two other cases is due to the installation of ventilation shafts for the vacuum system, which are not needed overground. Steel seems to be the costliest option, although this result should be taken with care, since a realistic cost of an optimised mass production of such steel tubes is yet to be established.

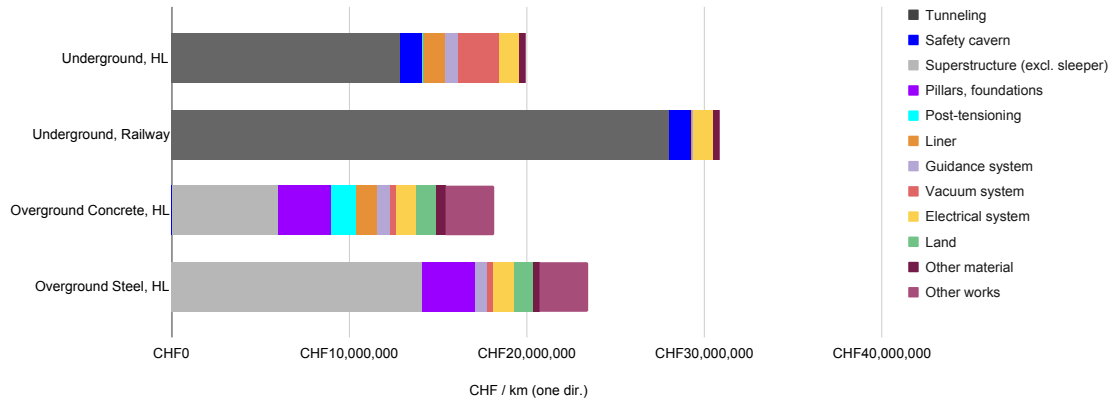


Figure 27: Cost per unidirectional kilometre for construction of linear infrastructure. Additional cost such as vehicles, stations and track-side launching are network dependent.

Fig. 27 also shows a first comparison with railway underground in terms of cost: Diameter and Tübbing/Vault sizes were taken analogously to Fig. 26. One can see that the cost of building a tunnel more than linearly scales with the diameter. The safety cavern was added analogously to the hyperloop scenario as well as the cost for electrical systems and sleepers. The estimate for the rail shall be taken with care since the approach to estimate such large diameters had to be modified. Overground railway can be assumed to be cheaper in terms of construction, but cost are still considerable: High-speed lines in the EU have been estimated to cost around 25 mill. Euros per two-lane kilometre on average [78]. Nevertheless, it can be seen as a first-order estimate.

5 Results for a small network (Swiss case)

For the network assessments most of the system settings introduced in section 4 have been kept the same. However, a few inputs have been adjusted either to conform to the specific network needs or to more thoroughly explore a subset of the parametric space. Considering the variable traffic demand and the relatively short distances of the Swiss case, the sensitivity analyses focus on settings that can affect the acceleration energy or the travel time. Table 7 summarises the system parameters that have been changed for the network analysis and the explored parametric space.

| Parameter | Value(s) | Source | Varied in sections | Value in ref. case |
|-------------------------------------------------------------|-----------------------------------------------------|-------------------------------------------------------|--------------------|--------------------|
| Traffic and Kinematics | | | | |
| Cruise speed | 167 – 250 m/s | own ass. | 5.1 – 5.4 | 250 m/s |
| Max. acceleration/deceleration rate | 1 – 2 m/s ² | own ass. | 5.1 – 5.4 | 2 m/s |
| Acceleration profile | linear / concave (gradually lower at higher speeds) | own ass. | 5.3, 5.4 | linear |
| Minimum headway | 110 s | more conservative ass. | fixed | - |
| Traffic capacity (in one direction) | 6'500 pax/h | based on new min. headway | fixed | - |
| Traffic demand (in one direction) | route-specific | derived in section 5.1 | 5.1 – 5.4 | - |
| Network length | 280+ km | depending on high- or slow-speed bypasses at stations | 5.3, 5.4 | 280 |
| Pod | | | | |
| Passenger capacity | 70 – 200 seats/pod, fixed in each route | based on traffic analysis of section 5.2.1 | fixed | 70 |
| Station | | | | |
| Share of acceleration propelled by track-side launcher | 0% – 100% | own ass. | 5.3, 5.4 | 100% |
| Share of brake energy recuperated by track-side recuperator | 0% | own ass. | fixed | 0% |
| Switch speed at through-stations | high (cruise speed) / low (≈ 50 km/h) | own ass. | 5.3, 5.4 | high |
| Passenger convenience | | | | |
| On- and off-boarding time | 0 – 8 min. | own ass. | 5.1 | 8 |
| Location of hyperloop stations | at railway stations / at highway ramps | own ass. | 5.1 | railway |

Table 7: Parameters changed compared to Table 6 for the investigation of the Swiss network.

The table introduces four additional parameters compared to Table 6 as they can significantly affect the acceleration energy and passenger demand in a network:

- **Acceleration profile:** for Switzerland, the authors had to investigate very small networks. This implies that the use of dozens of kilometres of track-side launching might be ineffective, and thus self-accelerating vehicles were looked at. The power needed to accelerate a vehicle is proportional to the velocity and given by:

$$P_{acc} = \vec{F} \cdot \vec{v} = (\vec{F}_{inertia} + \vec{F}_{EM} + \vec{F}_{aero}) \cdot \vec{v}$$

where the first is the force due to the inertia of the vehicle, i.e. $m \cdot \vec{a}$, the second it the drag due generated by the levitation system (which decreases with increasing speed) and the third the aerodynamic drag, increasing with speed.

It is therefore clear that on self-accelerating vehicles, an acceleration profile should not be linear, since one then over-sizes the motor to fit the power needed at the end of the acceleration phase. Or in different words: it is highly beneficiary to use a concave velocity profile during or combinations of track-side and pod-side accelerations.

- **Switch speed at through-stations:** the network is operated with pods directly travelling from origin to destination skipping intermediate stops. This implies that through-stations

(namely Bern and Lausanne) require a bypass line where transit pods can travel. Here two options are investigated: on one hand high-speed bypasses where transit pods maintain the regular cruise speed; this requires high-speed switches and long acceleration and deceleration ramps for the pods actually stopping at the intermediate stations. The low-speed bypasses version instead forces all pods to slow down at through stations: stopping pods then enter the airlocks and reach the platforms; transit pods remain in vacuum and re-accelerate using the same ramp (with or without launcher) of the stopping pods. This option does not require the complex engineering of high-speed switches and would likely entail significant savings in development and manufacturing costs. The length of the slow-speed bypass is also considerably shorter than the high-speed one and this solution is investigated in sections 5.3 and 5.4 for potential additional savings in costs and emissions.

- **On- and off-boarding time:** it is the sum of the two mode transfer times at the departure and arrival hyperloop stations. It only affects the travel demand (i.e. no impact on energy, emissions or costs) and it is further explored in the next section. In sections 5.3 and 5.4 it is assumed constant and equal to 8 minutes.
- **Location of stations:** two types of station locations are being considered for the hyperloop system: the first type involves locating the hyperloop stations at the same sites as the existing central railway stations; the second type involves positioning the hyperloop stations at the entrances of each city’s highways. This parameters clearly influences the attractiveness of the system for passenger and its impact on demand is investigated in the next section. While in principle the two solutions could also lead to different construction costs, such differentiation is omitted from this study due to the significant modelling and engineering work that would be required to quantify and discriminate the specific construction cost at every single location.

It is finally worth mentioning that while for the launcher the whole range from 0% (fully self-propelling pods) to 100% (full track-side acceleration) is explored, the track-side recuperator has been completely omitted. In preliminary analyses it was observed that the benefits brought by track-side recuperator are negligible compared to its environmental and financial costs. Intuitively, the energy integral that the recuperator captures from the braking pod is significantly lower than the energy integral supplied by the launcher for its acceleration: this is due to the friction forces that act against the pod and reduce the braking energy available for recuperation. Therefore, for the same size (hence footprint and cost) recuperators bring much less benefits to the system than launchers.

5.1 Passenger demand

5.1.1 Scenarios description for passenger simulation

The simulation model induced in the section on passenger demand section 3.3 is applied to various scenarios, depending on the location of hyperloop station, hyperloop operation speed and the transit time at hyperloop stations.

Hyperloop speed: Tests have been conducted for three different hyperloop kinematic profiles:

- “Fast hyperloop”: it achieves a maximum speed of 900 km/h with a constant acceleration of 2 m/s^2 ;
- “Slow hyperloop”: it achieves a maximum speed of 600 km/h with a constant acceleration of 1 m/s^2 ;
- “Slow hyperloop with slow-speed switches”: it operates with the same speed and acceleration of the slow case, but at through station all pods decelerate to allow the stopping ones to exit the main line at slow speed.

Hyperloop transit time: The on-and off-boarding time of passengers at the hyperloop station was taken into account and two different settings were considered. The first setting is referred to as “No transit time” indicating minimal or negligible time required for passenger transfers, which is an idealised scenario and mainly an intermediate step in the simulation process. The second setting “5+3 transit time” involved times of 5 and 3 minutes for on- and off-boarding, implying a more structured and defined process for passenger embarkation and disembarkation. A simulation for 20 minutes transit time was added as well for assumption of extensive security checks.

Hyperloop station: Both types of station locations are considered for the demand analysis. In the following sections they are referred to as “hyperloop at centre railway stations” and “hyperloop at highway entrance”.

We combined the aforementioned different settings to create 6 scenarios. We conducted separate simulations in each scenario to study potential hyperloop users based on whether they currently utilise public transport or private cars.

5.1.2 Average daily hyperloop passengers on each segment

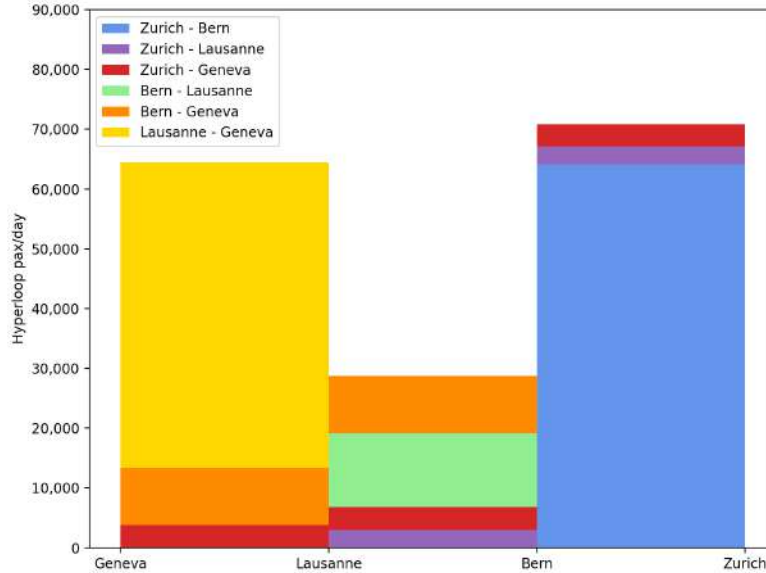


Figure 28: Average daily hyperloop passengers on each segment in 2050.

Fig. 28 illustrates the average daily hyperloop passenger numbers (y-axis) for each segment of the Geneva-Lausanne-Bern-Zurich line (x-axis) in both directions (i.e. summed for both ways). The data represent results obtained from passenger simulations conducted for the scenario “Fast hyperloop - No transit time - hyperloop at central railway stations” in the year 2050. These passenger numbers include individuals who currently use public transport, private cars, and aviation but would switch to the hyperloop system in the future.

Among the different segments, the Zurich-Bern sector stands out with the highest number of passengers, reaching 70,880 passengers per day. Notably, approximately 90% of these passengers travel specifically between Zurich and Bern, represented by the blue colour on the labels. The second-largest section is the one between Lausanne and Geneva, with 64,467 passengers per day. Within this segment, 79.2% of the passengers are individuals who specifically travel between Lausanne and Geneva, depicted by the yellow colour. On the other hand, the passenger flow between Lausanne and Bern is comparatively lower, with 24,956 passengers per day. Within this segment, only about 50% of the passengers are specifically travelling between Lausanne and Bern, indicated by the green colour on the labels. For passengers travelling between Zurich and Geneva (red colour), a significant portion of these passengers is expected to shift from aviation to the hyperloop system in the future.

Overall, the data suggest that the hyperloop line would have a substantial impact transport on the east-west connection. attracting a considerable number of passengers in each segment, particularly between major cities like Zurich and Bern.

5.1.3 Mode split of passenger-kilometres

In this section, Fig. 29 and Fig. 30 present the distribution of various transport modes based on passenger-kilometres per day (millions) for the years 2017 and the projected future of 2050 (entirety of Switzerland, not only the considered network). The x-axis displays the model split in passenger kilometres per day, while the y-axis represents the different transport modes. Each transport mode is represented by a distinct colour: blue corresponds to public transport (PT), red indicates hyperloop, green represents aviation, and yellow represents private cars. The presented results correspond to a specific scenario “Fast hyperloop - No Transit Time - hyperloop at Central Railway Stations”.

Fig. 29 focuses on the travel distances of passengers equal to or greater than 50 km, providing insights into how different transport modes were utilised in 2017 and how they are projected to be

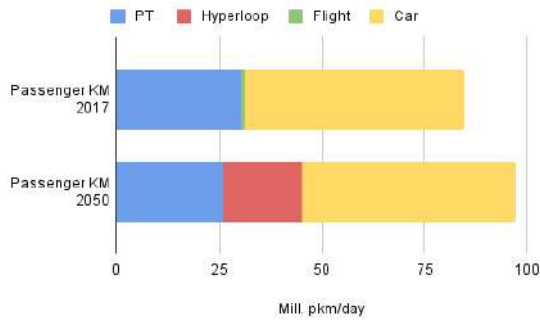


Figure 29: Mode split pkm (≥ 50 km).

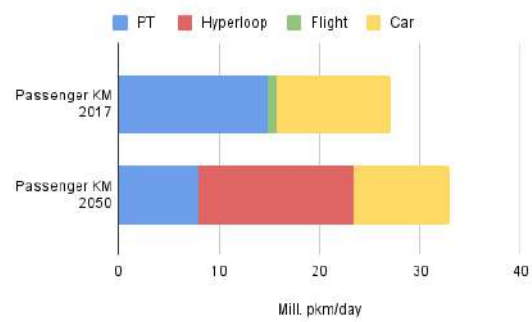


Figure 30: Mode split pkm (≥ 100 km).

used in 2050 for these longer journeys. By 2050, hyperloop is predicted to account for 19.7% of the overall transport market. Meanwhile, public transport is expected to experience a shift, slightly decreasing from 35.7% in 2017 to approximately 26.6% by 2050 for the selected distance.

Fig. 30, on the other hand, examines the model split for travel distances of passengers equal to or greater than 100 km, giving a specific analysis of the transport mode distribution for these even longer trips in the same years. The data depicted in the figure clearly illustrates the competitive edge of the hyperloop, particularly for long-distance travel. It shows that the hyperloop is poised to capture nearly half of the market share across all modes of transport. This dominance can be attributed to the significant advantage the hyperloop offers in terms of distance coverage and speed, making it an attractive choice for a large portion of travellers, especially for longer journeys.

5.1.4 Shift from each mode of transport to hyperloop

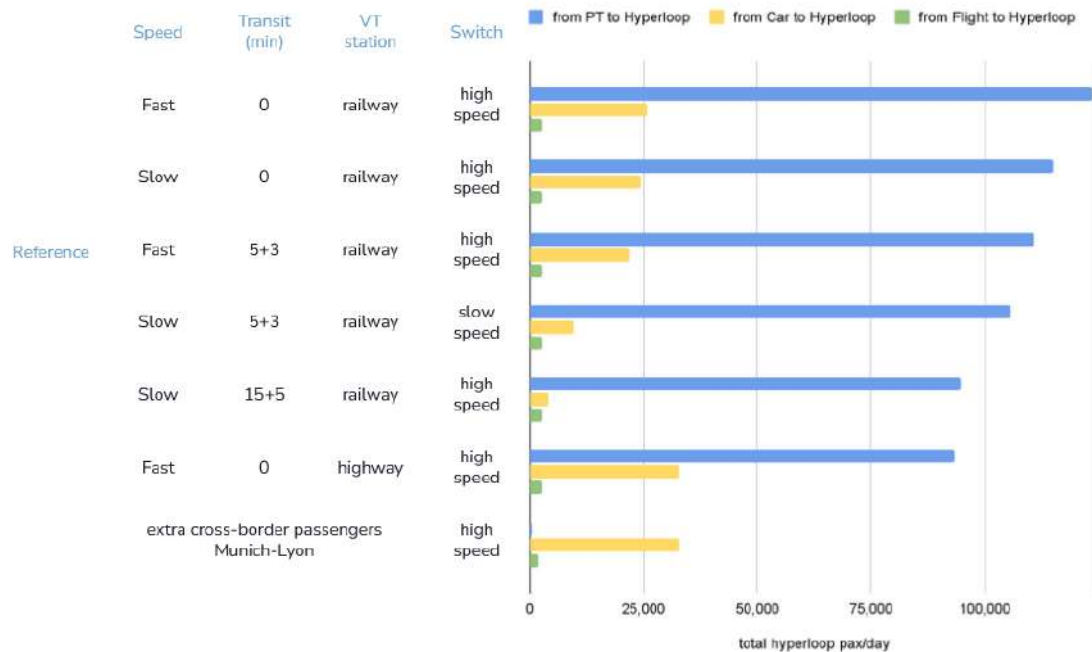


Figure 31: Shift from each mode of transport to hyperloop in 2050.

Fig. 31 presents various outcomes regarding the shift of passengers (per day, x-axis) from other transport modes, such as public transport, private cars, and aviation, to the hyperloop in different scenarios of passenger simulation (y-axis).

The reference scenario is “Fast hyperloop - 5+3 mins transit time - hyperloop at Central Railway Stations”. In this scenario, 142,067 passengers/day will travel by hyperloop in 2050. 81.3% of the hyperloop passengers are shifted from public transport (blue), 16.9% from private cars (yellow), and the rest from aviation (green). It is important to understand that with the growth projected for the number of railway passengers, this does not imply that the railway will experience a significant decrease in passengers, but that vacuum transport can help to accommodate all passengers.

| Travel times in min | Car | Railway 2023 | fast HL | slow HL | slow HL, slow-switches |
|------------------------|-----|--------------|---------|---------|------------------------|
| Zürich-Bern | 96 | 57 | 16 | 21 | 21 |
| Zürich-Lausanne | 156 | 135 | 22 | 30 | 36 |
| Zürich-Geneva | 195 | 163 | 26 | 36 | 47 |
| Bern-Lausanne | 77 | 73 | 15 | 19 | 19 |
| Bern-Geneva | 117 | 117 | 18 | 24 | 30 |
| Lausanne-Geneva | 58 | 37 | 12 | 14 | 14 |

Table 8: Comparison of travel times with car and rail today and the Hyperloop variants fast, slow, and slow with the need to slow down for switching as well. Passenger transit times are excluded.

When comparing the “Fast hyperloop” to the “Slow hyperloop”, it is observed that the number of passengers shifting from public transport and private cars to the hyperloop decreases. The reduction in the number of passengers from public transport is more significant than that from private cars.

Next, the analysis includes changes in transit time for passengers from “No Transit Time” (which was performed in the process of the simulation, but does not suggest to become reality) to “5+3 Transit Time”. In this case, it is shown that the number of passengers shifting to the hyperloop from public transport and private cars decreases further. This reduction is even more substantial compared to the shift observed with the “Slow hyperloop.” This finding emphasises the importance of efficient passenger organisation at hyperloop stations, as a fast and seamless entering and leaving process significantly impacts the demand for the hyperloop.

We also simulated the case of switches which work only at low speeds, since the proof of concept for a full-scale and full speed switch is yet to be performed. This means slowing down at stations in which the vehicle does not stop. As shown later in this work, for the small distances in Switzerland, this might be favourable compared to long on- and off-branching ramps.

Additionally, the study explores the effects of changing the hyperloop station location from “hyperloop at Central Railway Stations” to “hyperloop at Highway Entrance”. The results show a decrease in the number of hyperloop passengers coming from public transport, while the number of hyperloop passengers from private cars increases. However, the increase in passengers from private cars is lower than the decrease in passengers from public transport. Consequently, if the goal is to maximise the total number of hyperloop passengers, it is recommended to place hyperloop stations at central railway stations where accessibility from the cities is better. However, if future plans involve placing hyperloop stations at highway entrances, providing improved access to these stations from the cities is crucial.

Furthermore, the cross-border passengers between Munich and Lyon going through the Swiss corridor are also considered. The figures indicate that approximately 32,976 passengers per day will transition from private cars to the hyperloop, with the majority of this shift occurring between Lyon and Lausanne. An estimated 2,000 passengers per day will also switch to the hyperloop from the aviation sector, specifically from routes between Munich and Geneva, as well as between Lyon and Zurich. It’s important to note that these numbers represent the direct shifts without taking into account any additional induced demand arising from the convenience of the hyperloop service.

5.2 System operation and fleet sizing

5.2.1 Fleet sizing

Equation 1 shows that different traffic magnitudes can be accommodated by either adjusting the vehicle size or the travel frequency. Even though Fig. 36 shows that the traffic on each route depends on the exact system settings, the orders of magnitude are not significantly affected. In the interest of simplicity, this study thus assumes that a specific vehicle size is assigned to each route and that only the travel frequency is adjusted to meet different passenger demands. Therefore, a single demand scenario is analysed to heuristically determine the more appropriate vehicle sizes: the “Fast hyperloop” scenario without transit times is selected for this purpose. Even if this might not be the case closest to reality it is the most conservative one when sizing the vehicles/fleet.

Fig. 32 collects the outputs of the passenger demand module used to size the vehicles. The x-axis indicates the distance between origin and destination, which sets the requirement for the range of the vehicles. The y-axis displays the passenger traffic at rush hour, which relates to the seat capacity required to ensure a certain headway. From their placement in the plot two groups

of routes can be identified:

- connections requiring long range and lower seat capacity (Geneva – Bern, Geneva – Zurich, Lausanne – Zurich);
- connections requiring shorter range but larger seat capacity (Geneva – Lausanne, Bern – Zurich).

The Lausanne – Bern route could be served by either option, but in order to increase energy efficiency and headway between vehicles the larger short-range pods are assigned.

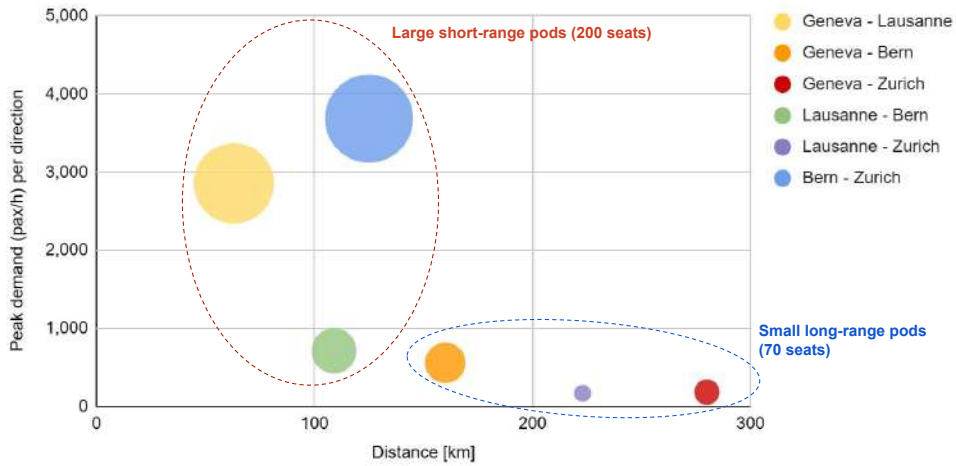


Figure 32: Rush hour passenger traffic (y-axis) and journey distance (x-axis) for each Swiss connection. These are the two main features used to group the routes into two categories, so that each that can be served by a unique vehicle type. The bubble size is proportional to the average daily traffic.

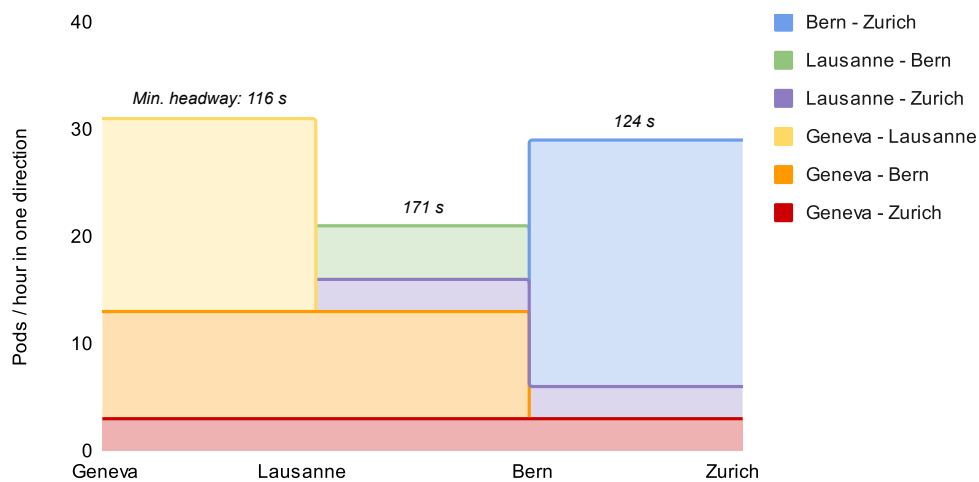


Figure 33: Pod traffic at rush hour on each segment of the network for the “fast hyperloop” scenario; the colours identify the origin – destination routes travelled by the pods.

This results in a simple hyperloop system with just two types of vehicles that complementarily serve all routes of the network without excessive over-dimensioning. In addition, the reciprocity between pod ranges and seat capacities minimises the requirements on the infrastructure side, e.g. when designing a track-side launcher suitable for both types of vehicle.

The range of the two vehicle types is set based on the longest served route with the addition of a small buffer: this results in 150 km and 300 km of range respectively. The seat capacity is heuristically determined to fulfil the headway requirements set in section 3.4.1: pod capacities of 70 and 200 seats turn out to be suitable. Fig. 33 shows the resulting hyperloop traffic *at rush hour* on each segment of the network; it resembles Fig. 28, but with the y-axis representing pods travelling in each direction and not passengers. The plot height inversely correlates to the headway

between the vehicles, which is reported in text above each segment. With the demand derived from the “fast hyperloop” scenario and the assigned seat capacities, the minimum headway at rush hour is 116 seconds and occurs between Geneva and Lausanne.

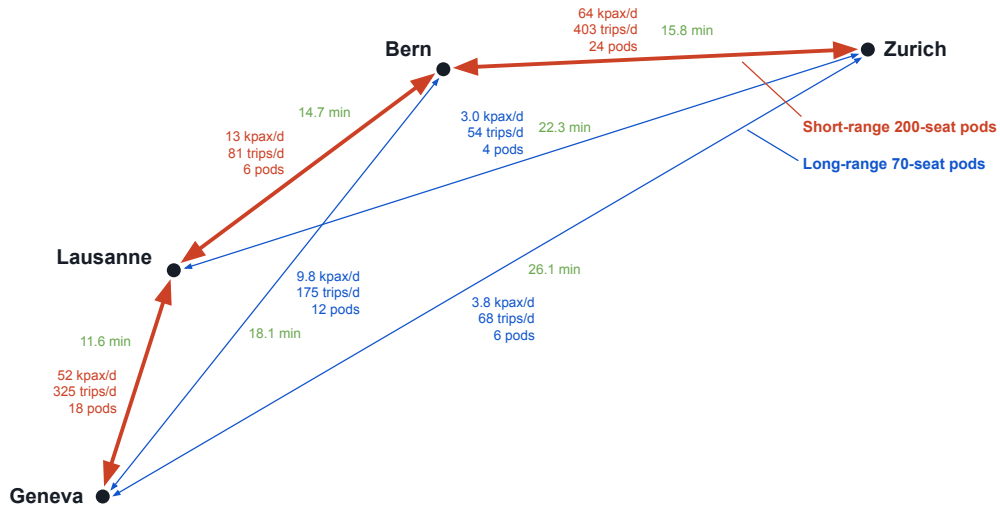


Figure 34: Daily passenger and pod traffic in both directions for each route of the network for the “fast hyperloop” scenario. Also the travel time and the minimum number of vehicles dedicated to each route is indicated. The colour refers to the assigned vehicle type.

Fig. 34 summarises the main operational features of the hyperloop network for the “fast hyperloop” demand scenario and the chosen vehicle sizes. Beyond passenger and pod traffic, the plot reports the number of vehicles simultaneously assigned to each route. This follows from the traffic at rush hour and the time it takes for a pod to return to the station of origin and be available for a new departure (assumptions made in the “system design” module). Despite their higher capacities and shorter distances, the network still requires more large pods, as the traffic in the Geneva – Lausanne and Bern – Zurich routes is particularly significant.

5.3 Network life-cycle assessments

In the following environmental and economic assessments the parametric space explored slightly differs from Section 5.1. The purpose here is to identify the system design that minimises the environmental impact and/or the system costs, thus parameters that solely influence the demand without impacting the design have been neglected. Namely:

- the **on- and off-boarding time** has been fixed to 8 minutes: it goes without saying that reducing it is beneficial for the system, but varying it does not help identifying the optimal macro design features (e.g. cruise speed).
- the **location of hyperloop stations** has been fixed to “centre railway station”, as it gave the best traffic outcome in Section 5.1. In reality, the actual location of the hyperloop stations would significantly affect the costs and at some extent also the LCA, but the complexity of such modelling is out of this study’s scope, as is the precise routing of the line.

All other kinematic parameters of Table 7 instead influence both the system design (hence costs and emissions) and the passenger demand and have thus been investigated⁹. A good share of the parametric space explored with the sensitivity analyses can be graphically summarised with Fig. 35, which depicts six examples of the acceleration profiles tested in the investigation.

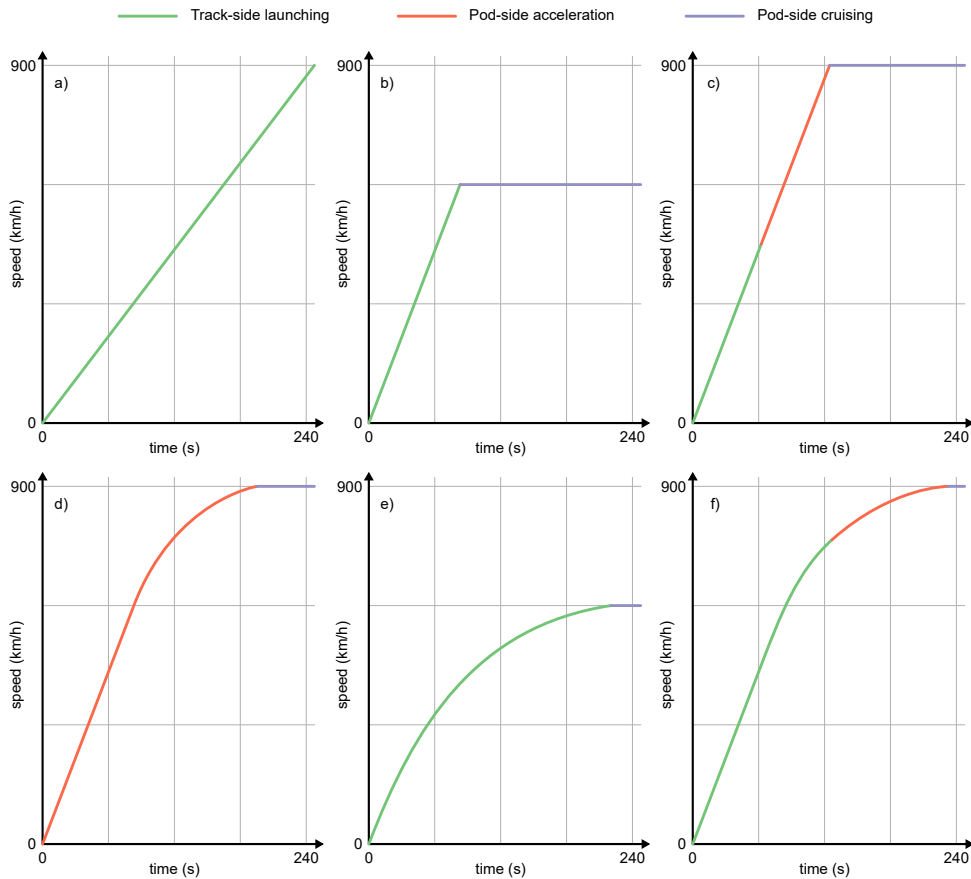


Figure 35: Six examples of pod acceleration profiles that have been tested in the study. The colour indicates whether the pod is being accelerated by the launcher, by its own propulsion, or it is simply cruising. a) is the reference case from section 4, with a slow 1 m/s^2 acceleration to the top speed of 900 km/h fully propelled by the launcher; case b) depicts a launcher-propelled 2 m/s^2 acceleration to 600 km/h ; in case c) the acceleration is provided by the launcher up to 450 km/h , then by the pod; case d) shows a fully self-accelerated pod, but with a gradually lower acceleration rate at higher speeds; case e) displays a fully concave acceleration profile propelled by the launcher; case f) combines all of the above, with a concave acceleration profile propelled by both launcher and pod. All these combinations and more have been tested in the simulation.

In general, any combination of 1) cruise speed, 2) acceleration rate, 3) shape of acceleration profile, and 4) share of launcher-aided acceleration has been tested in the following sections. The

⁹For the cruising speed, 600 km/h ($= 167 \text{ m/s}$) has been chosen for the lower end.

5th and last parameter explored in the following analyses is the speed of switches and transit bypasses at through stations. The combination of these 5 features results in the simulation and evaluation of approximately 2'000 different system configurations.

5.3.1 Travel time sensitivity

The system configurations tested in the network assessment exceed the 6 demand scenarios tested in Section 5.1 and presented in Fig. 31. In order to approximately estimate the passenger demand for all these new cases, Fig. 36 presents a generalisation of the passenger demand results.

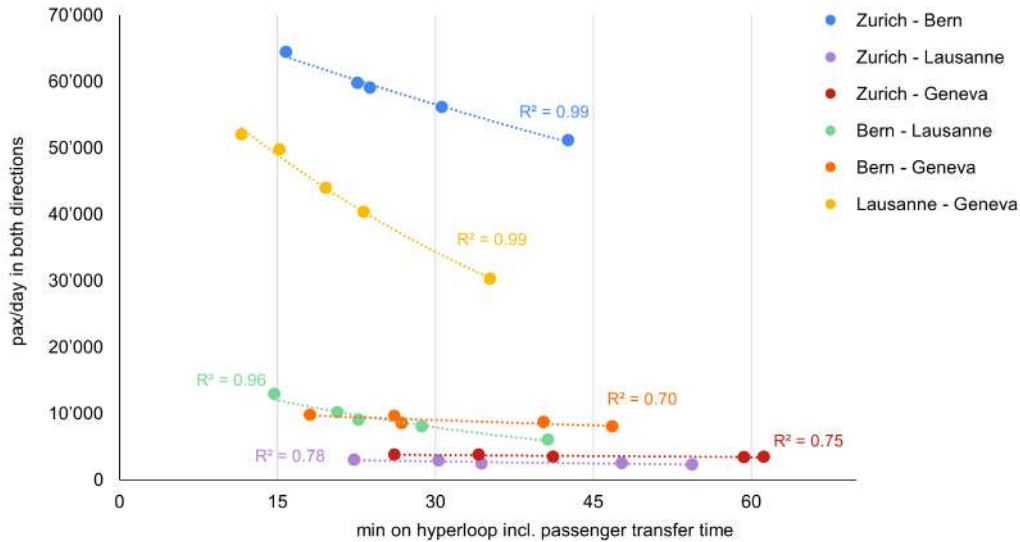


Figure 36: Bi-directional daily passenger flow by hyperloop (y-axis) for a given total travel time (x-axis) on each route. The travel time includes the time needed to change mode (if required) at both origin and destination. Passenger numbers include modal shift from road, rail, and plane and are set in 2050.

For each route, Fig. 36 presents the total travel time (on-route and transit, x-axis) and the total hyperloop traffic in 2050 (pax/day in both direction, y-axis) including mode shift from public transport, private cars and domestic aviation. The plot predictably reveals a clear correlation between passenger demand and total travel time, especially evident for the more crowded Zurich – Bern and Lausanne – Geneva segments.

In order to derive a consistent fitting line, only the 5 scenarios of Fig. 31 where the the hyperloop stations are located at central railway stations are included. Exponential functions of the form $y = e^{-ax}$ have been chosen for the interpolation due to their monotonicity and strict positiveness; the coefficients of determination (R^2) also display an adequately high score.

These functions are used to automatically link the “system design” and “passenger demand” modules of Fig. 11 by returning the passenger flow on each route for a given total travel time.

5.3.2 Energy consumption

Fig. 37 presents the overall annual results of the network in terms of passenger traffic and energy consumption for all the explored system configurations. Each point corresponds to a different combination of the 5 varied system settings mentioned in Table 7. Overall, higher passenger traffic can be achieved by increasing the total energy consumption, but the milder solutions on the left seem to be more energy-efficient in terms of kWh/pkm.

The cruising speed has the highest impact on the travel time, hence on the passenger traffic, and the different system configurations can be clustered into two blocks, with the points on the left with a cruising speed of 600 km/h and the ones on the right with 900 km/h. Beyond the passenger traffic, speeds strongly impacts the energy demand, with all points to the left displaying lower annual or specific energy consumptions than the right ones.

The presence of a launcher also significantly affects the energy consumption: yellow points refer to purely self-propelled vehicles and display higher energy demands than the purple points, which describe systems with track-side launchers.

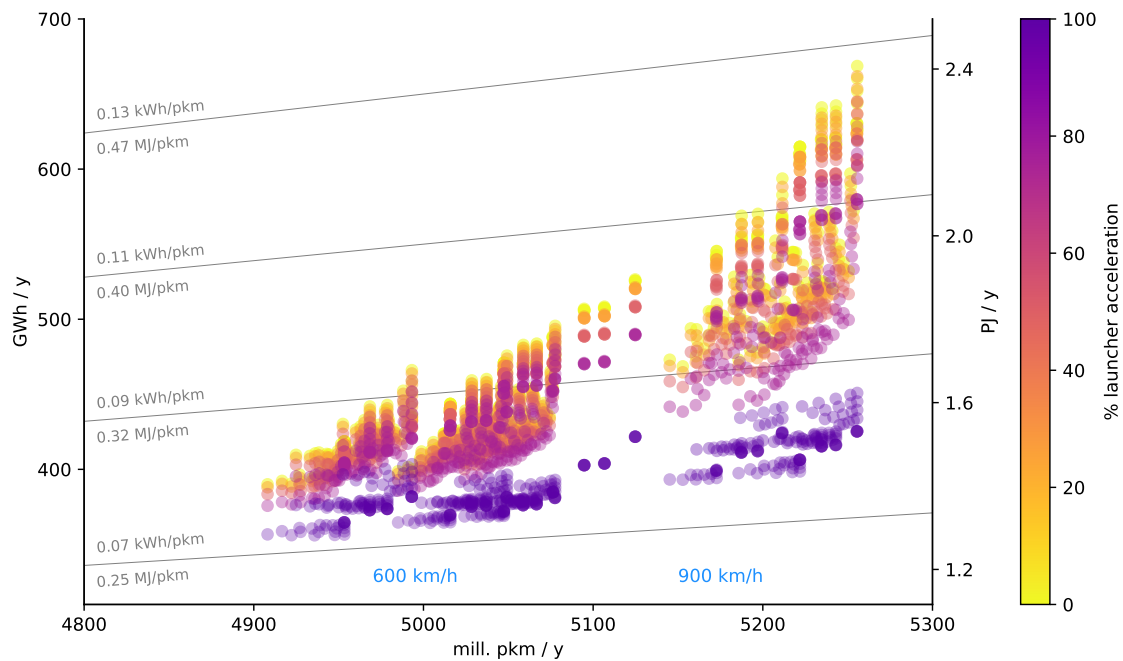


Figure 37: Annual electricity consumption (left and right y-axes) and passenger traffic (x-axis) for different system configurations. The colour indicates the share of the acceleration phase propelled by the track-side launcher. The points to the left correspond to system configurations with a cruising speed of 600 km/h, the points to the right to 900 km/h.

The role of the launcher in the energy consumption is more visible in the breakdown displayed in Fig. 38. The large variety of system configurations displayed in Fig. 37 is compressed into 10 groups based on cruise speed and share of acceleration propelled by the launcher. The stacked coloured bars show the breakdown of the average energy consumption in each group, while the variability lines show the range of net total energy consumption in each group (by changing the other three parameters: acceleration rate and profile and transit bypass speed).

For shorter routes in the Swiss network case, the relative impact of various energy components shifts noticeably. Vehicle acceleration and vacuum assurance become more significant contributors to energy consumption than aerodynamic or electromagnetic drags when the vehicle is at top speed. Consistent with general sensitivity analyses, the analysis shows that higher speeds inevitably lead to increased energy consumption, particularly due to the elevated energy requirements for acceleration.

The launcher emerges as a pivotal element in this energy equation. By taking over the demanding acceleration phase, the launcher not only reduces the energy consumption but also contributes to making the pods lighter and more energy-efficient. This reduction in pod weight is further influencing the decrease in brake energy recuperation, a mechanism that operates with constant efficiency and is always situated on the pod side. Its efficiency varies directly with the available kinetic energy before the braking process begins.

Conclusively, from an energy consumption perspective, the most optimal configurations are those that feature lower top speeds, higher acceleration rates, and a launcher-aided acceleration phase. These configurations result in an energy consumption rate of approximately 0.075 kWh/pkm for pod operation and vacuum assurance.

5.3.3 Life-cycle assessment

Fig. 39 shows the specific global warming potential of the full life-cycle of the hyperloop system, measured in gCO₂-eq./pkm. The same grouping and visualisation notation of Fig. 38 is used. Beyond the different system configurations, the variability lines here account also for different geological contexts (e.g. different soils or shares of under- and over-ground tubes compared to the 50%-50% scenario here investigated). This explains why the range of the variability lines exceeds the minimum and maximum points of Fig. 40.

The largest contributor to emissions in the system is the linear infrastructure, which includes el-

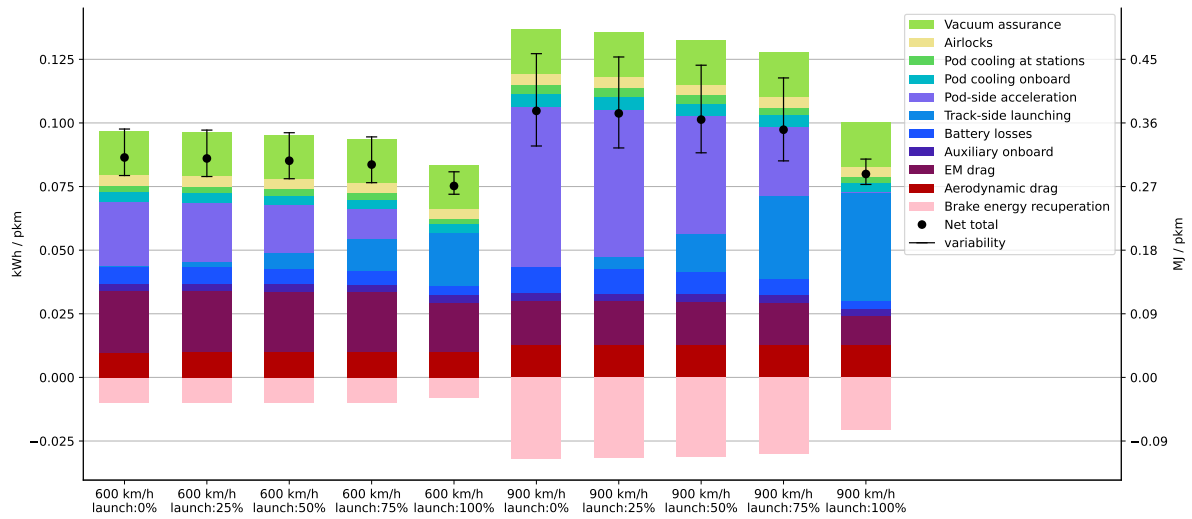


Figure 38: Breakdown of the specific energy consumption per pkm for various system configurations, grouped by cruising speed (600 or 900 km/h) and share of acceleration propelled by the track-side launcher.

ements in grey and purple shades but excludes buildings. This is in line with the findings presented in Fig. 26¹⁰. Following closely behind in terms of climate impact are the pods, particularly due to the consumption of fuselage and electrical batteries. The consumption rate of these components is assumed to be simply proportional to the number of cycles experienced by the pods, i.e. by the number of end-to-end trips (see Table 6 for the specific values). The impact of speed, heating or other characteristics on these consumption rates has thus been neglected.

Interestingly, the use of the launcher for acceleration does reduce battery consumption, but it also increases the upstream emissions related to its production. This is especially true for higher speeds, as the length of the launcher must be increased, thereby enlarging its environmental footprint. It shall be noted that the introduction of solid-state batteries might increase the lifetime and environmental impact considerably by 2050.

Energy consumption is a less significant factor, thanks to the clean electricity mix used, as detailed in Table 6. In addition to the energy used for propelling the pods and maintaining the vacuum, energy for cooling the infrastructure has also been considered, although it has not been explicitly modelled. This was estimated based on railway requirements for tunnel cooling, as cited in [79].

Lastly, when comparing the ten different groups, they all show a similar range of emission values. However, the self-propelling cases generally perform better than those that rely on launchers. Interestingly, a launcher-based approach with a 50 percent contribution shows slightly lower emission values, indicating that there is an environmental trade-off between investing in pod batteries and track-side motors.

However, a large share of the variability remains unexplained by the speed or the launcher configuration. The scatter plot of Fig. 40 shows that a third feature has the largest influence on the system GWP: the speed of the transit bypasses in through stations.

By avoiding the long ramps required for high-speed bypasses, solutions with slow bypasses achieve significant savings in grey emissions for the infrastructure. This follows from the prominent role that the linear infrastructure has in the overall system footprint. The slow-bypass configuration (red points) clearly leads to less traffic due to the longer travel times, but Fig. 40 shows that this is balanced out by the emissions savings: slow-bypass solutions achieve not only lower total emissions (y-axis) but also lower specific emissions per pkm (grey lines). Slow-bypass systems approach specific emissions in the order of 8.5 gCO₂/pkm.

The demand reduction due to the slower bypasses speed is not particularly significant because the affected routes are not the most relevant for the network traffic. Figures 28 and 36 show that the large majority of hyperloop traffic is on the Zurich–Bern and Lausanne–Geneva routes, both of which have no intermediate stops and thus are not affected by the bypass speed.

Systems where either Bern (orange) or Lausanne (green) has slow bypasses while the other

¹⁰Assuming that the infrastructure is made of concrete and is equally divided between underground and above-ground structures.

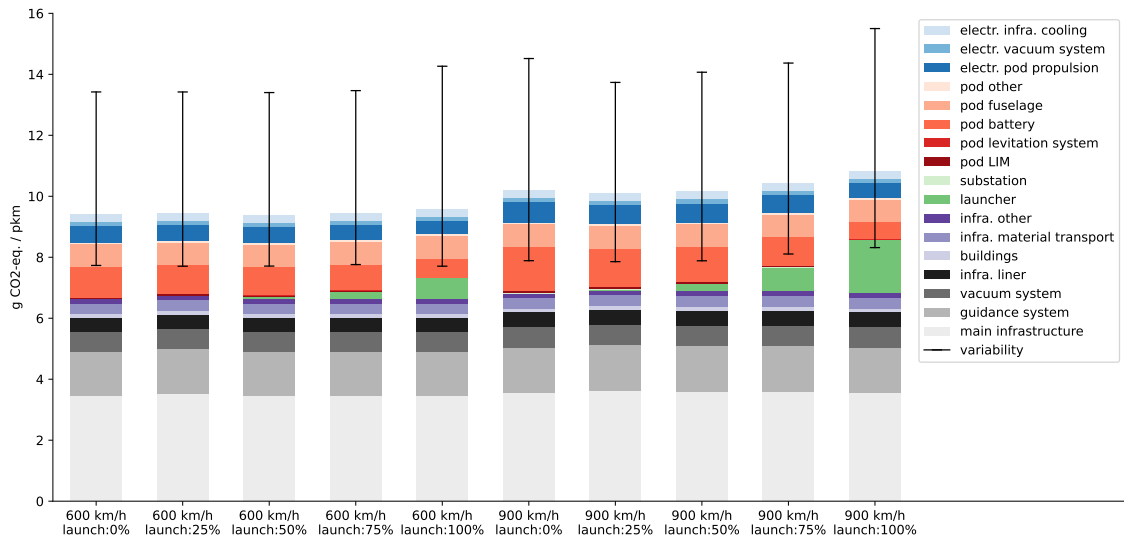


Figure 39: Breakdown of the specific LCA emissions per pkm for various system configurations, grouped by cruising speed (600 or 900 km/h) and share of acceleration propelled by the track-side launcher.

station has faster ones behave similarly to each other. Interestingly, in terms of annual emissions the two solutions are virtually identical, but in terms of passenger traffic placing the slow bypasses in Bern is more beneficial. This is due to the higher passenger demand from/to Bern compared to Lausanne: forcing all vehicles to slow down in Bern is less detrimental than doing so in Lausanne because there is a larger share of traffic that would have stopped in Bern anyway; in Lausanne instead there is a larger share of transit passenger that would find themselves slowing down without the need to stop there.

Finally, constructing high-speed bypasses at both stations (blue points) obviously leads to the highest passenger traffic, but the price in terms of grey emissions does not seem to pay off.

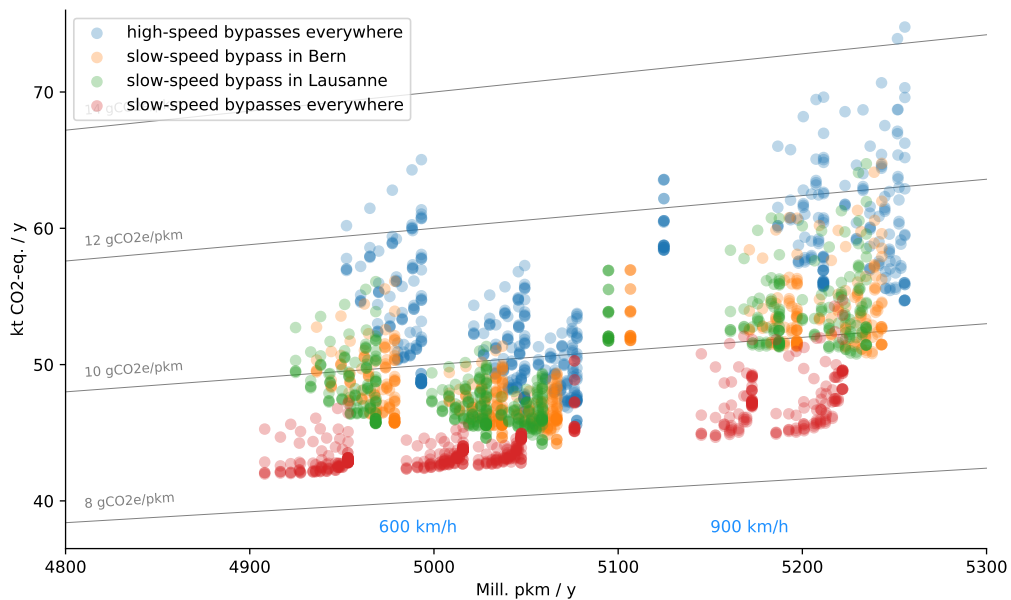


Figure 40: Annualised life-cycle emissions (y-axis) and passenger traffic (x-axis) for different system configurations. The colour indicates which through stations employ high- or slow-speed transit bypasses. The points to the left correspond to system configurations with a cruising speed of 600 km/h, the points to the right to 900 km/h.

5.4 Network economic assessments

Fig. 41 presents the investment costs (i.e. CAPEX) required to build the whole system, grouped by the same speed and launch parameters as Fig. 38 and 39. These expenditures exclude the purchase of vehicles as their renewal rate is rather high and we consider them as operational costs (i.e. OPEX). As for the LCA, also here the variability lines account for different system configurations, soil composition and shares of under- and over-ground structures.

The proposed Swiss hyperloop network could be constructed for 15–25 bill. CHF depending on the specific configuration (excluding any type of development cost). The relatively low estimate follows naturally from the costs per km of linear infrastructure seen in Section 4.5. The estimate can likely increase if a larger share of network has to be moved underground, which is plausible scenario in Switzerland. Moreover, unforeseen additional costs are common to occur in large infrastructure projects (e.g. 50% more for the Gotthard base tunnel). These factors combined could lead to a network cost of 30–40 bill. CHF.

The CAPEX distribution between the different subsystems follows the breakdown of Fig. 27, with the non-marginal addition of buildings for the stations. The high cost of stations is primarily due to their modelling, which follows the realised historical expenditures to build railway stations in Switzerland: being large in volume and often underground in cities, the construction of railway stations has been considerably expensive and this is likely to apply also to hyperloop stations.

By comparing the CAPEX and LCA breakdowns (Fig. 41 and Fig. 39) one can see an interesting shift from metal-based components to concrete-based components; namely, launcher and guidance system have a relatively higher importance in the system footprint than in the capital expenditure. This is because the cost factor between steel and aluminium on one side and concrete on the other is lower than the corresponding environmental factor.

Overall, the 10 different macro-configurations show similar total values and breakdown, since the largest CAPEX component (linear infrastructure) is not influenced by the two varied parameters. Fig. 43 will show that adjusting the bypass speed and length has a stronger impact on the total system costs and explains most of the observed variability.

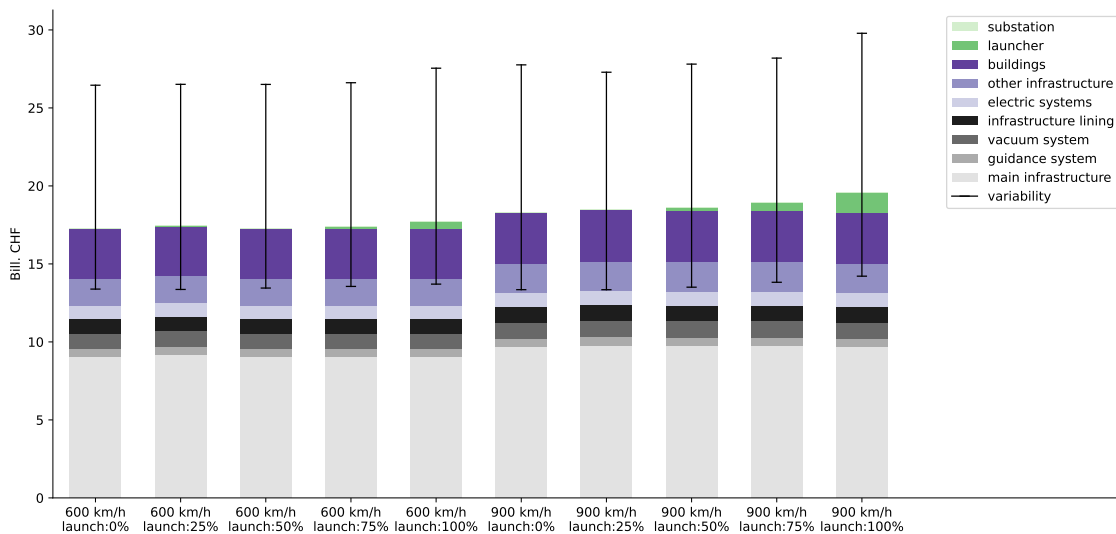


Figure 41: Breakdown of the full CAPEX of the network for various system configurations, grouped by cruising speed (600 or 900 km/h) and share of acceleration propelled by the track-side launcher.

Fig. 42 shows the annual operating costs of the system with the same visualisation notation of the previous plots. The variance in each group reduces as no impact of the route or geology is modelled for the OPEX.

While significant, the purchase and maintenance of the pods is not a particularly large component of the OPEX. However, there is a shift in the relative importance of pod components compared to the LCA: batteries are responsible for more than 50% of the vehicle-related CO₂ emissions, but account for less than 20% of their costs. This is thanks to the huge cost reduction that batteries have achieved in recent years, while the price of pods is based on large Maglev trains that have not reached mass-production yet and may not benefit from the same economies of scale.

As in most transport companies, the largest source of OPEX is the cost of personnel. Even in a substantially automatized and concentrated transport business like hyperloop it is important to

have personnel at the stations and in the vehicles supporting passengers and all processes. This unavoidably increases the operational costs.

In terms of OPEX, adding a launcher is purely beneficial: on one side the system becomes more energy efficient and all electricity-related expenditures reduce, on the other the battery requirements drop and their management becomes cheaper.

Fig. 44 shows from an annualised perspective the trade-off between more CAPEX-intensive systems with a launcher and more OPEX-intensive configurations without it.

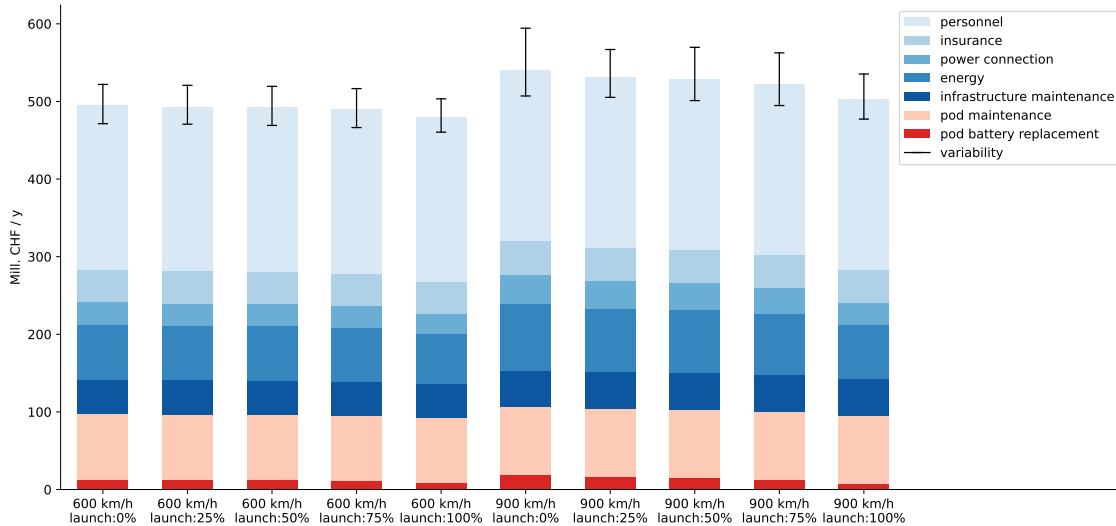


Figure 42: Breakdown of the annual OPEX of the network for various system configurations, grouped by cruising speed (600 or 900 km/h) and share of acceleration propelled by the track-side launcher.

In Figures 43 and 44 and CAPEX and OPEX have been aggregated by annualising the CAPEX via their lifetimes. The original lifetime of all components has been used, with a cap at 60 years; i.e. infrastructure components with a likely lifetime of 80–100 years have been annualised so that they would be depreciated in “just” 60 years. This is more aligned with standard investment evaluations, where a financial payback time is employed rather than the technical lifetime of the components. After taking into account the shorter lifetimes of other components such as liner and pumps, the average CAPEX lifetime results in the order of 53 years. Importantly, no discount factor has been taken into account as this work is not comparing investments strategies between different infrastructure projects (no revenue is estimated). The goal is simply to estimate the total system costs over the plausible lifetime of the infrastructure.

Fig. 43 compares the annualised expenditure with the induced passenger traffic and shows a more compromising solution than the corresponding environmental assessment (see Fig. 40). Faster hyperloop configurations naturally attract more passengers, but the cost for this service is not significantly higher. Indeed, the normalised cost per pkm is approximately even, as also visible in Fig. 44.

However, Fig. 43 clearly highlights the superiority of the slow-speed bypasses. As observed above, the CAPEX are heavily weighted on the linear infrastructure and avoiding the long ramps required for high-speed bypasses brings important financial savings. This cost reduction is stronger than the penalty in lost travellers and overall also the CHF/pkm metric rewards the slow bypass systems.

In Fig. 44 the annualised expenditures have been divided by the captured passenger traffic to compare the net costs per travelled pkm. The breakdown shows that annualised costs are dominated by the OPEX, which cover more than 60% of the total costs. The variation between the 10 groups is minimal, with the savings in energy and battery replacement slightly surpassing the depreciation of the launcher.

Overall, systems with lower cruising and bypass speeds and with launcher-aided acceleration display the lowest specific costs, approaching 0.17 CHF/pkm.

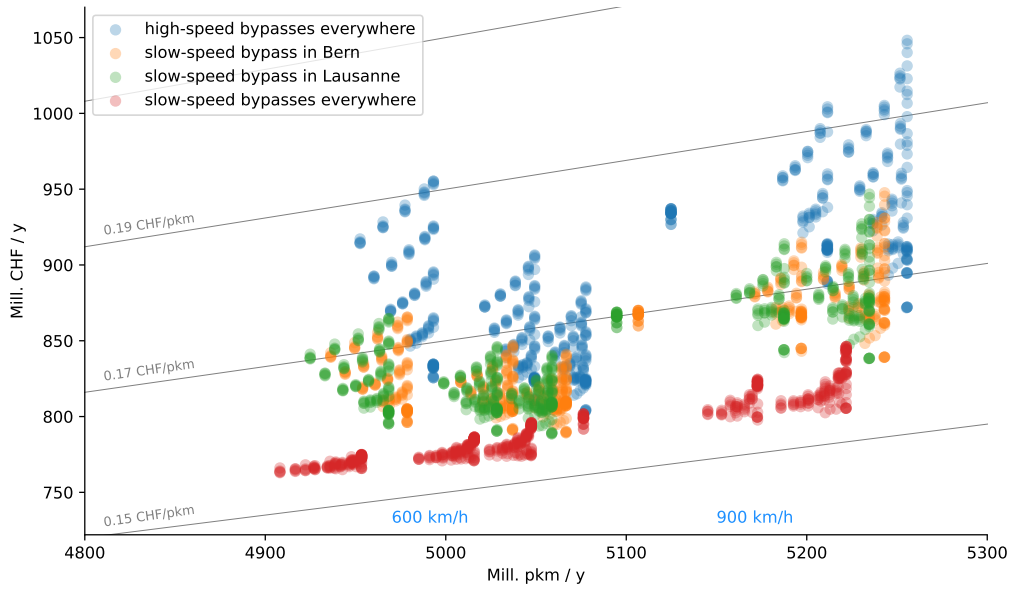


Figure 43: Annualised system costs (y-axis) and passenger traffic (x-axis) for different system configurations. The colour indicates which through stations employ high- or slow-speed transit bypasses. The points to the left correspond to system configurations with a cruising speed of 600 km/h, the points to the right to 900 km/h.

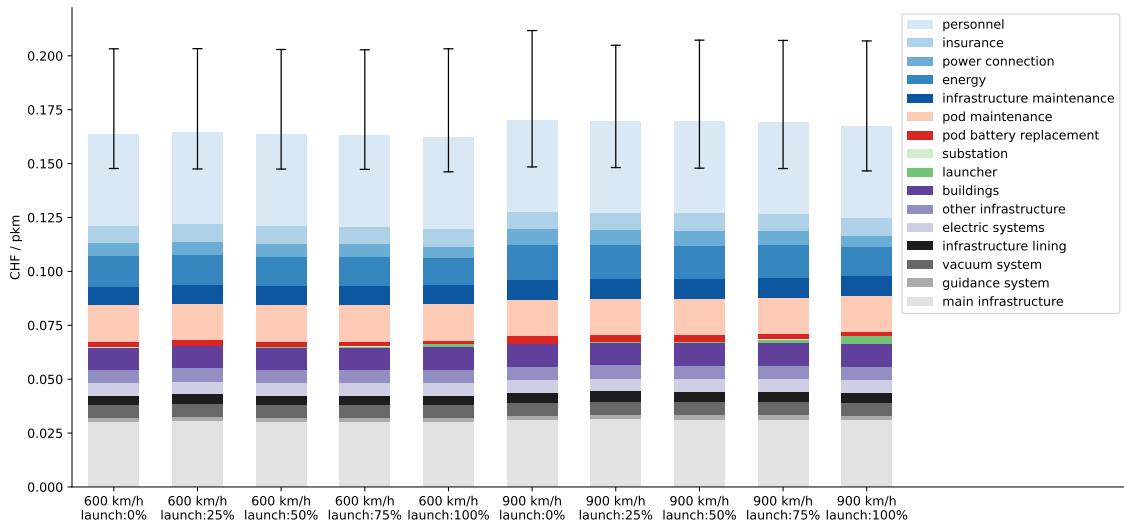


Figure 44: Breakdown of the total costs of the system (CAPEX depreciation and OPEX) per pkm for various system configurations, grouped by cruising speed (600 or 900 km/h) and share of acceleration propelled by the track-side launcher.

6 Overall assessment of hyperloop in Switzerland

6.1 Cost and emissions trade-off

Fig. 45 summarises the specific costs and environmental impacts of all tested network configurations. Given the importance of both metrics, the plot can be used to identify Pareto-optimal points, where both measures are optimised in the sense that no metric can be further improved without worsening the other one. The figure shows that the Pareto-optimal line is actually quite concentrated in a bunch of points at the bottom-left corner of the figure; in other words, both the specific emissions and costs are minimised for approximately the same configurations. This is due to the paramount role that the infrastructure has in both costs and emissions, so that both metrics are minimised when the “consumption of infrastructure per pkm” is reduced.

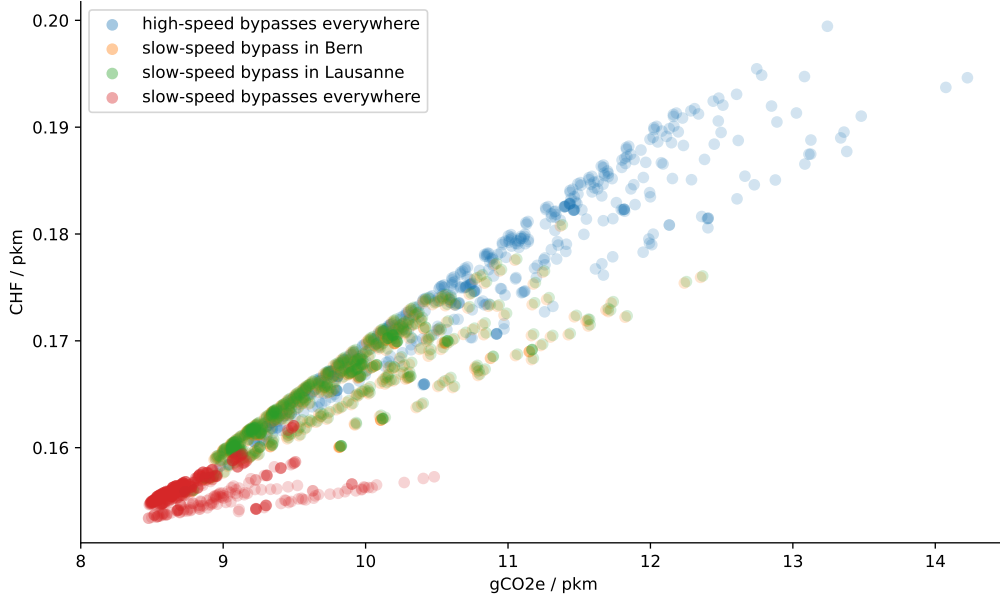


Figure 45: Summary of total costs (y-axis) and life-cycle GHG emissions (x-axis) for all tested network configurations. The colours indicates the presence of slow- or high-speed bypasses at through stations.

This characteristic simplifies the identification of systems that perform better under both points of view. From the plot it is already visible that the systems with only low-speed switches and bypasses achieve better scores thanks to the shorter ramps at the through stations, hence the reduced need for infrastructure.

To provide a conclusive description of the optimal system configuration (among the explored ones) we develop the aggregated metric “ $\text{gCO}_2\text{-eq.} + \text{Rp.}/\text{pkm}$ ”, where 1 Rp. represents 0.01 CHF. This metric is an adequate proxy for the overall system performance since $\text{gCO}_2\text{-eq.}/\text{pkm}$ and $\text{Rp.}/\text{pkm}$ display a comparable standard deviation among the network configurations¹¹.

This metric can help identifying the “best” overall system; however, given the large size of the explored parametric space and the uncertainties underlying some assumptions, we average the features of the 20 best performing systems. Table 9 summarises the main inputs and outputs of the resulting average hyperloop system (excluding parameters such as pressure, blockage ratio, etc. that have been fixed for all network configurations – see Tables 6 and 7 for the omitted features).

¹¹In Fig. 45 the points span a comparable range of values on the x-axis ($\text{gCO}_2\text{-eq.}/\text{pkm}$) and on the y-axis multiplied by 100 (which from CHF/pkm becomes Rp./pkm).

| Parameter | Value | | |
|-------------------------------------------------------------------------|---------------------------------------------------------|--------------------------------|-----------------------|
| INPUTS | | | |
| Cruise speed | 167 m/s | | |
| Max. acceleration/deceleration rate | 1.85 m/s ² | | |
| Acceleration profile | linear up to 38% of cruise speed, then gradually lower | | |
| Pods passenger capacity | 70 or 200 seats/pod based on route, as shown in Fig. 32 | | |
| Share of acceleration propelled by track-side launcher | 90% | | |
| Share of brake energy recuperated by track-side recuperator | 0% | | |
| Switch and bypass speed at through-stations | low at all stations | | |
| On- and off-boarding time | 8 min. | | |
| Location of hyperloop stations | at central railway stations | | |
| OUTPUTS | | | |
| Passenger traffic | | | |
| Annual traffic | 45 mill. pax/y 5'032 mill. pkm/y | | |
| Max. traffic at rush hour | 3'620 pax/h on Zurich–Bern | | |
| Min. headway at rush hour | 132 s on Geneva–Lausanne | | |
| Key network dimensions | | | |
| Network length | 326 km | | |
| Total hall and platform area of all stations | 148'000 m ² | | |
| Peak power demand of network | 101 MW | | |
| Peak power demand at single station | 33 MW in Bern | | |
| Energy consumption | | | |
| | Annual | Specific | |
| Pod operation (incl. propulsion, cooling and brake energy recuperation) | 302 GWh/y | 0.060 kWh/pkm | |
| Vacuum assurance of infrastructure | 75 GWh/y | 0.015 kWh/pkm | |
| Cooling of infrastructure (high uncertainty) | ~137 GWh/y | ~0.027 kWh/pkm | |
| Total (excl. infrastructure cooling) | 377 GWh/y | 0.075 kWh/pkm | |
| Total (incl. infrastructure cooling) | ~514 GWh/y | ~0.102 kWh/pkm | |
| Life-cycle GWP | | | |
| | Annualised emissions | Specific emissions | |
| Infrastructure | 29'514 tCO ₂ -eq./y | 5.87 gCO ₂ -eq./pkm | |
| Launcher & substation | 1'729 tCO ₂ -eq./y | 0.34 gCO ₂ -eq./pkm | |
| Pods | 7'663 tCO ₂ -eq./y | 1.52 gCO ₂ -eq./pkm | |
| Energy supply | 4'000 tCO ₂ -eq./y | 0.80 gCO ₂ -eq./pkm | |
| Total | 42'906 tCO ₂ -eq./y | 8.53 gCO ₂ -eq./pkm | |
| Costs | | | |
| | CAPEX | Annualised costs | Specific costs |
| Linear infrastructure | 12'436 mill. CHF | 240.6 mill. CHF/y | 4.78 Rp./pkm |
| Launcher & substation | 226 mill. CHF | 3.8 mill. CHF/y | 0.07 Rp./pkm |
| Station building | 3'214 mill. CHF | 53.6 mill. CHF/y | 1.06 Rp./pkm |
| Pods | | 94.5 mill. CHF/y | 1.88 Rp./pkm |
| Energy | | 87.8 mill. CHF/y | 1.74 Rp./pkm |
| Personnel & insurance | | 255.1 mill. CHF/y | 5.07 Rp./pkm |
| Infrastructure maintenance | | 38.9 mill. CHF/y | 0.77 Rp./pkm |
| Total | 15'875 mill. CHF | 774.1 mill. CHF/y | 15.38 Rp./pkm |

Table 9: Main input parameters and output results of the average best-performing configurations for a Swiss hyperloop network; 1 Rp. = 0.01 CHF.

As observed in the previous sections and in Fig. 45, the optimal hyperloop configuration entails low cruising and bypass speeds. This is primarily due to the small size of the investigated network, where the time gains on the relatively short trips do not justify particularly high speeds. In addition, the two routes that make up most of the passenger traffic (Zurich–Bern and Geneva–Lausanne, see Figures 28 and 36) connect neighbouring cities, reducing even further the effective travel time of the average passenger. These two routes do not cross any intermediate station, meaning that raising the speed of switches and transit bypasses increases infrastructure costs with no real benefit. Supposedly, if one were to insert a station (e.g. Lucerne) between Zurich and Bern, the slowing-down option would probably be worse in terms of LCA than a high-speed infrastructure

bypass.

Table 9 confirms that the launcher is beneficial to the system, at least until the pod reaches about 90% of the target cruising speed. A concave acceleration profile starting at 1.85 m/s^2 is also identified as optimal, although the detailed picture in Fig. 46 reveals a rather mild decrease in the acceleration rate at higher speeds.

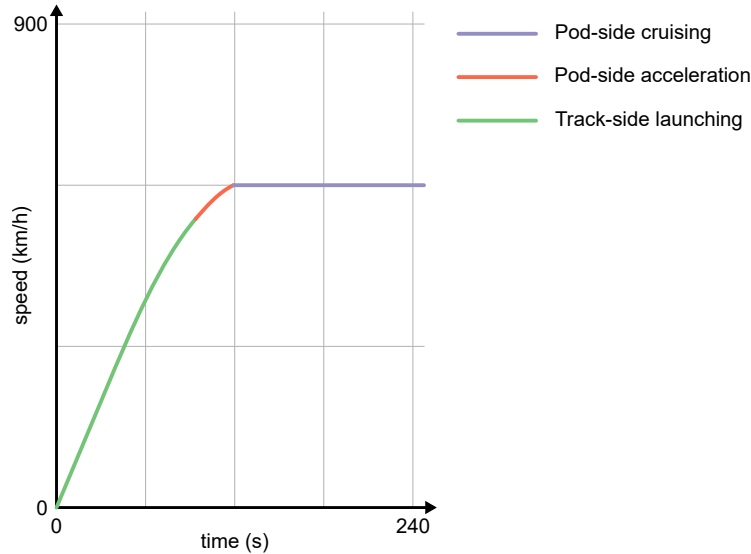


Figure 46: Pod acceleration profile for the average best-performing hyperloop configurations, using the notation of Fig. 35.

The generally low speed of the system leads to a passenger demand closer to the low end of the investigated spectrum: about 5'000 mill pkm/y. It is important to highlight that this passenger traffic neglects any potential rebound effect due to the introduction of this fast mode of transport, as well as any international travel as the Swiss system is simulated in isolation. The resulting rush-hour traffic is well within the safe operating zone, with a minimum headway of more than 2 minutes observed on the Geneva–Lausanne segment at 5 p.m.

The maximum passenger traffic and minimum headway occur at two different routes because of the different pod composition on the two segments. This is visible by comparing Fig. 28 with Fig. 33: while the Geneva–Lausanne segment sees more pod travelling in absolute terms, many are 70-seaters travelling from Geneva to Bern; on the other hand, the seemingly lower traffic on the Zurich–Bern segment is mostly composed of the 200-seat pods travelling from only between Zurich and Bern.

The detail breakdowns in energy, LCA emissions and costs follow the observations made in the previous sections. Thanks to the alignment between CO₂- and cost-optimal systems, the lowest values of Figures 38, 39 and 44 are all reachable with the same average configuration, namely 0.075 kWh/pkm, 8.5 gCO₂-eq./pkm and 0.17 CHF/pkm¹²

With these values, the next sections compare the hyperloop network to other modes of transport.

¹²For sake of completeness all numbers account for the energy needed to cool the infrastructure, but no explicit modelling has been performed and the reader should take the estimate with caution.

6.2 Environmental benchmark with alternative modes of transport

The comparison of the life-cycle GHG emissions between hyperloop and other modes of transport is displayed in Fig. 47. For aviation, two comparisons are provided: with conventional fossil jet fuel and with synthetic kerosene. The synthetic kerosene is produced via Fischer-Tropsch and water electrolysis, the CO₂ comes from Direct Air Capture (DAC) whose heat requirements are provided by heat pumps. All electricity needs for e-kerosene production are supplied by wind generation, while all other modes employ local electricity, specifically assumed to be today’s consumption mix of the Swiss Federal Railways (SBB) [57]. All extraction and conversion processes occurring upstream of the transport service are also assumed to take place with today’s technology and energy mix.

For each mode of transport the GWP is split by source of emissions: infrastructure (stations, airports, tubes, rails), vehicles (pods, planes, trains), electricity during operation (and for e-kerosene production), upstream fuel supply (especially for aviation) and other emissions during operation (SO_x, NO_x, SF₆ refrigerants) ¹³.

Conventional aircrafts display the largest environmental impact especially due to the combustion of fossil fuels during their operation. However, also aircrafts running on e-kerosene still require the same energy intake as their predecessors. In addition, the low electricity-to-fuel conversion process for e-kerosene makes the net electricity consumption of these aircrafts considerably higher than trains or hyperloop. Even if all electricity is generated from wind farms, the LCA of such electricity consumption heavily penalises e-kerosene aircrafts ¹⁴.

The GWP related to electricity consumption is rather comparable for train and hyperloop, with the former performing slightly better. Considering that the two systems are supplied with the same electricity mix, this means that trains consume marginally less electricity per-pkm than the reference case of hyperloop. However, based on the variability associated with different hyperloop designs (see Fig. 24) for any practical purpose we can conclude that hyperloop and railway consume on average a comparable amount of electricity per-pkm.

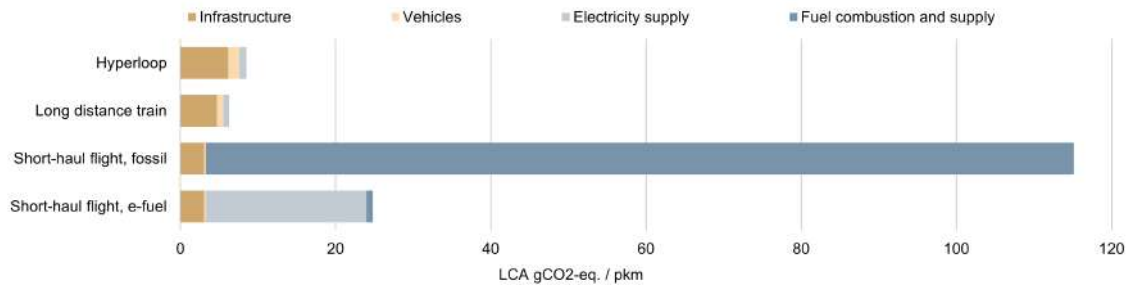


Figure 47: Comparison of the specific life-cycle emissions per passenger-kilometre between different modes of transport, split into the main sources of emissions.

Aviation performs better than trains and hyperloop in the vehicle life-cycle, mostly due to the large number of passenger-kilometres carried by planes during their lifetimes. Hyperloop’s vehicles particularly show a significant footprint and this is primarily due to the central role that electric batteries have in the pod life-cycle, as highlighted in Fig. 39.

The infrastructure footprint for all modes of transport is surprisingly similar: in the case of aviation, despite the no need for a connecting infrastructure, airports still display a large environmental impact. This comes from their extensive land use, the substantial consumption of heat and electricity for the buildings, the fuel consumption for ground operations and the resources needed for aircraft maintenance ¹⁵.

The difference between rail and hyperloop infrastructure is instead primarily due to the assumed utilisation of the lines. On one hand, the average seat offer of railway is about 36% lower than for hyperloop, because the latter is sized to serve the most crowded Swiss corridor (Zurich–Bern), while the former comes from an average of Swiss long-distance train services [81]. On the other hand, the load factor employed for long-distance trains is 28% [81] while for hyperloop an utilisation rate of 80% is assumed. The latter estimate can be considered achievable thanks to the

¹³Non-CO₂ climate forcers like cirrus clouds are excluded from the analysis due to the large range of uncertainties.

¹⁴It is to be noted that the SBB electric mix employed by trains and hyperloop is also extremely clean (8 gCO₂-eq/kWh_{el}), hence comparable with wind power (14 gCO₂-eq/kWh_{el}).

¹⁵For all other modes, vehicle maintenance is included in the “vehicle” segment; but for aviation the maintenance of aircrafts is partly assigned to airports in the original ecoinvent data set [80].

higher modularity of the vehicles and their more frequent departures, which may allow for a better demand-following timetable and a higher occupancy rate. In addition, load factors of 80% are typical for aviation and have been employed in the present LCA [73, 82].

6.3 Economic benchmark with alternative modes of transport

The most sensible metric to benchmark a system which would have to be newly introduced is in cost per passenger-kilometre. A direct CAPEX comparison is not possible with infrastructure that has grown over centuries (in the case of railway). Therefore, we estimated the OPEX of a potential hyperloop system and a depreciation cost for the CAPEX needed, while fetching OPEX and depreciation from annual reports of the entities shown in Fig 48. Although the absolute value should be taken with care, one can already see that hyperloop will not be financially able to compete with aviation, a system that does not need a linear infrastructure such as railway or hyperloop. However this applies to the current market and regulation environment, with a higher CO₂ price and a reduction of the tax advantages on kerosene, this could considerably evolve. The very strong difference in the split of OPEX is also explained by that: Aviation need to spend large amounts of money on fuel and personnel, but almost none on infrastructure.

Compared to railway, hyperloop seems to be able to compete with the companies in the DACH-region (Germany, Switzerland, Austria). There are several factors that could explain the large difference between railway and the estimated hyperloop values: The network shown here is only operating on four stations in large cities on a single line. Compared to this, a state railway is distributing people much more granular on a network which becomes "thinner" in terms of passenger flows the further one goes from urban centres - in short, a state railway only operated on the suggested hyperloop line might perform similarly.

However, hyperloop as it is envisioned, is thought to have indeed less personnel (per pkm of course), again only operating stations at centres with a lot of passenger throughput each day.

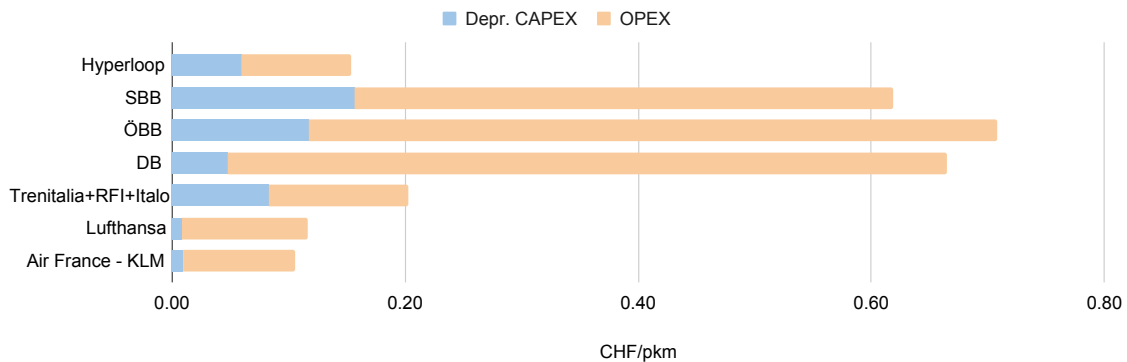


Figure 48: Cost per passenger-kilometre for different modes of transport. The railway and aviation data are taken from annual reports of the corresponding entities for the year 2022.

The cost estimate provided shall give an order of magnitude of a first estimate. It shall however be clear that this does not include the following points

- Development cost
- Certification cost
- Cost for connecting vacuum piping within the ground
- Cost for possible electric grid reinforcements to deal with the additional power requirements
- We assumed that the entire length of the tunnel can be done with TBMs, which might be an optimistic, but really the only achievable, generalised approach. In any case, for a real tender or similar, one should include unexpected cost due to difficulties in the ground or in cities that appear in any real-world project.

6.3.1 Comparison with other sources

The cost estimated for the construction of a two lane hyperloop in this work are in the order of 36 mill. CHF overground and 38 mill. CHF underground per kilometre of tube/tunnel. *Hyperloop Connected*, as a first comparison, estimate roughly 36 mill. USD for and overground track, although for a smaller diameter [83]. The tunnelling cost given is on the order of 60 mill USD. This however assumes, to the authors understanding, an additional construction for vacuum proofing inside the tunnel (e.g. placing a steel tube inside the tunnel). Also do they assume the same land cost for

overground and underground, which seems unrealistic.

Virgin hyperloop estimated around 52 mill. USD per kilometre for a projected line between Dubai and Abu Dhabi [84], although not clearly stating if this would include the station construction. Various other studies suggest cost in the range of 38 and 56 mill. USD and are summarised in a report by *Aecom* [85]. *HTT* assume a cost between 20-40 mill. USD, which is in a similar range [86]. *Swissmetro* estimated for Lausanne - Geneva a cost of 2.654 bill. CHF for 85 km. This results in (inflation corrected) 51 mill. CHF per kilometre of double track [32].

6.4 Further economic considerations

Although the evaluation of socio-economic benefits was neither the scope nor focus of this study, a quick order of magnitude estimate is performed to put the shown cost above into perspective. The following are "back-of-the-envelope calculations" and should therefore be repeated by experts in the field.

Value of time travel savings In the financial evaluation of public transport enhancements, the inclusion of the Value of Travel Time Savings (VTTS) can add to a comprehensive cost-benefit analysis. VTTS quantifies the economic utility gained from reduced travel duration, thereby serving as a proxy for increased societal productivity and well-being. According to Axhausen et al. [87], an average hour spent on public transport amounts to 14.90 CHF of VTTS (in 2003, likely higher today). Considering this to be a conservative estimate, this amounts to (assuming the VT passengers would take the train with today's travel times instead) 450 mill. CHF of VTTS annually, which puts the annualised system costs in Fig. 43 into perspective by adding indirect value creation (cost reduction) of almost half the annualised cost.

Noise reduction The external cost caused by noise exposure were estimated to be 2.8 bill. CHF in 2019 [88]. The "Switzerland noise fact sheet 2021" by the European Environment Agency estimates that of the people exposed to high noise pollution (More than 55 dB during the day and more than 50 dB during the night), 18% on average are caused by rail [89]. If one scales the resulting external cost caused by noise with the passenger numbers of SBB in 2019 [69], one obtains roughly 0.026 CHF per pkm of noise cost caused by rail. This would amount to roughly 125 mill. CHF savings in noise cost annually through the projected hyperloop system in this study, when looking at the amount of people that would use rail instead in the future without a hyperloop present.

This does of course not include noise cost caused by the construction of the new system.

Cost in aviation Airbus predicts roughly 40'000 new airplanes are needed to cover the projected demand until the year 2042 [38]. The concerns about developing many potentially needed hyperloop vehicles can therefore be put somewhat in perspective.

7 Conclusion

7.1 Key Findings

In this study, the following key statements were established:

- **Energy consumption:** The estimates of this report show that hyperloop indeed can provide high-speed ground based transport for a comparably small cost in terms of operational energy, which can be as little as 0.075 kWh/pkm for a small Swiss network. In comparison, this amounts to roughly a fifth of the railway energy consumption¹⁶.
- **Environmental impact:** It is demonstrated, using in-depth life-cycle assessments, that hyperloop is indeed at the same level of conventional trains (8.5 gCO₂ per pkm) in terms of greenhouse gas emissions. There is a strong dependence on the cleanliness of the electricity mix, i.e. meaning the numbers for gCO₂/pkm will change substantially when transferred to a country which has a different mix of power sources.
For the construction, the creation of the main structure (i.e. the tunnel) already contributes to half of the emissions. The remarkable second biggest contributor is the guide way, which means the aluminium and steel profiles needed for guidance and propulsion. The annualised emissions would amount to roughly 0.1 % of what Switzerland yearly emits¹⁷.
- **Construction Cost:** The construction cost of a Swiss network as projected in the study is estimated to be around 15 –25 bill. Swiss Francs, having in mind that unforeseen costs such as in the Gotthard might likely add another 50%. Although surely unforeseen cost will arise, it shall be noted that this is potentially less than what will be spent on gradual improvements of the rail system in the combined extension steps 2025 and 2035 [2, 3], for which roughly 20 bill. CHF have been reserved. While the authors in no way imply to choose either or, it shall be stated that although considerable, the cost is in the realm of possibility. This is underlined by the unavoidability of big investments needed if any of the climate targets are to be met [92].
- **Estimated total cost of ownership:** The first estimate presented in this study suggests a cost of approximately 0.15 – 0.17 CHF/pkm for the proposed network or roughly CHF 775 mill./year. Although the estimates for socio-economic benefits should be repeated by experts in the field, the reduction in travel time and noise reduction by removing passengers (roughly the amount by which today’s volume is expected to rise in 2050) from the rail are estimated to lead to more than CHF 500 mill./year in savings of socio-economic cost factors. The lower cost compared to railway might largely be due to the simple, highly frequented network of hyperloop compared to the exhaustive grid of railways.
Balancing the cost with ticket pricing would implicate roughly 50 CHF for a ticket from Zurich to Geneva, while the current railway is at 44 CHF (including Half-fare card). However, as mentioned above, one might have to include development cost and assume that the shown cost will increase due to unforeseen factors, so the ticket price could be substantially higher. If the system became part of the Swiss public infrastructure, subsidies might be possible as well.
- **Passenger prediction:** The 2050 projection for the Geneva-Lausanne-Bern-Zurich hyperloop line reveals a strong passenger demand, particularly along vital city-to-city connections such as Zurich-Bern and Lausanne-Geneva. Notably, the hyperloop is poised to capture a substantial market share in long-distance travel, particularly for journeys surpassing 100 km. Sensitivity analyses underscore the pivotal role of factors like travel time, station locations, and streamlined processes in encouraging shifts from conventional transport modes. The strategic placement of hyperloop stations is pivotal for accessibility, while passenger responsiveness to hyperloop travel time highlights the significance of speed. Additionally, cross-border routes show the hyperloop’s potential to influence travel patterns, attracting passengers from Munich, Lyon, Geneva, and Zurich.
As passenger demand grows by 2050, hyperloop is expected to help accommodate this surge, diverting long-distance travel. Comprehensive mobility policies are crucial for achieving a significant transition from cars to the hyperloop or public transport, with the hyperloop

¹⁶Our estimates show roughly 0.5 TWh/y while railway amounts to 2.5 TWh according to [90]

¹⁷According to [91], Switzerland emits about 45 Mill. tons CO₂-equivalent, while the annualised emissions of the envisioned system is in the order of 0.05 Mill tons.

standing out as a key solution to revolutionise regional transport dynamics by providing an attractive and sustainable alternative.

- **Capacity:** With the vehicle defined in the reference case and a safety distance that allows for breaking behind an instantly stopping vehicle, a capacity to cover the full rush hour between Zurich and Bern can be achieved. This capacity can also be provided from the electrical grid side, as demonstrated in section F. Therefore, doubts about the capacity of hyperloop are somewhat unjustified. Since the aerodynamic drag only marginally depends on the vehicle length, this almost proportionally reduces the specific operational energy consumption (MJ/pkm).
- **Adaption of hyperloop for Switzerland:** Comparing sections 4 and 5, one can see the immense dependency of ideal system configuration and thus performance of the hyperloop system: While the consensus within the field is to develop high-speed switches, it seems that for a Swiss network of the size as projected above, this might actually not be beneficial due to the immense off- and on-ramps needed to be constructed on top, impacting more the environment than slowing down and speeding up again. This both depends on the distances in the network but also the demand distribution, i.e. if the main traffic were to be between Geneva and Bern, it might be worth to build a high-speed bypassing Lausanne, which currently it is not.
Little surprising, the top speed is recommended to be reduced compared to a continental network. It seems to be the case that a hybrid of launcher and self-acceleration yields an optimum in terms of environmental impact.
- **Technology:** Already today, many of the key technologies needed to construct a hyperloop exist and have undergone proof of concept. With the improvements to come in the next few years, the key performance indicators of the hyperloop have the potential to significantly improve. The most influential parameters about the performance of the system (from energy point of view) are much less technology predictions (motor power density etc.) than “design choices”, i.e. speed, acceleration profiles, operating pressures. This shall be considered as a positive result, since these can be much more controlled by the developers than e.g. battery density improvements.
- **Framework (hyperloop modelling tool):** A framework has been established to evaluate different design configurations and address fundamental hyperloop design questions. This method can be used (and extended) in the future to further investigate the many design choices yet to be made and to identify the most pressing topics for further research.
- **Export and Swiss Pioneer spirit:** The introduction of a hyperloop system in Switzerland would present a new flagship in transport, similar to the introduction of AlpTransit in the last decades. Regardless of a potential introduction, the research and development of components related to the technology could benefit the Swiss industry through export of innovative products such as vacuum proof tunnelling technologies, motor development etc.

Overall, the study indicates that a hyperloop system indeed could provide the speed of a plane at the ecological footprint and capacity of a train, closing a large gap in the future network of transport. It can be seen as a first needed step in the context of a large scale study, that should include a mobility concept for the country after 2050, a nation wide demographic model and close collaboration with railway. To underline once more, the authors envision hyperloop to be an addition to the future public transport infrastructure, extending railway with a new high-speed network to cope with the presumed growth in demand. It would also add a step to complete a Swiss cross-network, bringing east and west together in a manner that the Gotthard-Basetunnel provided for North and South.

7.2 Identified bottlenecks in technology

In short, the study emphasises the following key technologies that need to either yet be developed or significantly more knowledge about is needed:

- **Levitation systems:** Have to be built at scale and the assumed values confirmed.
- **Tunnelling:** The concept of a vacuum-tight, and maintenance friendly tunnel has yet to be validated or even created in reality. The importance of such a realised prototype cannot be overstated, not only for Switzerland but for a global context.

- **Thermal batteries:** In theory, as done in this work, one could use water/ice or similar phase-changing materials. In this work, the performance of such a system was estimated, but the development of it is yet to be done at scale. A first step toward this will be done by EuroTube in 2024 in an Innosuisse collaboration with the Hochschule Luzern.
- **Efficiencies:** The realisation of efficiencies at the level projected in this study have yet to be achieved. By this we mean the efficiencies of motors involved, discharging of batteries etc.
- **Standards:** A critical future objective for the hyperloop community is to establish a set of unified standards that will ensure the seamless integration of a Europe-wide hyperloop network.
- **Highspeed Switching:** Concerns about the feasibility of highspeed switches are yet to be silenced. EuroTube is following closely the development of the *European Hyperloop Centre*, in which Hardt Hyperloop is supposed to demonstrate their switch concept in late 2024.

Technologies that are worth investigating but not crucial or not endangering a realisation of hyperloop (e.g. they have been demonstrated in similar applications already):

- **Compressor:** Several key players in the hyperloop field (e.g. Zeleros) aim at relatively high pressures in the tube and the implementation of a compressor on board. The impact of a heavy, fast-rotating device onboard the pod, the additional heat generated as well as the additional energy consumption needed could be benchmarked against a low-pressure, compressor-free solution.
- **Virtual coupling:** Pods re-entering the main tube from the intermediate station would have to merge with the high-speed traffic and, to minimise energy consumption, a possible re-connection with the fast-travelling pods could be considered; this calls for further investigations on the topic of virtual coupling (like wagons in a train).
- **Development of life support systems:** The life support system on a hyperloop pod needs to be developed. In principle the system used in submarines could be implemented, however hyperloop can take advantage of some peculiar features: typically, cyclic CO₂ scrubbers either use vacuum, heat or their combination to desorb the CO₂ scrubber. With joule heating and a low-pressure environment, both inputs are already provided in hyperloop and can be exploited for an efficient life-support system.
- **Tunnelling technologies:** Alternative tunnelling systems are to be investigated and the progress in industry shall be followed. One example of such is *HyperTunnel* from England who aim to increase tunnelling times by a factor of 10 and half cost through the use of swarms of robots. However, this is still on a prototype scale.

7.3 Limitations of the model and outlook

The following aspects modelled in this work have substantial room for improvement and shall be taken with care.

- **Air leakage:** Whether or not the leakage rate for overground systems can be transferred to a tunnel is yet to be proved and should be pursued further to allow any realisation of an underground system with a reasonable performance.
- **Levitation:** Although the system envisioned in this work is based on a series of publications and was discussed with researchers in the field, potential caveats, problems or changes in performance have to be expected when building a full-scale system. Even though there exist already fully functioning and commercially implemented levitation systems, further work is needed to find the optimal (economically viable, most ecological, most reliable and switch-compatible) solution for a completely new large-scale infrastructure. The same reasoning holds for the linear propulsion system.
- **Tunnelling:** It is clear that there will be, as in any real-life projects, limits to the modelling approach in which one can go several kilometres uninterrupted with a TBM. One should therefore expect additional cost due to unforeseen obstacles that come with such works.
- **Efficiencies:** Efficiencies of motors of around 90% have yet to be proven at that scale and can of course completely change the performance of a hyperloop system if not achieved.

- **Transit times:** Although overhead calculations of the authors indicate that e.g. a doubling of the here assumed transit time is not strongly changing results, it shall be stated that (coming from a safety discussion) longer transit times should be included in further evaluations.
- **Cooling of tunnels:** While one of the first concerns of people entering the discussion about hyperloop is always concerning the energy needed for vacuum assurance, our literature value for the cooling of railway tunnels suggest that this might be of even bigger influence. Therefore, in a continuation, one should pay considerable attention to this problem.
- **Demand:** Demand modelling is in itself a highly complex topic. In addition to considering passengers' total travel time, ticket price stands as another pivotal factor for predicting passenger demand, underscoring the necessity to analyse how hyperloop transport services should be priced to both attract passengers and ensure the financial sustainability of the hyperloop system. In the metrics used in 5.1 strongly influence the KPIs estimated in this work. It is therefore to be noted that governance, economic development and regulations might have significant influence on the passenger demand and are outside the realm of predictability. This holds for any behavioural prediction, but especially one that is on a nation-wide scale in infrastructure and therefore strongly regulated.
- **Aerodynamics:** Despite the extensive work undertaken on the system aerodynamics there remain many challenges that should be investigated further. The pressure drag experienced by the vehicle is still, although being in vacuum, the major energy consumption contributor. Reliable KPIs can only be established with in-depth simulations of drag forces. Turbulent and unsteady phenomena like vehicle oscillations should be analysed since they may significantly affect the lateral stability of the pod as well as the effective blockage ratio and drag. Vertical forces (lift) caused by the air flow should be quantified as they may perturb the distance between vehicle and rail. Depending on its direction, this lift may also significantly relieve or additionally strain the levitation system. Friction and pressure drags contribute to the heating up of the system (tube and vehicle) and a precise estimation of this heat generation would be important to adequately size the heat dissipation mechanism of the infrastructure and the pod.
- **Material bills:** The material bill for the current launcher is based on a design used in a 120 metre demonstration tube. Therefore, an optimised design could substantially reduce the materials needed and alter the outcome of the comparison between track-side and pod-side acceleration in terms of environmental footprint and costs.
- **Safety:** Several safety concepts were suggested and looked at, such as bypasses, valve to divide the line into sectors and minimal braking distances. However, safety and governance remain crucial areas for future study. Tailored safety protocols, distinct from existing rail and aviation guidelines, are essential to address hyperloop-specific conditions like low-pressure environments and high G-forces. On the governance side, a pivotal decision awaits: should Hyperloop be regulated more like aviation or rail in terms of safety? Should hyperloop adopt aviation's "no-fail" safety policy? This choice will significantly impact both development and public acceptance. While not the focus of this technical report, these safety and governance considerations are vital for hyperloop's future.

Acknowledgements

The authors would like to thank the following entities and people for their valuable technical contribution to this report: Christian Bauer and Dr. Romain Sacchi from PSI, Julien Pouget from HES-SO, Implenia Schweiz AG, Sika Schweiz AG, Leybold GmbH, Herrenknecht AG, EBP Schweiz, the expert group around Stephan Husen at FOT, as well as Jean-Loup Robineau and Nicolas Macabrey at Planair for their constructive feedbacks.

Significant help within EuroTube came from Dr. Lorenzo Benedetti, Antoine Juge, Gregory Inauen, Dr. Rajdeep Dep, and Ioannis Stravopolous.

We would also like to express our gratefulness to Tristan Chevroulet for supporting our initiative.

References

1. Bundesamt für Statistik BFS. *Mobility and Transport* , last accessed: 2023-08-16. <https://www.bfs.admin.ch/bfs/de/home/statistiken/kataloge-datenbanken/publikationen.assetdetail.21826261.html>.
2. Federal Office of Transport. *Railway Infrastructure Expansion Step 2025* , last accessed: 2023-08-30. <https://www.bav.admin.ch/bav/en/home/modes-of-transport/railways/rail-infrastructure/expansion-programmes/expansion-step-2025.html>.
3. Federal Office of Transport. *Railway Infrastructure Expansion Step 2035* , last accessed: 2023-08-30. <https://www.bav.admin.ch/bav/en/home/modes-of-transport/railways/rail-infrastructure/expansion-programmes/expansion-step-2035.html>.
4. Musk, E. *Hyperloop Alpha* last accessed: 2023-08-22. https://www.tesla.com/sites/default/files/blog_images/hyperloop-alpha.pdf.
5. TÜV SÜD. *TÜV SÜD zertifiziert TUM Hyperloop Demonstrator* , last accessed: 23-09-11. July 2023. <https://www.tuvsud.com/de-de/presse-und-medien/2023/juli/tuev-sued-zertifiziert-tum-hyperloop-demonstrator>.
6. CEN-CENELEC. *Railways and Hyperloop Systems* , last accessed: 23-09-11. Access Year. <https://www.cenelec.eu/areas-of-work/cenelec-sectors/transport-and-packaging-cenelec/railways-and-hyperloop-systems/>.
7. Hyperloop Hype. *Construction of the European Hyperloop Centre is well underway* , last accessed: 2023-09-12. <https://hyperloophype.com/construction-of-the-european-hyperloop-centre-is-well-underway/>.
8. EIT InnoEnergy. *Hardt Hyperloop secures EUR 12M investment for the groundbreaking European Hyperloop Center* , last accessed: 2023-07-26. <https://www.innoenergy.com/news-events/hardt-hyperloop-secures-eur-12m-investment-for-the-groundbreaking-european-hyperloop-center/>.
9. Nevomo. *Nevomo has been awarded with up to EUR 17.5 million in total from the EIC Accelerator issued by the European Commission* , last accessed: 2023-07-26. <https://www.nevomo.tech/en/nevomo-has-been-awarded-eur-175-million-total-eic-accelerator-issued-european-commission/>.
10. IEEE Spectrum. *The Hyperloop Is Hyper Old* , last accessed: 2023-08-16. <https://spectrum.ieee.org/hyperloop-is-hyper-old#toggle-gdpr>.
11. Schafer, A. & Victor, D. G. The future mobility of the world population. *Transportation Research Part A: Policy and Practice* **34**, 171–205. ISSN: 0965-8564. <https://www.sciencedirect.com/science/article/pii/S0965856498000718> (2000).
12. Marchetti, C. Anthropological invariants in travel behavior. *Technological Forecasting and Social Change* **47**, 75–88. ISSN: 0040-1625. <https://www.sciencedirect.com/science/article/pii/0040162594900418> (1994).
13. IPCC. *Climate Change 2022, Mitigation of Climate Change, Summary for Policymakers* , last accessed: 2023-08-16. https://www.ipcc.ch/report/ar6/wg3/downloads/report/IPCC_AR6_WGIII_SPM.pdf.
14. IEA. *Electric Vehicles* , last accessed: 2023-08-16. <https://www.iea.org/energy-system/transport/electric-vehicles>.
15. Mission Possible Partnership. *Making Net-Zero Aviation possible* , last accessed: 2023-08-16. <https://missionpossiblepartnership.org/wp-content/uploads/2023/01/Making-Net-Zero-Aviation-possible.pdf>.
16. Çabukoglu, E., Georges, G., Küng, L., Pareschi, G. & Boulouchos, K. Battery electric propulsion: An option for heavy-duty vehicles? Results from a Swiss case-study. *Transportation Research Part C: Emerging Technologies* **88**, 107–123. ISSN: 0968-090X. <https://www.sciencedirect.com/science/article/pii/S0968090X18300470> (2018).
17. Bundesamt für Energie BFE. *E-Scooter – Sozial- und naturwissenschaftliche Beiträge zur Förderung leichter Elektrofahrzeuge in der Schweiz* , last accessed: 2023-08-16. http://www.ikaoe.unibe.ch/forschung/e-scooter/Schlussbericht_E-Scooter_2013.pdf.
18. IEA. *GHG intensity of passenger transport modes, 2019* , last accessed: 2023-08-16. <https://www.iea.org/data-and-statistics/charts/ghg-intensity-of-passenger-transport-modes-2019>.

19. EEA. *Specific CO2 emissions per passenger-km and per mode of transport in Europe, 1995-2011* , last accessed: 2023-08-16. <https://www.eea.europa.eu/data-and-maps/figures/specific-co2-emissions-per-passenger-3>.
20. Lindfeldt, A. *Railway capacity analysis, Methods for simulation and evaluation of timetables, delays and infrastructure* , last accessed: 2023-08-16. <https://www.diva-portal.org/smash/get/diva2:850511/FULLTEXT01.pdf>.
21. Bosquet, R., Vandanjon, P.-O., Coiret, A. & Lorino, T. Model of High-Speed Train Energy Consumption. *International Journal of Energy and Power Engineering* **7**, 767–771. ISSN: eISSN: 1307-6892 (2013).
22. Bundesamt für Verkehr BAV. *Perspektive BAHN 2050* , last accessed: 2023-08-16. <https://www.bav.admin.ch/bav/de/home/publikationen/berichte/perspektive-bahn-2050.html>.
23. International Transport Forum. *Alternative Solutions to Airport Saturation: Simulation models applied to congested airports* , last accessed: 2023-08-16. <https://www.itf-oecd.org/sites/default/files/docs/alternative-solutions-airport-saturation-simulation-models.pdf>.
24. EUROCONTROL. *European Aviation in 2040, Challenges of Growth, Annex 4, Network Congestion* , last accessed: 2023-08-16. <https://www.eurocontrol.int/sites/default/files/2019-05/challenges-of-growth-2018-network-congestion-21122018.pdf>.
25. IEA. *ETP Clean Energy Technology Guide* , last accessed: 2023-08-16. <https://www.iea.org/data-and-statistics/data-tools/etp-clean-energy-technology-guide>.
26. IEA. *Aviation* , last accessed: 2023-08-16. <https://www.iea.org/energy-system/transport/aviation>.
27. Brazzola N. Patt A., W. J. *Definitions and implications of climate-neutral aviation - Nature Climate Change* — *nature.com* <https://www.nature.com/articles/s41558-022-01404-7#citeas> . , last accessed: 2023-08-16.
28. Our World in Data.
29. Concessioni Autostradali Venete - CAV S.p.a. *Dettagli procedura* , last accessed: 2023-08-16. <https://cavspa-appalti.maggiolicloud.it/PortaleAppalti/it/homepage.wp?actionPath=/ExtStr2/do/FrontEnd/Bandi/view.action¤tFrame=7&codice=G00658&csrf=IOL8UDEBSMVGUVTOIVOQMASUXJJOXC>.
30. Hyperloop Development Program. *Hyperloop could replace 66 percent of European flights in 2050 – Hyperconnected Europe vision paper shows* ”, last accessed: 2023-08-08”. <https://hyperloopdevelopmentprogram.com/hyperloop-could-replace-66-of-european-flights-in-2050-hyperconnected-europe-vision-paper-shows/>.
31. Infrastructure Outlook. *Forecasting infrastructure investment needs and gaps* , last accessed: 2023-08-16. <https://outlook.gihub.org/>.
32. Bundesamt für Verkehr BAV. *Fachbericht zu einer erstetn Überprüfung des Konzessionsgesuches für eine SWISSMETRO-Pilotstrecke Genf-Lausanne durch die Bundesverwaltung* , last accessed: 2023-08-16. <https://swissmetro-ng.org/wp-content/uploads/Swissmetro-Fachbericht-Konzessionsgesuch-Pilotstrecke-Genf-Lausanne.pdf>.
33. Kirschen, P. & Burnell, E. *Hyperloop System Optimization* 2021. arXiv: 2104.03907 [cs.CE].
34. Bundesamt für Raumentwicklung ARE. *National passenger transport model* , last accessed: 2023-08-04. <https://zenodo.org/record/5700957#.Ya8x2NCZ04Q>.
35. Bundesamt für Statistik BFS. *Services of private passenger transport by road* , last accessed: 2023-08-04. <https://www.bfs.admin.ch/asset/de/13967139>.
36. EUROSTAT. *Air passenger transport between the main airports of Switzerland and their main partner airports (routes data)* , last accessed: 2023-07-18. https://ec.europa.eu/eurostat/databrowser/view/AVIA_PAR_CH__custom_6946177/default/table?lang=e.
37. Bundesamt für Raumentwicklung ARE. *Verkehrsperspektiven 2050* , last accessed: 2023-07-18. www.aren.admin.ch/aren/de/home/mobilitaet/grundlagen-und-daten/verkehrsperspektiven2050.html.
38. Airbus. *Global Market Forecast 2023-2042* , last accessed: 2023-07-18. www.airbus.com/en/products-services/commercial-aircraft/market/global-market-forecast.

39. Powell, J. P. & Palacín, R. Passenger stability within moving railway vehicles: limits on maximum longitudinal acceleration. *Urban Rail Transit* **1**, 95–103 (2015).
40. Flight Safety Foundation (FSF). *Approach-and-Landing Accident Reduction (ALAR) – Briefing note 8.4 – Braking devices* tech. rep. (2000). flightsafety.org/files/alar_bn8-4-braking.pdf.
41. Quagliaetta, E., Wang, M. & Goverde, R. M. P. A multi-state train-following model for the analysis of virtual coupling railway operations. *Journal of Rail Transport Planning & Management* **15**. Best Papers of RailNorrköping 2019, 100195. ISSN: 2210-9706 (2020).
42. Mendes Borges, R. & Quagliaetta, E. Assessing Hyperloop Transport Capacity Under Moving-Block and Virtual Coupling Operations. *IEEE Transactions on Intelligent Transportation Systems* **23**, 12612–12621 (2022).
43. Timperio, C. *Linear Induction Motor (LIM) for Hyperloop Pod Prototypes* tech. rep. (ETH Zurich, 2018). <https://www.research-collection.ethz.ch/handle/20.500.11850/379531>.
44. Hao, L., Huang, Z., Dong, F., Qiu, D. & Jin, Z. Study on Electrodynamics Suspension System with High-Temperature Superconducting Magnets for a High-Speed Maglev Train. *IEEE Transactions on Applied Superconductivity* **PP**, 1–1 (Nov. 2018).
45. Dong, F. *et al.* An on-board 2G HTS magnets system with cooling-power-free and persistent-current operation for ultrahigh speed superconducting maglevs. *Scientific Reports* **9**, 11844. ISSN: 2045-2322. <https://doi.org/10.1038/s41598-019-48136-x> (Aug. 2019).
46. Chen, X., Zhao, L., Ma, J. & Liu, Y. Aerodynamic simulation of evacuated tube maglev trains with different streamlined designs. *Journal of Modern Transportation* **20**, 115–120 (2012).
47. Markish, J. Jan. 1970. <https://dspace.mit.edu/handle/1721.1/16871>.
48. Boeing. *Boeing 787 from the Ground Up*, last accessed: 2023-08-16. https://www.boeing.com/commercial/aeromagazine/articles/qtr_4_06/article_04_2.html.
49. Bizzozero, M., Sato, Y. & Sayed, M. A. Aerodynamic study of a Hyperloop pod equipped with compressor to overcome the Kantrowitz limit. *Journal of Wind Engineering and Industrial Aerodynamics* **218**, 104784. ISSN: 0167-6105. <https://www.sciencedirect.com/science/article/pii/S0167610521002622> (2021).
50. Oh, J.-S. *et al.* Numerical Analysis of Aerodynamic Characteristics of Hyperloop System. *Energies* **12**. ISSN: 1996-1073. <https://www.mdpi.com/1996-1073/12/3/518> (2019).
51. EBP Schweiz AG. *Optimierung des Energieverbrauchs, der Kosten sowie der Klimawirkung beim Bau und Betrieb von Bahntunnel: Schlussbericht im Projekt «Graue Energie Bahntunnel» (GrETu)* tech. rep. (Bundesamt für Verkehr, Zürich, Schweiz, Feb. 2023). <https://www.bav.admin.ch/dam/bav/de/dokumente/verkehrstraeger/eisenbahn/gretu/schlussbericht-gretu.pdf.download.pdf/Projektschlussbericht%20GrETu.pdf>.
52. Personenverkehr, S. *Ein- und Aussteigende an Bahnhöfen*, last accessed: 2023-11-10. https://data.sbb.ch/explore/dataset/passagierfrequenz/table/?disjunctive.kt_ct_cantone&disjunctive.isb_gi&sort=dtv_tjm_tgm&refine.jahr_allee_anno=2022.
53. ISO. *Environmental management - Life cycle assessment - Principles and framework (ISO 14040:2006)* tech. rep. (International Organization for Standardization, 2006). www.iso.org/standard/37456.html.
54. ISO. *Environmental management - Life cycle assessment - Requirements and guidelines (ISO 14044:2006)* tech. rep. (International Organization for Standardization, 2006). www.iso.org/standard/38498.html.
55. Mutel, C. Brightway: An open source framework for Life Cycle Assessment. *The Journal of Open Source Software* **2**, 236 (2017).
56. Steubing, B., de Koning, D., Haas, A. & Mutel, C. L. The Activity Browser – An open source LCA software building on top of the brightway framework. *Software Impacts* **3** (2020).
57. ecoinvent. *Data release ecoinvent v3.8*, last accessed: 2023-07-10. 2022. www.ecoinvent.org/the-ecoinvent-database/data-releases/ecoinvent-3-8/#1610466712722-d74b0f24-6896.

58. Sacchi, R. *et al.* PROspective EnvironMental Impact asSEment (premise): A streamlined approach to producing databases for prospective life cycle assessment using integrated assessment models. *Renewable and Sustainable Energy Reviews* **160** (2022).
59. Aboumahboub, T. *et al.* REMIND - REgional Model of INvestments and Development - Version 2.1.0 2020. www.pik-potsdam.de/en/institute/departments/transformation-pathways/models/remind/remind.
60. Stehfest, E., van Vuuren, D., Bouwman, L., Kram, T., *et al.* *Integrated assessment of global environmental change with IMAGE 3.0: Model description and policy applications* www.pbl.nl/sites/default/files/downloads/pbl-2014-integrated_assessment_of_global_environmental_change_with_image30_735.pdf (Netherlands Environmental Assessment Agency (PBL), 2014).
61. Swiss Federal Office of Energy. *Energy perspectives 2050+* , last accessed: 2023-07-10. 2023. www.bfe.admin.ch/bfe/en/home/policy/energy-perspectives-2050-plus.html/.
62. Houghton, J. T., Jenkins, G. J. & Ephraums, J. J. *Climate change – The IPCC scientific assessment* tech. rep. , last accessed: 2023-07-28 (IPCC, 1990). <https://www.ipcc.ch/reports/?rp=ar1>.
63. Fazio, S. *et al.* *Supporting information to the characterisation factors of recommended EF Life Cycle Impact Assessment methods* tech. rep. (European Commission, Joint Research Centre, Publications Office, 2019). www.eplca.jrc.ec.europa.eu/permalink/TR_SupportingCF_FINAL.pdf.
64. Hyperloop Connected. *The future of hyperloop* ”, last accessed: 2023-08-08”. <https://hyperloopconnected.org/2019/06/report-the-future-of-hyperloop/>.
65. hausinfo.ch. *Wieviel kostet Bauland in der Schweiz* last accessed: 2023-08-08. <https://hausinfo.ch/de/bauen-renovieren/haus-planen/bauland-kaufen/kosten-bauland.html>.
66. Kanton Zürich. *Kanton Zürich* , last accessed: 2023-08-08. https://www.web.statistik.zh.ch/cms_bodenpreise/bom.php?bfs=999.
67. HS2. *A guide to tunneling cost* , last accessed: 2023-08-17. https://assets.publishing.service.gov.uk/government/uploads/system/uploads/attachment_data/file/434516/HS2_Guide_to_Tunnelling_Costs.pdf.
68. Group, L. *Annual Report 2022* , last accessed: 2023-08-30. <https://investor-relations.lufthansagroup.com/fileadmin/downloads/en/financial-reports/annual-reports/LH-AR-2022-e.pdf>.
69. Swiss Federal Railways (SBB). *Verkehr - SBB Statistikportal* , last accessed: 2023-08-29. Swiss Federal Railways. <https://reporting.sbb.ch/verkehr?=&years=1,4,5,6,7&scroll=748>.
70. Eidgenössische Elektrizitätskommission (ElCom). *Strompreise Schweiz* , last accessed: 2023-08-30. <https://www.strompreis.elcom.admin.ch/?category=C7&priceComponent=energy>.
71. Hyperloop Transportation Technologies. *Great Lakes Hyperloop Feasibility Study* , last accessed: 2023-08-29. <https://www.hyperlooptt.com/2019/great-lakes-hyperloop-feasibility-study/>.
72. Swissgrid. *Tariffs and remuneration rates for the transmission grid* , last accessed: 2023-08-30. <https://www.swissgrid.ch/en/home/customers/topics/tariffs.html#tariffs-and-remuneration>.
73. Notten, P., Althaus, H.-J. & Burke, M. *Life cycle inventories of global air freight - Global* tech. rep. (ecoinvent, Cape Town, 2018).
74. Chisholm, S. A., Rufin, A. C., Chapman, B. D. & Benson, Q. J. *Forty Years of Structural Durability and Damage Tolerance at Boeing Commercial Airplanes* in (2017). <https://api.semanticscholar.org/CorpusID:199394956>.
75. Professional Pilots Rumour Network. *Airliner life/cycles* , last accessed: 2023-08-30. <https://www.pprune.org/tech-log/240269-airliner-life-cycles.html>.
76. Cox, B., Bauer, C., Mendoza Beltran, A., van Vuuren, D. P. & Mutel, C. L. Life cycle environmental and cost comparison of current and future passenger cars under different energy scenarios. *Applied Energy* **269**, 115021. ISSN: 0306-2619. <https://www.sciencedirect.com/science/article/pii/S030626192030533X> (2020).

77. Hill, N. *Determining the environmental impacts of conventional and alternatively fuelled vehicles through Life Cycle Assessment* 2019. https://www.upei.org/images/Vehicle_LCA_Project_FinalMeeting_All_FinalDistributed.pdf.
78. Of Auditors, E. C. *A European high-speed rail network: not a reality but an ineffective patchwork* , last accessed: 2023-08-30. <https://op.europa.eu/webpub/eca/special-reports/high-speed-rail-19-2018/en/>.
79. Spielmann, M., Bauer, C., Dones, R. & Tuchschnid, M. Transport services: Ecoinvent report no. 14. *Swiss Centre for Life Cycle Inventories, Dübendorf*. https://db.ecoinvent.org/reports/14_Transport.pdf (2007).
80. Spielmann, M. *ecoinvent 3.8 Dataset Documentation - 'airport construction - RER'* , last accessed: 2023-08-30. 2021. <https://ecoquery.ecoinvent.org/3.9.1/cutoff/dataset/8812/documentation>.
81. Ecoinvent. *Ecoinvent Transport Report* , last accessed: 2023-08-31. https://db.ecoinvent.org/reports/14_transport.pdf.
82. International Civil Aviation Organization (ICAO). *Air Transport Monthly Monitor - March 2022* , last accessed: 2023-08-31. https://www.icao.int/sustainability/Documents/MonthlyMonitor-2022/MonthlyMonitor_March_2022.pdf.
83. Hyperloop Connected. *A Closer Look at the Infrastructure Costs.* , last accessed: 2023-08-29. <https://hyperloopconnected.org/2019/02/a-closer-look-at-the-infrastructure-costs/>.
84. Frontiers. *A Critical Review of Hyperloop (Ultra-High Speed Rail)*. *Frontiers*. <https://www.frontiersin.org/articles/10.3389/frsc.2022.842245/full> (2022).
85. AECOM. *PRELIMINARY FEASIBILITY OF HYPERLOOP TECHNOLOGY* , last accessed: 2023-08-30. <https://tc.canada.ca/en/innovation-centre/priority-reports/preliminary-feasibility-hyperloop-technology>.
86. Khaleej Times. *World's first hyperloop to cost up to \$40m per km, to recoup investment in 8-15 years*. *Khaleej Times*. <https://www.khaleejtimes.com/business/worlds-first-hyperloop-to-cost-up-to-40m-per-km-to-recoup-investment-in-8-15-years> (2020).
87. Axhausen, K. W., König, A. & Abay, G. *Swiss Value of Travel Time Savings*. *Arbeitsberichte Verkehrs und Raumplanung* **253**. Additional authors: John J. Bates, Michel Bierlaire. <https://doi.org/10.3929/ethz-a-005240096> (2006).
88. Federal Office for the Environment (FOEN). *Noise and vibrations: In brief* , last accessed: 2023-08-29. Swiss Federal Office for the Environment. <https://www.bafu.admin.ch/bafu/en/home/topics/noise/in-brief.html>.
89. European Environment Agency. *Switzerland Noise Fact Sheet 2021* , last accessed: 2023-08-29. European Environment Agency. <https://www.eea.europa.eu/themes/human/noise/noise-fact-sheets/noise-country-fact-sheets-2021/switzerland-noise-fact-sheet-2018>.
90. Bundesamt für Verkehr BAV. *ESöV Faktenblatt* Swiss Federal Office of Transport. , last accessed: 2023-11-09. May 2018. https://www.bav.admin.ch/dam/bav/de/dokumente/themen/umwelt/energiestrategie-projekte/esoev-factsheet-fakten-zahlen.pdf.download.pdf/ES%C3%B6V_Faktenblatt_A4_final_DE_180523.pdf.
91. Bundesamt für Umwelt (BAFU). *Klima: Das Wichtigste in Kürze* Swiss Federal Office for the Environment. , last accessed: 2023-11-09. 2023. <https://www.bafu.admin.ch/bafu/de/home/themen/klima/inkuerze.html>.
92. Klaaßen, L. & Steffen, B. *Meta-analysis on necessary investment shifts to reach net zero pathways in Europe*. *Nature Climate Change* **13**, 58–66. ISSN: 1758-6798. <https://doi.org/10.1038/s41558-022-01549-5> (2023).
93. Bundesamt für Statistik BFS. *Alpine and cross-border passenger transport* last accessed: 2023-08-04. <https://www.bfs.admin.ch/bfs/en/home.assetdetail.25905617.html>.
94. Nevomo. *Magrail - The next generation of high-speed railways* , last accessed: 2023-07-10. 2022. www.nevomo.tech/en/magrail/.
95. Swiss Federal Railways (SBB). *Noise protection* , last accessed: 2023-07-26. <https://company.sbb.ch/en/the-company/responsibility-society-environment/sustainability/environmental-protection/noise-protection.html>.

96. Air Transport Action Group (ATAG). *Aviation: Benefits Beyond Borders* , last accessed: 2023-07-26. https://aviationbenefits.org/media/167517/aw-oct-final-atag_abb-2020-publication-digital.pdf.
97. Bossi, O. *Contribution au dimensionnement et à la gestion par optimisation de systèmes de stockage d'énergie pour les réseaux électriques ferroviaires* Theses (Université Grenoble Alpes, Jan. 2016). <https://theses.hal.science/tel-01279238>.
98. Mayet, C. et al. *Different models for the simulation of DC railway systems supplied by non-reversible substations* in *2019 IEEE Vehicle Power and Propulsion Conference (VPPC)* (2019), 1–6.
99. Pouget, J. et al. *Energetic simulation of DC railway micro-grid interconnecting with PV solar panels, EV charger infrastructures and electrical railway network* in *2020 IEEE Vehicle Power and Propulsion Conference (VPPC)* (2020), 1–7.
100. Allenbach, J.-M., Chapas, P., Comte, M. & Kaller, R. *TRACTION ELECTRIQUE* <https://www.epflpress.org/produit/364/9782880746742/traction-electrique> (EPFL Press, 2017).

Appendix A Calibration of passenger simulation

We have chosen to focus our passenger simulation model calibration on individuals travelling between Arth-Goldau and Bellinzona via the Gotthard Tunnel. This particular route is characterised by passengers predominantly travelling between major cities such as Basel, Zurich, Lucerne, Bellinzona, and Lugano. This selectivity ensures a higher proportion of passengers travelling between significant urban centres rather than between small towns and cities, making the data set more homogeneous and easier to validate.

To calculate the number of passengers projected to travel between Arth-Goldau and Bellinzona through the Gotthard Tunnel, we have adopted the methodology outlined in section 3.3. According to our calculations, the average daily passenger count is estimated to be 5,471 individuals.

In order to validate the accuracy of our model, we have cross-referenced our results with the passenger data made available by the Federal Statistical Office (Bundesamt für Statistik) [93]. Their data indicate an average daily passenger volume of 5,425 individuals, with a margin of error of approximately $\pm 9.1\%$.¹⁸

Through this comparative analysis, we observe that our simulation model produces accurate predictions that fall within the expected range of variation. This validation reinforces the reliability of our model’s projections for passenger flow between Arth-Goldau and Bellinzona through the Gotthard Tunnel, considering the inherent uncertainties associated with such estimations.

Appendix B Intermodality

Intermodality and interaction with other modes of transport is a highly discussed topic, both within the hyperloop community but also in the work with different mobility and logistics partners. The following key messages have been identified:

- **Interoperability - technical aspects:** The levitation technology assumed in this study requires landing wheels that are compatible with the current standard rail. This means that the vehicles are theoretically equipped to run on conventional rail without levitating. However, there are also technical solutions to make hyperloop vehicles levitate on “upgraded” conventional rail [94].
- **Interoperability - hyperloop on rail (speed limitation):** The current railway lines (especially in Switzerland) include bends that are too narrow for travel at the speeds of a hyperloop, even if the top speed was limited to only three or four hundred kilometres per hour.
- **Interoperability - Disentanglement of modes (railway grid limitation):** As stated very clearly in the *Perspektive BAHN 2050* by the FOT, one of the major limitations of the capacity of current railway lines is the difference in speed between intercity and regional/S-Bahn trains. Therefore, it is stated that “[...] In case of grid extension, a disentanglement is to be pursued [...]”. This means that there is a need for separate lines for high- and low-speed lines, and hyperloop running on existing lines would only aggravate this problem.
- **Interoperability - last mile improvement:** Since the vehicle can potentially run on conventional rail, connections to important hubs without any direct hyperloop connections could be improved: this would allow for connections between two major cities on a high-speed hyperloop line, and then cover the last kilometres to airports (for example on conventional rails).
- **Point of access within a city:** Hyperloop aims, among other things, at replacing – to a certain extent – short-haul flights across the European continent or even within a country. Ideally, with special concern to the problem of the last mile, hyperloop ideally is being integrated in existing train stations, directly in the city centres, compared to airports which are located further away from cities because of the lack of space availability. Airports, however, have exactly this advantage of space to build stations as well as to have a much higher range for people to access long-haul flights. For example, with a Zurich-Geneva hyperloop, it would be feasible for Genevoises to travel to Zurich Airport to take intercontinental flights.

¹⁸Based on BFS data, there is only a marginal increase in the number of passengers between 2015 and 2017, indicating that the comparison falls within an acceptable range of error.

Appendix C Freight use case

EuroTube does not see cargo as the main use case for Switzerland, since the short distances within the country make the increase of cargo shipment speed along the network backbone of secondary importance compared to first-mile/last-mile delivery. However, in the model, the tube diameter is chosen in a way to allow for cargo transport of regular 20ft or 40ft containers. Furthermore, the size of the tube would allow customers to board with their cars onto the pods and travel on hyperloop, if the demand and business case for this are given. Pods carrying containers may have a large blockage ratio - hence a higher energy consumption (see Fig. 25a) - but this could be offset by reducing the usually not-necessary very high speed of freight pods. In order not to interfere with the faster passenger service, cargo vehicles could for example be launched during the night and they would not face the night noise issues typically common with freight trains as reported also by SBB [95].

It is out of the scope of this project to investigate exactly if and which kind of business cases exist for freight transport with hyperloop. However, there is no reason to doubt that logistic and shipping companies could find beneficial exploiting an already existing hyperloop infrastructure (built for a passenger-driven business). At this point, it is relevant to draw the reader's attention to Italy's Hypertransfer project [29] that is aimed at alleviating cargo traffic that is particularly heavy on the transalpine axis to Austria and Germany. In addition, the demand for fast international freight via air cargo - which already accounts for 35% of internationally traded value of goods [96] - is expected to keep growing at an annual rate of 3.2% for the next decades [38]. Therefore the cargo application remains an important potential use case of hyperloop depending on the local and regional demand.

Appendix D The impact of the electricity mix

Electricity consumption has a tangible impact on the GWP of all electrified transport systems even with very clean electricity mixes assumed. It is thus interesting to explore what happens when a wider range of electricity intensities is taken into consideration. Fig. 49 shows how the overall life-cycle GHG emissions of the various transport systems evolve when the GHG intensity of the grid is gradually raised. For this analysis, the reference case from section 4 has been used.

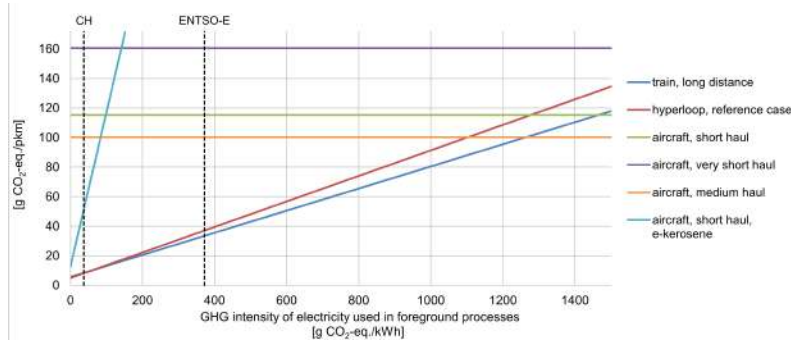


Figure 49: Life-cycle GHG emissions of different transport systems for a given GHG intensity of the electricity consumed during operation (or e-kerosene production).

For traditional aircrafts the impact of the electricity mix is minimal since the electricity consumption during operation is negligible. However, it can be appreciated that medium haul aircrafts have a lower specific footprint compared to short and very short haul planes due to the relatively lower role that take-offs have compared to cruise ¹⁹.

Hyperloop and railways display analogous trends due to the similar footprint breakdown. Their higher efficiency compared to aviation is such that grid carbon intensities higher than 1200 gCO₂-eq/kWh (the intensity of old lignite power plants) are necessary to reach GWP parity. In the range of the Swiss (CH) or European (ENTSO-E) electricity mixes both hyperloop and railway

¹⁹Ecoinvent classifies aircrafts according to the following ranges: very short haul: <800 km; short haul: 800-1500 km; medium haul: 1500-4000 km; long haul: >4000 km. Hyperloop applications typically consider ranges of 300-1000 km, i.e. in the range of very short and short haul aircrafts. For an impartial assessment, the better-performing short haul aircrafts are then used for comparison (also with e-kerosene).

dramatically outperform aviation. This holds also when synthetic jet fuel is employed because of the multiplication effect that the low well-to-wake efficiency of e-kerosene has on the carbon intensity of the electricity.

Increasing the GHG intensity of the electricity mix however amplifies the slightly different energy consumption observed between railway and hyperloop shown above. For the very clean SBB mix employed in this study, hyperloop’s reference design is similar to railway, but with increasing carbon intensities the higher electricity consumption starts penalising hyperloop. For GHG intensities higher than 60 gCO₂-eq/kWh hyperloop’s reference case has a larger GWP than railway.

Variations of the hyperloop system have only a small impact on the overall behaviour. Building the tube with steel shifts the hyperloop’s footprint to higher values and then maintains a stable pattern parallel to the reference case. Moving instead the pod acceleration from the track to the vehicle results in the cleanest system when the electricity comes with practically no environmental burden (e.g. the SBB mix), but it quickly deteriorates for higher carbon intensities due to the lower system efficiency. For grid intensities higher than 25 gCO₂-eq/kWh the pod-accelerated hyperloop system performs worse than the track-side counterpart and for intensities higher than 37 gCO₂-eq/kWh it also exceeds railway’s climate impact.

Appendix E Technical descriptions

E.1 Alternative levitation technologies

This is a very brief overview of alternative levitation systems considered within the community:

- Air Bearings: The Alpha Paper [4] initially suggested to suck in air at the front of the vehicle and exhaust at the bottom of the vehicle to make the vehicle slide on an air cushion. This idea however is followed by no major hyperloop company, due to various technical difficulties.
- Wheels: At the suggested speeds, wheels are disadvantageous in terms of noise, stability and also wear and tear.
- Electromagnetic Suspension: This technology consists of magnets (either electromagnetic or superconductive) being attracted to a steel beam on the track side. The advantage of this is a good “lift-to-drag ratio”, meaning how much electromagnetic drag is generated per unit force of lift. The drawback in the use of these systems is that they are intrinsically unstable and require a high-frequency feedback loop with a fast control system of the magnetic force. Also, the “lift-to-weight”, meaning the self-weight of a system normalised to the force that it provides, is rather poor, at least with classical electromagnets. This system can be applied from the top or bottom of the tube, however, there exists no passive switching mechanism (elaborated later) for the bottom version. According to the authors, analysing a EMS system would be important and they do not have a preference of technology.
- Magnetic reluctance: It is a phenomenon that can be used to stabilise a rail between two magnets and thus, when placed appropriately, be used for levitation. However, to the best of the authors’ knowledge, no large-scale transport application exists today. However, this technology is of interest to be investigated in the future.

E.2 Levitation System Details

An EDS levitation system using conventional magnets would have a considerable self-weight, which would be disadvantageous. The model includes the use of ReBCO superconducting tapes, which can behave as a resistance-free electromagnet. They only have to be charged initially at the station, and their temperature has to be kept below the critical current. However, these superconducting tapes have remarkable currents densities even at 77 K, the vapour point of liquid nitrogen. Other magnetic levitation trains such as the SCMaglev in Japan use liquid helium, which is substantially cooler, but also more expensive and more difficult to handle. The technology to store liquid nitrogen safely is well established and used in various industries, and the cost of ReBCO-tapes is below 40 CHF per metre. The use of liquid nitrogen is included in the model as well as the LCIA. The modelling of a flux pump to charge the superconductor was outside the scope of this project. Energy needed for lateral stabilisation is not included and negligible compared to levitation.

Appendix F Detailed study on launcher power management

The hyperloop solution proposed by EuroTube is briefly presented in Fig. 50. Firstly, the capsule train is accelerated with a linear motor installed along the track. The capsule train reaches the maximum speed at the end of the launching process. Secondly, in the constant speed area, the capsule train is supplied by an on-board battery to maintain the maximum speed. Finally, when the capsule arrives at the destination, it will be braked by a recuperator section. The regenerative braking energy can be harvested for further acceleration of other capsule trains running in the opposite direction. In addition, the total power from the substation is often limited, which is defined in the contract with the transmission system operator (TSO, Swissgrid) or the local distribution system operator (DSO). A high-power storage (HPS) module is thus studied to shave the peak power in the morning and evening peak periods.

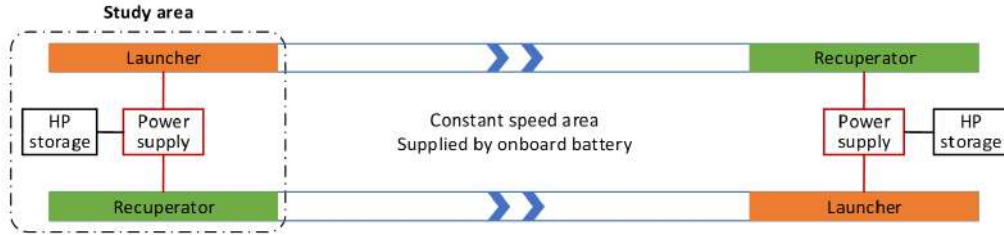


Figure 50: hyperloop rail line with launcher in green and recuperator in orange

It is highlighted that this section focuses on acceleration and deceleration areas (launcher and recuperator) that are supplied by the substation. The following aspects have been studied:

- Modelling of hyperloop electrical network with moving train loads
- Electrical grid topology and substation configuration
- Comparison of DC and AC grid solutions
- hyperloop electrical microgrid study

The aim of the model developed in this study is to provide a design tool that enables the economical and technical feasibility of such a system for a later stage.

The railway electrification system model contains two main parts. The first part is the cinematic model of the trains, namely the capsule train model. The model helps compute their behaviour according to parameters such as the line profile, the planning timetable, the train features, and the supply voltage [97]. The built model allows to obtain the time positions of the trains and their time power consumptions. The second part deals with the supply voltage calculated by an electrical model of the railway [98].

The Modified Nodal Analysis (MNA) is introduced to model the railway electrical network [99]. The detailed modelling methodology will be presented in the following subsections.

F.1 Modelling of the train traction system

The dynamic train traction model and its input data are briefly presented in this part. The detailed design and the parameter configurations are provided in the deliverable simulation model with Matlab/Simulink. Firstly, the dynamic traction equation of the train can be given by :

$$F_t - F_d - F_f = m \cdot a = m \cdot \frac{dv(t)}{dt} \quad (3)$$

where m represents the total mass of the pod, a is the acceleration speed, v is the speed, F_d is the air drag force, F_f is the friction force and F_t is the total traction force of the train . The general inputs of passenger pod and freight pod are summarised in Table 10. For both cases, in equation 3, the maximum speed is 250 m/s, and the acceleration is 1 m/s². The passenger pods are assumed to have a capacity of maximum 70 persons, the weight of each person is set at 100 kg. The maximum weight of a passenger pod with 70 persons will be a mass of $m=26.6$ tons. The freight mass is set to $m=50.1$ tons.

The calculated launching period is rounded to the next 15 seconds. There are 8 different launching periods from 30 seconds to 840 seconds for the passenger pods as shown in Table 4.2.

| Universal inputs | | | |
|-----------------------------|---------------|---------------------------|----------------------|
| Top speed v | 250 m/s | Top acceleration a | 1 m/s ² |
| Pod curb weight (for both) | 19.6 tons | | |
| Passenger pod inputs | Values | Freight pod inputs | Values |
| Pod capacity (persons) | pax 70 | Pod capacity | 1 FEU type container |
| Pax pod payload | 7.0 tons | Freight pod payload | 30.6 tons |
| Pax pod weight | 26.6 tons | Cargo pod weight | 50.1 tons |

Table 10: General inputs of passenger and freight pods

The morning peak occurs around 7:00 am, and the evening peak between 16:00 and 17:00, with a launching frequency of 30s. The launching frequency of freight pods is set to be 105 seconds. The capsule train traction model is built with Matlab/Simulink as shown in Fig. 51 The capsule train speed is the input, which is generated according to the timetable defined in Table 10. The position profiles are calculated in real time according to the speed information. While the models used are similar, here the catenary voltage is referring to the voltage in the launcher at the pod position and not to a “standard” catenary system. The connecting point of each capsule train is updated from the MNA-based calculation results of the electrical network. The next section will present how to model the hyperloop electrification system and how to connect the moving train loads (the train current) with a fixed electrical network.

| Hour | Traffic (pax/h) | Raw launching frequency (s) | Launching frequency (s) | Launches/h |
|------|---------------------------------|-----------------------------|-------------------------|------------|
| 1 | No passenger pods, only freight | | 105 | 35.8 |
| 2 | | | 105 | 35.8 |
| 3 | | | 105 | 35.8 |
| 4 | | | 105 | 35.8 |
| 5 | 976 | 258 | 240 | 15 |
| 6 | 4179 | 60 | 60 | 60 |
| 7 | 6986 | 36 | 30 | 120 |
| 8 | 5560 | 45 | 45 | 80 |
| 9 | 4470 | 56 | 60 | 60 |
| 10 | 4075 | 62 | 60 | 60 |
| 11 | 4790 | 53 | 60 | 60 |
| 12 | 4771 | 53 | 60 | 60 |
| 13 | 4902 | 51 | 45 | 80 |
| 14 | 4403 | 57 | 60 | 60 |
| 15 | 5082 | 50 | 45 | 80 |
| 16 | 6911 | 36 | 30 | 120 |
| 17 | 8212 | 31 | 30 | 120 |
| 18 | 6654 | 38 | 45 | 80 |
| 19 | 4483 | 56 | 60 | 60 |
| 20 | 2928 | 86 | 90 | 40 |
| 21 | 2097 | 120 | 120 | 30 |
| 22 | 1605 | 157 | 180 | 20 |
| 23 | 942 | 268 | 240 | 15 |
| 24 | 302 | 836 | 840 | 4.3 |

Table 11: Launching frequencies of passenger and freight pods

The train speed and the position simulation curves for an example of launching frequency 30 seconds are shown in Fig. 52. At this frequency, there will be a maximum of 2×8 capsules running

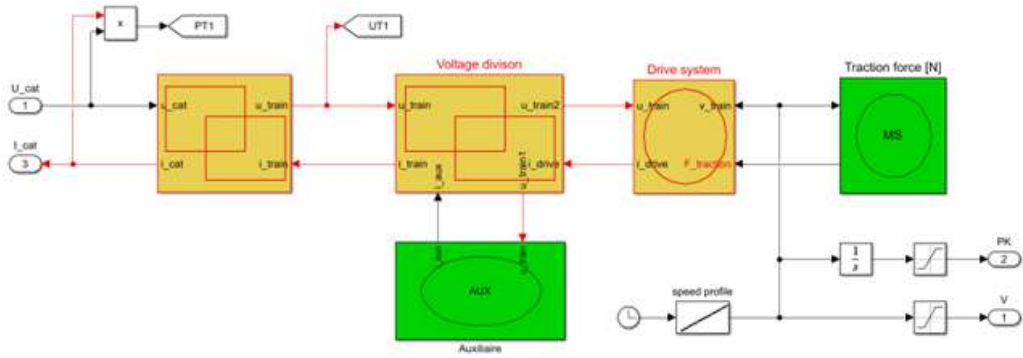


Figure 51: Capsule train traction model with Matlab/Simulink

simultaneously in the launcher and recuperator zones, namely, 8 capsules are under acceleration and 8 capsules are under deceleration.

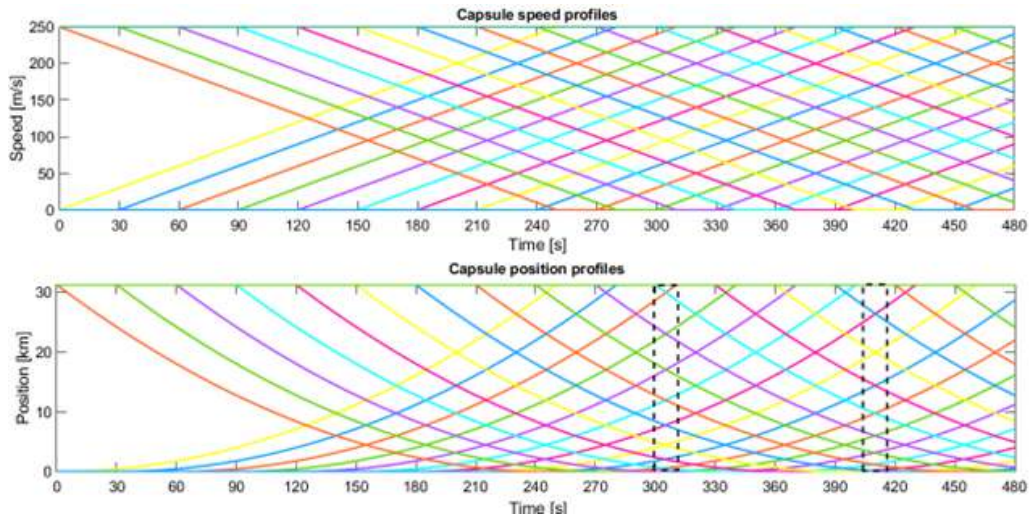


Figure 52: Speed and position profiles of each capsule train

F.2 Modelling of electrical network with moving loads

The equivalent circuits of the traditional and the hyperloop electrical railway network are respectively shown in Fig. 53. Compared to the traditional railway network, there is no real rail connection in the MAGLEV case. The distribution electrical network is modelled with equivalent resistances. The per-unit-length resistance of the contact line and its return line are summed together to provide an equivalent per-unit contact line resistance. Such a simplification allows reducing the number of nodes by considering a perfect current return path. The final resistances of each subsection of the circuit are calculated by multiplying their length by the equivalent per unit resistance as follow:

$$\Delta U(x) = T_{train} \cdot R_{eq} \cdot 2 \cdot x \cdot \frac{\rho_c}{S_c} \quad (4)$$

where c is the resistivity of cable, S_c represents the surface of cable, x represents the distance between the train and the voltage source.

However, unlike the classical power grids, the railway power grid contains the moving train loads where the electrical topology changes according to the schedule of the trains. A critical question is how to model the moving train loads for a fixed topology. A common solution to consider a mobile load on an electrical line is to split it up to create multiple nodes in the corresponding circuit, to locate the train displacements as shown in Fig. 54. According to their position, the trains are connected to the closest node of the network. When enough nodes are added by creating subsections, every train can be connected to the network without adding or removing nodes. In this way, the resulting network has a fixed topology. If a train is connected to a node, the load value of the node is set to the train power. Otherwise, it is set to zero.

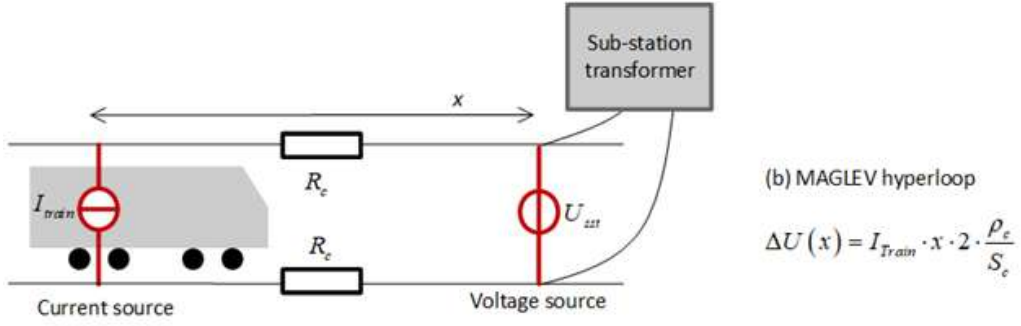


Figure 53: Equivalent circuits of the electrical railway network

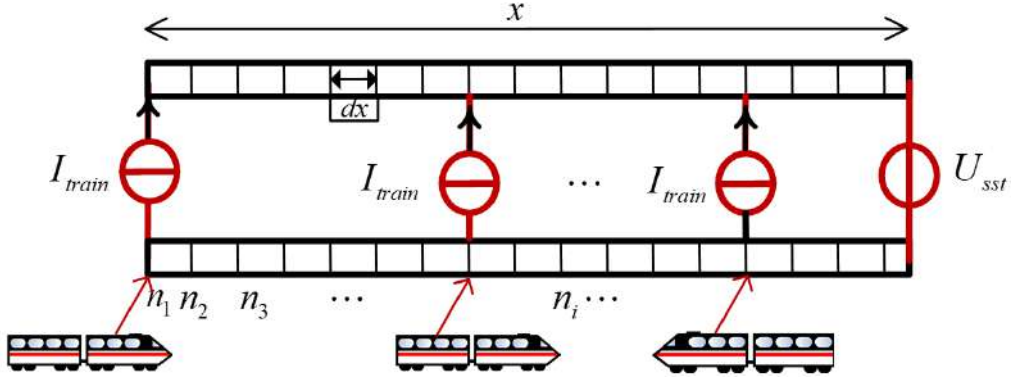


Figure 54: Modelling solution of the moving train loads

The electrical railway network can be modelled by using the Modified Nodal Analysis (MNA). The MNA mathematical representation is formulated by

$$[U_n I_{SSE}] = [G - BB^t - R]^{-1} [JE] \quad (5)$$

Where:

- the vectors J and E are the variables of the known initial currents and voltages
- the vector J should be updated with the moving trains loads
- the contact lines are split into small elements to formulate the conductance matrix G
- the B matrix is 1 if the voltage source m corresponds to the subsystem at node i, and 0 elsewhere,
- the R matrix is the internal source resistance, with the R_{sst} very small for an infinite power system
- the output vectors are the unknown voltages and the currents at each node. In this case, the output variables are the current flowing from each substation ISST and the voltages with respect to each node U_n .

In the simulation, the cable parameters are configured according to the standards suggested in [100], the cable surface is set to 400 mm², the electrical resistivity of copper is considered with a value of 16.8 nΩm. Besides, the energy conversion efficiencies of the train traction system and power electronics converter are both set to 95 percent. The simulation model under Matlab/Simulink is shown in Fig. 55

F.3 Substation configuration

F.3.1 MVAC vs MVDC

This motor located on the track side is representing a load of several dozens of MW that will be distributed across a 10 to 20 km launcher in a full-scale system. The motor is composed of primary

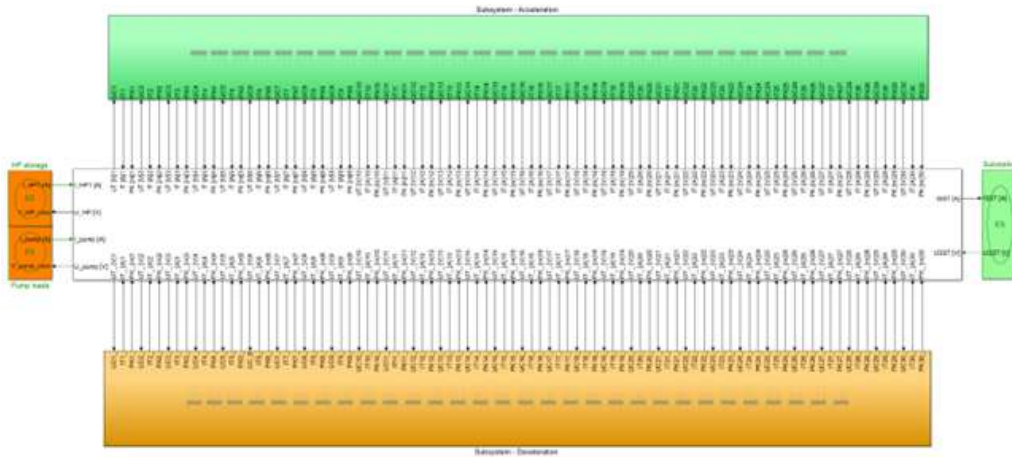


Figure 55: Complete simulation model of hyperloop electrical microgrid with Matlab/Simulink

elements placed in series that are powered and switched successively to propel the vehicle. The switches are not represented on the drawing. The system is composed of multiple drives placed along the launcher. The exact topology is not known yet and will depend on the result of the first prototypes, but distributed inverters will be used and could be parallelized. In this study, the inverters are considered as one block of 95

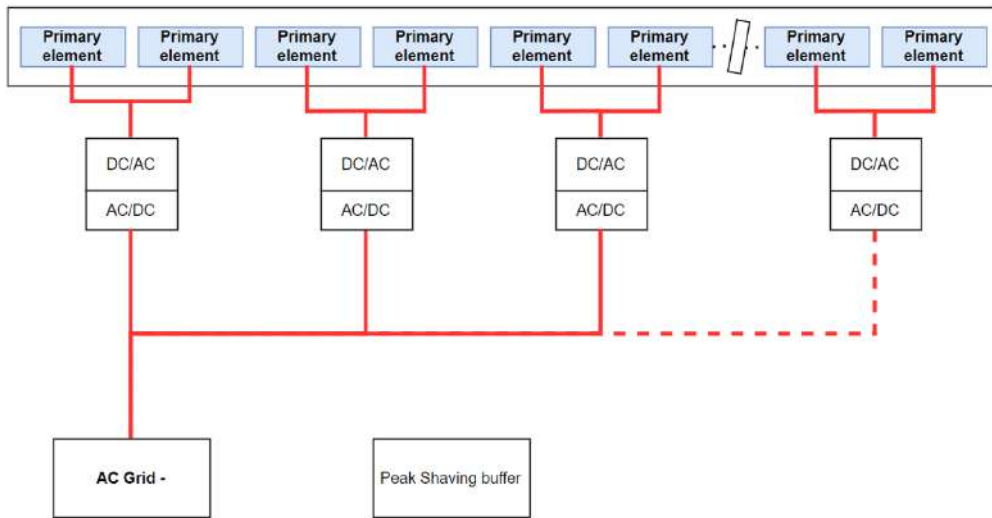


Figure 56: MVAC (Medium Voltage Alternating Current) Topology

AC power systems were originally used because of their efficiency and ease of voltage manipulation thanks to power transformers. But the technological progress in the last decade as well as the current trends towards DC allow such systems to be re-considered. On top of being more efficient at the same voltage, MVDC system removes the need for the power factor compensation as well as the frequency synchronisation to connect two systems. In such topology it is also easier to integrate renewable energy and electrical energy storage. On the other hand they require more complex protection schemes for short circuits management and usually require more CAPEX. In the case of hyperloop propulsion, a unique rectifier will not be needed for each inverter, and thus a DC distribution can actually be competitive even over the initial investment. For such a system to work without additional power converters (DC/DC converter), strict requirements over the bus voltage are needed. For the voltage at the input of the drives inverter (DC/AC converter) a limit of $\pm 10\%$ is considered. This limit is more strict than traditional railway which requires the voltage to stay within $[-33\% : 20\%]$ of the nominal voltage for DC and $[-24\% : +15\%]$ for AC. The AC and DC electrification systems are both simulated in this work. A group of classical voltages of AC 25kV, AC 15kV, DC9 kV, DC 15 kV are respectively tested and compared. It is noted that the braking power generated by each capsule train is assumed to be consumed by the capsules close to it. From the basic Ohm's law, if the transmission power is fixed, the current that flows in the cable increases under a lower transmission voltage, and the voltage drops increase on

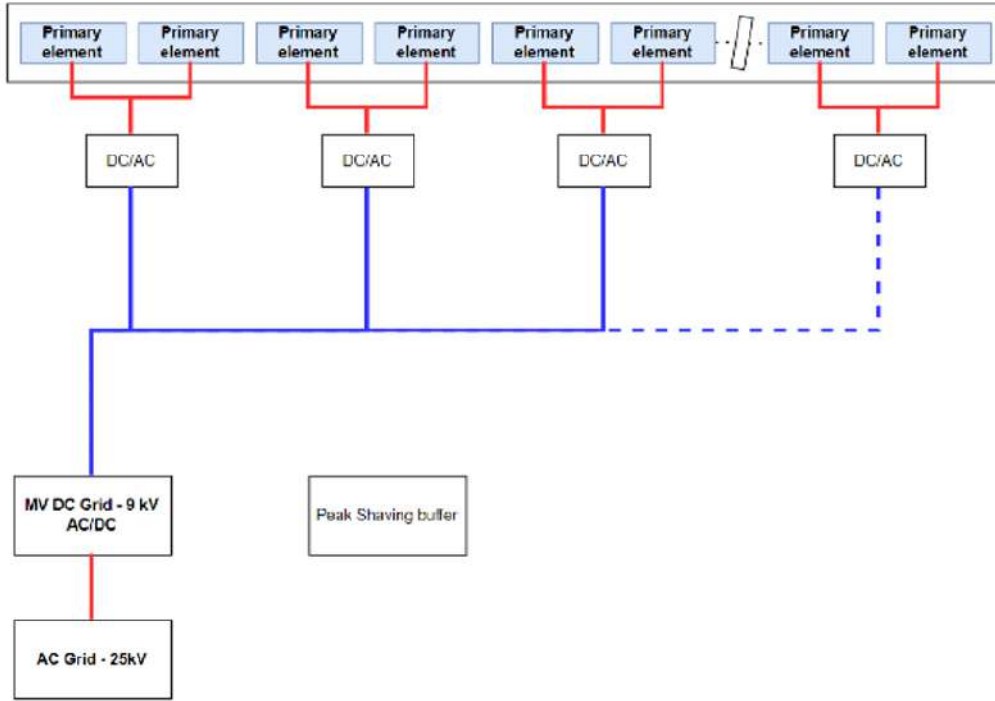


Figure 57: Fig. MVDC (Medium Voltage Direct Current) Topology

the transmission lines. As shown in Figs. 58-60, if the transmission voltage is set to be too low, for example, AC 15kV and DC 9kV, the absolute voltage drop will be larger than 10% of the rated voltage. If we choose transmission voltage to be AC 15kV and DC 9kV, the voltage variations are maintained to be $\pm 10\%$. Besides, the voltage profiles perform very similarly for AC and DC cases under such a configuration.

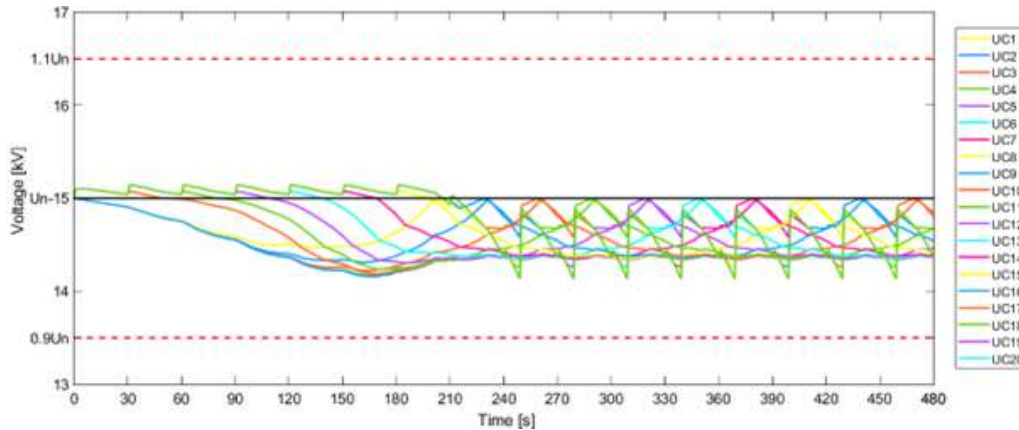


Figure 58: Voltage profile of each capsule train for 15kV DC electrification system

In conclusion, the substation can be configured with a rated voltage of 15kV for the DC system or 25kV for AC case. However, the DC voltage value is relatively low compared to that of the AC grid, which will have a lower insulation requirement on power converters as well as transmission cables. The cables and power electronic elements impose less rapid ageing problems under a relatively lower voltage environment.

F.3.2 Energy management system

In the acceleration and deceleration areas, there are several challenges to be addressed. Firstly, the loads change sharply: The train's load power can be very large at the end of the acceleration area and in the beginning of the deceleration area. Secondly, there are multiple capsules running in the launcher and recuperator simultaneously in the morning and evening peak time. The load peak would be larger than the maximum power that can be supplied by the substation, which

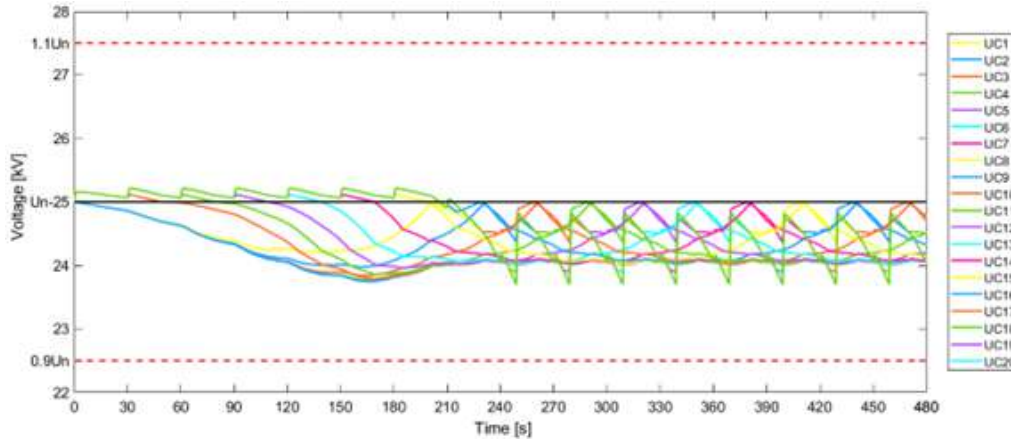


Figure 59: Voltage profile of each capsule train for 25kV AC electrification system

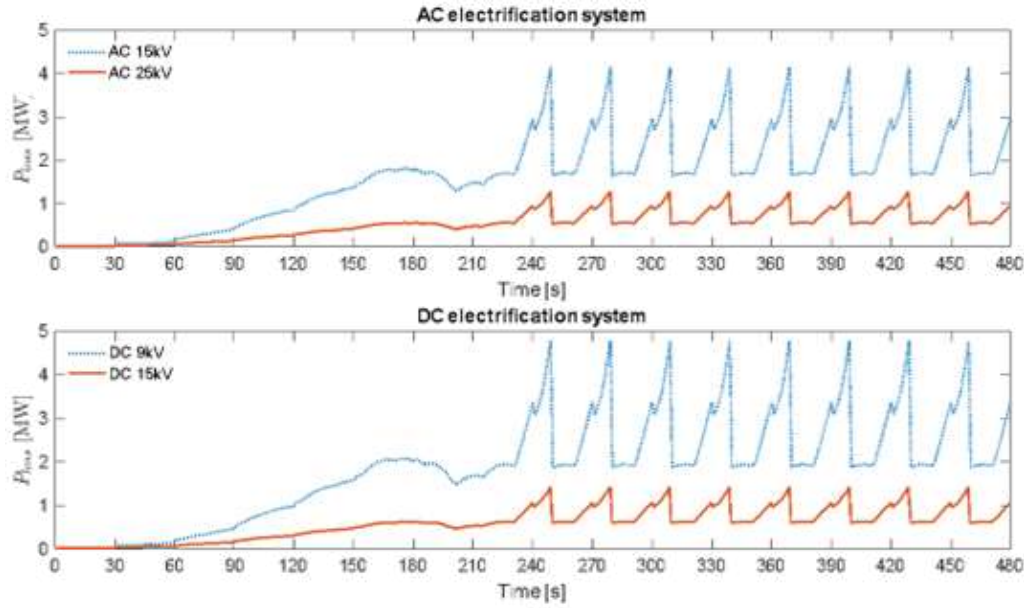


Figure 60: Line power loss under different voltage configurations

results in financial extra power penalties. One solution is to change the contract for a larger power limitation with DSO or TSO, which means a higher annual payment on the increased power demand. However, most of the time in a day, the power would be lower than the power limitations, this solution seems to be not very economical.

The launching time delay between two capsules ranges from 30s to 840s as given in Table 10. Three cases are simulated as shown in Fig. 61, with launching periods of 30s, 45s, and 105s. The total power supplied by the substation is periodically changing, depending on the running capsule trains. The peak power decreases when the delay time between two capsules increases, as there will be less capsules running in the launcher and the recuperator. There will be maximum 8×2 capsules who are simultaneously running in the study zone for a time delay of 30 seconds. The power demand from the substations reaches a maximum peak power of 39.6 MW. However, for the largest part of the day, the power demand will be less than the maximum power. It is important to underline at this point that the power needed is significant but still in the range of current technology and power grid. The station would need to be connected to a line $> 50\text{kV}$ directly.

In this chapter, a microgrid concept for a hyperloop electrical system is proposed: it consists of a substation, moving capsules loads, HPS (high power storage) modules, and other consumptions. The HPS module is used to stabilise the peak power demand. The droop control-based energy management system is designed to exactly address the issues mentioned above.

As stated above, the voltage and energy profile have similar forms but different absolute values, which leads to different battery sizes. The 15kV DC grid will be considered in the following studies.

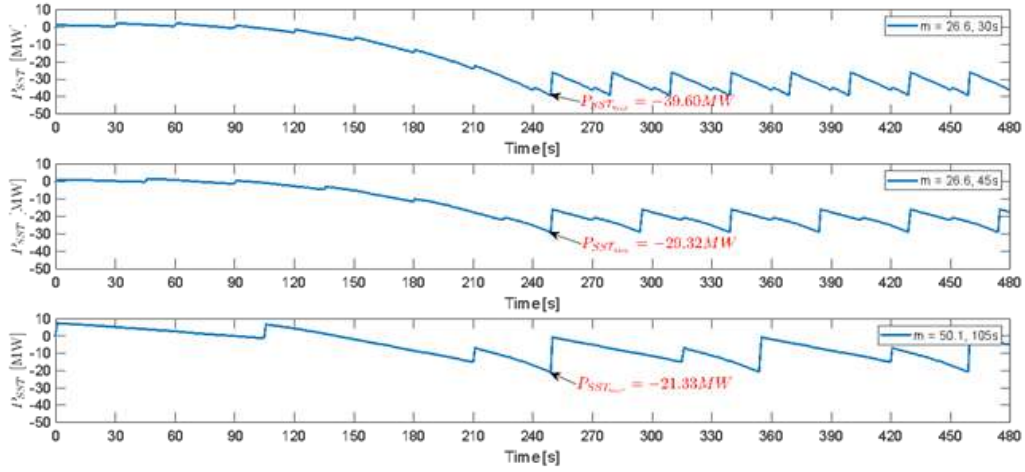


Figure 61: Substation total power curves for DC electrification system

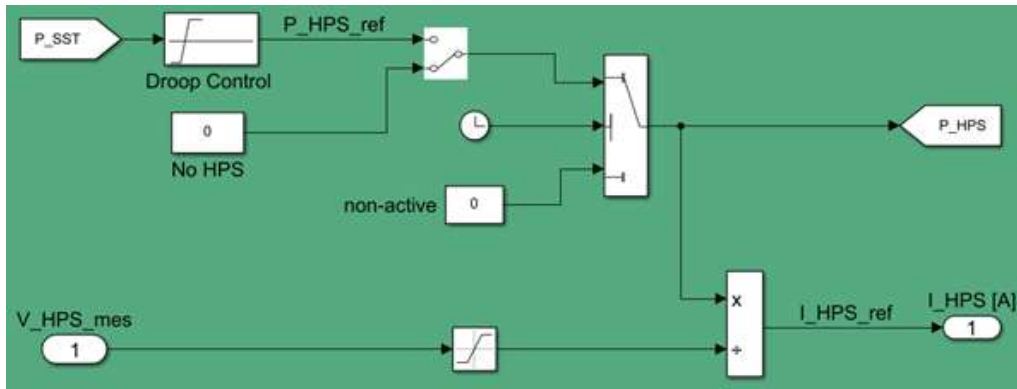


Figure 62: HPS module integration in hyperloop microgrid

The HPS module is integrated near the substation as a buffer as shown in the Fig. 62. The droop control is the core of EMS to regulate the power peak. The input information of the droop control is the total power measured at the transformer; the output is the suggested charging or discharging power for the battery. The droop control is simple and very efficient, though the energy management is a suboptimal design.

From this study, it can be concluded that the AC electrical grid can be configured with installation position PK-SST = 0.65L and voltage level 25kV. The DC electrical grid can be PK-SST = 0.65L and voltage level 15kV. Compared to the AC grid, however, the DC grid solution needs less power electronics elements. However, the reduced peak power value is not proportional to the installed HPS capacity, because the droop control performs a nonlinear behaviour. The capacity of 2.6 MW can be fully used in the peak time, however, the utilisation rate for 10.4MW decreases to 55.9 %. Therefore, it is suggested to configure the HPS with a total capacity of 5.2MW, which has a very high utilisation rate as well as a relatively large reduction in peak power. As shown in Fig. 60, the state of charge (SOC) of the HPS will come back to the original state in each period, the net energy into the battery is zero for a complete period. To complete 1 cycle the required capacity is of 9.91 KWh, a relatively low value. Current technology like Electric Double Layer Capacitor (EDLC) can already be used to realise this type of storage. By then considering the grid provider contract cost and the acceptable depth of discharge (90 % for EDLC) it is possible to compute the cost savings and total investment needed for such a solution both in OPEX and in CAPEX.

Appendix G Sankey diagram of the life-cycle assessment

The following page shows the distribution of GHG emissions along the whole cradle-to-grave chain of processes and system components. The upstream processes are shown at the top while the final transport service that combines all subsystems is at the bottom. The diagram refers to the reference case presented in section 4.3, with the infrastructure entirely overground and made of reinforced concrete.

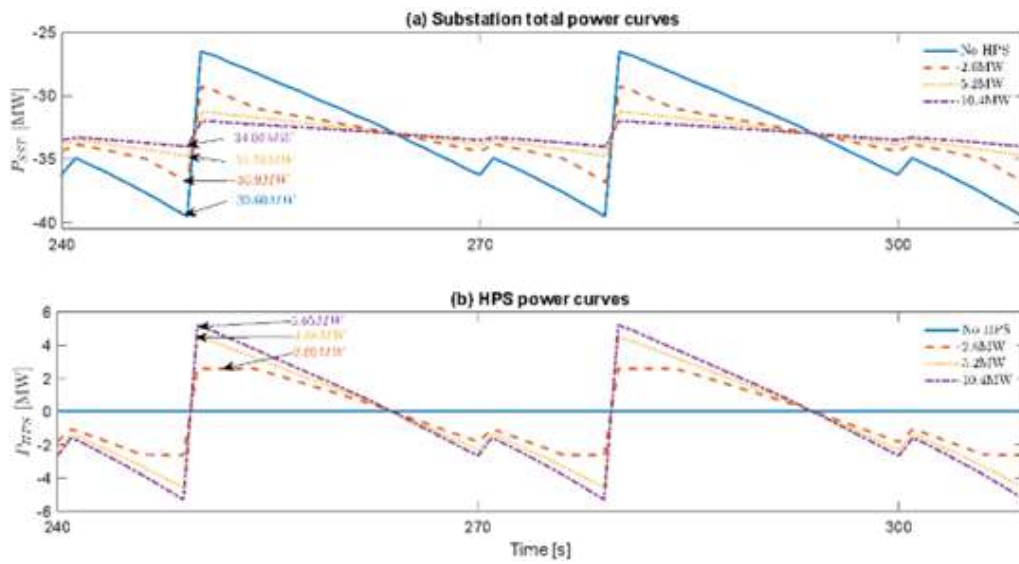


Figure 63: Partial zoom results of substation power curves and HPS behaviour curves